FRIENDS OF THE PLEISTOCENE PACIFIC CELL FIELD TRIP
NORTHERN WALKER LANE AND NORTHEAST SIERRA NEVADA
October 12-14, 2001.

Contributors:

Ken Adams[1], Rich Briggs[2], Bill Bull[3], Jim Brune[4], Darryl Granger[5], Alan Ramelli[6], Clifford Riebe[7],

Tom Sawyer[8], John Wakabayashi[9], Chris Wills[10]

[1]*Desert Research Institute, Reno, Nevada, kadams@dri.edu*

[2]*Center for Neotectonic Studies, University of Nevada, Reno, NV 89557, briggs@seismo.unr.edu*

[3]*Department of Geosciences, University of Arizona, Tucson, AZ 85721, bill@activetectonics.com*

[4]*Seismology Laboratory 714, University of Nevada, Reno NV 89557, brune@seismo.unr.edu*

[5]*Department of Earth and Atmospheric Sciences & PRIME Lab, Purdue University, West Lafeyette, IN 47907, dgranger@purdue.edu*

[6]*Nevada Bureau of Mines and Geology, MS 178, University of Nevada, Reno, NV 89557, ramelli@unr.edu*

[7]*Department of Earth and Planetary Science, University of California, Berkeley, CA 94720, riebe@seismo.berkeley.edu*

[8]*Piedmont Geosciences, Inc., 10235 Blackhawk Dr., Reno, NV 89506, piedmont@USA.com*

[9]*1329 Sheridan Lane, Hayward, CA 94544, wako@tdl.com, http://www.tdl.com/~wako/*

[10]*California Division of Mines and Geology,185 Berry St Suite 210, San Francisco CA 94107, cwills@consrv.ca.gov*

SPECIAL THANKS TO: Friends of the Pleistocene Pacific Cell website manager, Doug La Farge (doug@holdit.com), for managing the Pacific Cell website (http://pacific.pleistocene.org/), including facilitating production of online field trip guides, and coordination of group emails. Special thanks also to the Ramelli family, for allowing our trip to use their property as the meeting place.

INTRODUCTION

John Wakabayashi, 1329 Sheridan Lane, Hayward, CA 94544; wako@tdl.com

This field trip examines stops related to the neotectonics, paleoseismology, and evolution of the northern Walker Lane, as well as general controls on erosion rates, and topographic evolution of the Sierra Nevada. In addition to showing participants field localities relevant to research on the above topics, the trip should also make it clear to participants that so much research in this area has been conducted at barely a reconnaissance level, leaving many inviting targets for future study. Figure In-1 shows a generalized road map with stop and camp locations (same as the map on the Pacific Cell website, except that the location of Stop 9 has been changed). Figures In-2 and In-3 show the general geology and faults, respectively, of the Sierra Nevada and northern Walker Lane with stop and camp locations. For participants interested in further exploration of this area on their own, there is a full color field trip guide published by the California Division of Mines and Geology (CDMG Special Publication 122) that has trips that include additional neotectonics-related stops in this area (Wakabayashi and Sawyer, 2000; Wagner et al. 2000).

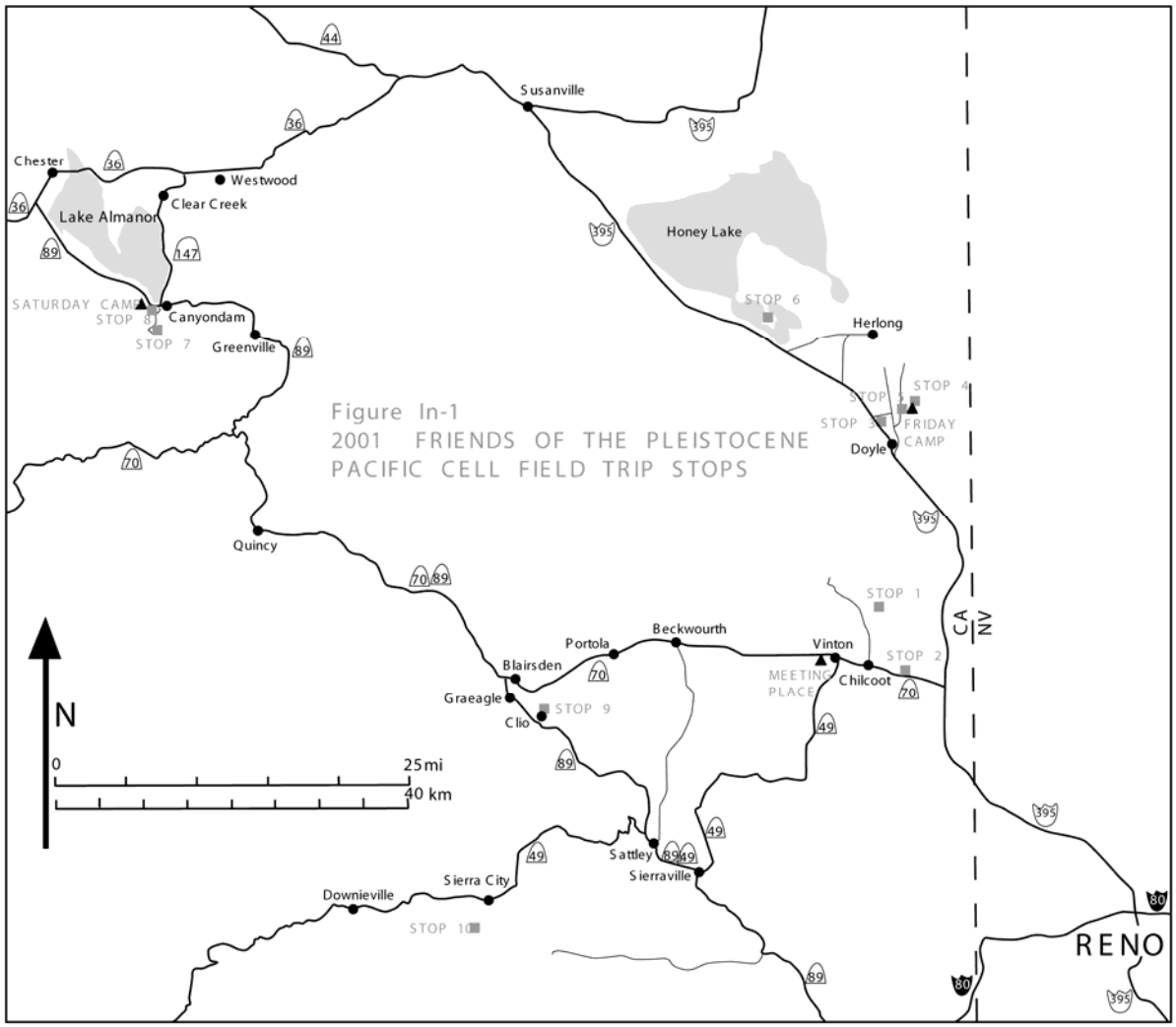

Tectonic Setting

The Walker Lane is the most active element of the 'eastern branch' of the Pacific-North American plate boundary, a zone of dextral shear separating the Basin and Range province on the east from the Sierra Nevada microplate to the east (Fig. In-2, inset A, B). Collectively the Walker Lane and Basin and

Range accommodate 20-25% of Pacific-North American plate motion; the remaining motion occurs on the San Andreas fault system (e.g., Argus and Gordon, 1991; Dixon et al., 2000). The westernmost part of the Walker Lane is the Sierra Nevada Frontal fault system (Frontal fault system), a zone of dextral, oblique, and down-to-the-east normal faults that bounds the eastern margin of the Sierra Nevada block, and forms the eastern escarpment of the range (Fig. In-2; In-3). The Sierra Nevada is California's most prominent mountain range, extending for over 650 km, with peak elevations that exceed 2000 m over a distance of 500 km, and 3000 m over a distance of 350 km (In-4). The Sierra Nevada is part of the Sierra

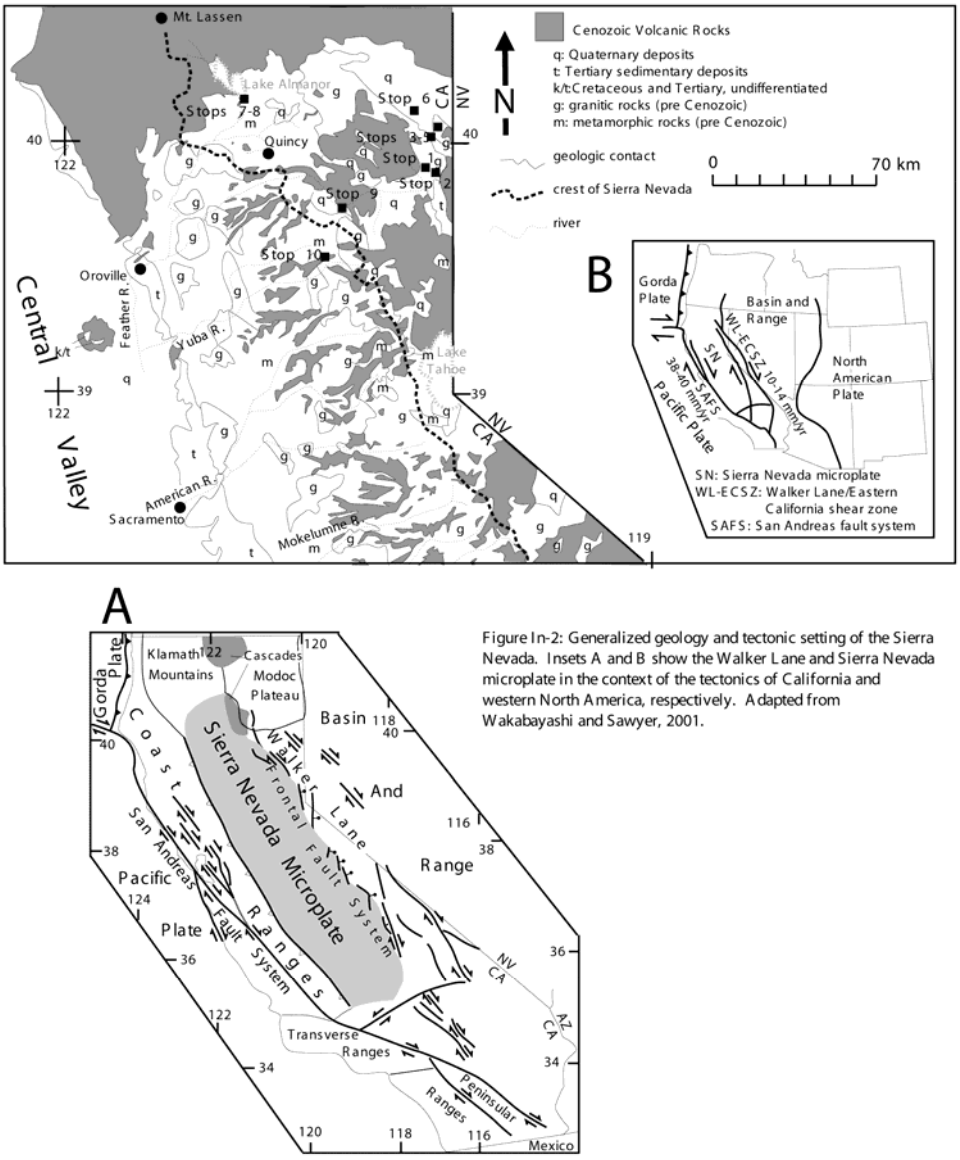

Figure In-2: Generalized geology and tectonic setting of the Sierra Nevada. Insets A and B show the Walker Lane and Sierra Nevada microplate in the context of the tectonics of California and western North America, respectively. Adapted from Wakabayashi and Sawyer, 2001.

Nevada microplate, bounded on the west by the California Coast Ranges, and on the east by the Frontal fault system. The Sierra Nevada itself is a west-tilted fault block range, with comparatively little internal deformation and significant variation in topographic expression along strike (e.g., Wakabayashi and Sawyer, 2000; 2001). Note that the eastern boundary of the Sierra Nevada, as defined above, follows the "tectonic" definition of the Sierra Nevada as a comparatively rigid microplate with little internal deformation (implicit in geodetic studies; e.g., Argus and Gordon, 1991, Dixon et al., 1995; 2000; explicit in geologic summaries of Wakabayashi and Sawyer, 2000; 2001). The eastern boundary of the Sierra Nevada is defined as the westermost strand of the Frontal fault system.

Northern Walker Lane faulting appears to be accommodated in two major zones: a western zone known as the Mohawk Valley fault zone an eastern zone called the Honey Lake fault zone. The Walker Lane currently accommodates 10-14 mm/yr of dextral shear in its southern reaches, most of this shear occurring several well-defined fault zones, including the Owens Valley and Fish Lake-Death Valley fault zones (e.g., Dixon et al., 2000). In contrast to the southern and central Walker Lane, comparatively little data exists on the kinematics of the northern Walker Lane, and the distribution of faulting within it, because: (1) geologic slip rate studies are lacking, with the exception of the Honey Lake fault zone (Wills and Borchardt, 1993), and (2) because stations used for geodetically determined slip rates are located well beyond the eastern border of the northern Walker Lane, so it is difficult to assign slip rate to specific fault zones. Dixon et al. (2000) estimated an aggregate slip rate of 7 mm/yr for the northern Walker Lane and assigned 5 mm/yr of this slip rate to the Mohawk Valley fault zone on the basis of subtracting Wills and Borchardt's (1993) ~2 mm/yr slip rate estimate for the Honey Lake fault zone (see Stop 3.), and the geodetically determined slip rate for the Central Nevada Seismic Belt (CNSB) from the velocity between Ely and locations such as Quincy and Oroville; such an approach assumes negligible deformation between the CNSB and the Honey Lake fault zone. Further discussion of the geodetic data bearing on the slip rate of Mohawk Valley fault zone and local geologic features will be presented at Stop 9. There have been no geologic dextral slip rate estimates for the Mohawk Valley fault zone. Long-term (post 5-Ma) vertical separation rates for the Mohawk Valley fault zone have been estimated at 0.1 to 0.24 mm/yr on this dominantly dextral fault zone (Wakabayashi and Sawyer, 2000). Whether or not slip rates are indeed as high as 5 mm/yr for this zone remains to be verified by detailed geologic studies. There are not that many places in the western United States where 5 mm/yr of slip rate is unaccounted for! The Honey Lake and Mohawk Valley fault zones have produced features typical of strike slip fault systems, such as linear scarps, sag ponds and shutter ridges, but it is the subordinate normal faulting (or component of normal slip) that has produced the most noticeable geomorphologic signature in the form of major topographic escarpments and features such as the graben of Mohawk Valley. Piercing points for determining long-term slip displacement and slip rates have not been found across the major fault zones of the northern Walker Lane.

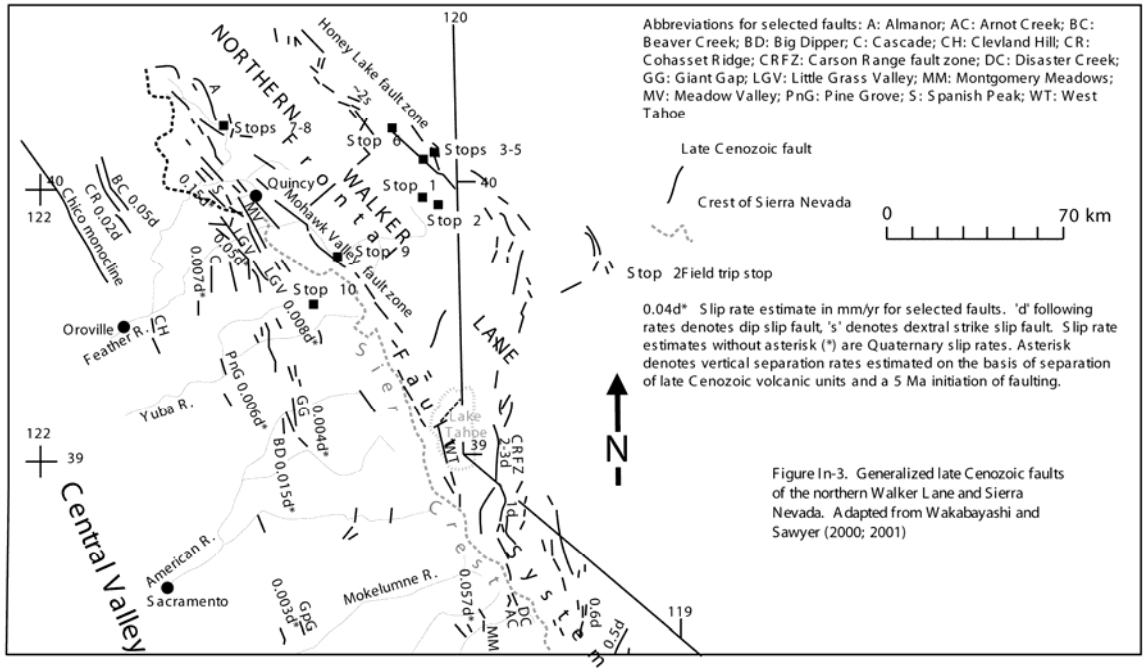

Both the Mohawk Valley and Honey Lake fault zones appear to have formed comparatively recently in geologic time. The Honey Lake fault zone may have started moving between about 10 and 5

Ma, and the Mohawk Valley fault zone started movement shortly after about 5 Ma; the initiation of movement on these fault zones appears to be related to the progressive encroachment of the Walker Lane into the Sierran microplate (Wakabayashi and Sawyer, 2000; 2001). This encroachment is ongoing in the North Fork Feather River area, where some faults apparently did not start moving until after about 600 ka (Wakabayashi and Sawyer, 2000),(discussed at Stop 7).

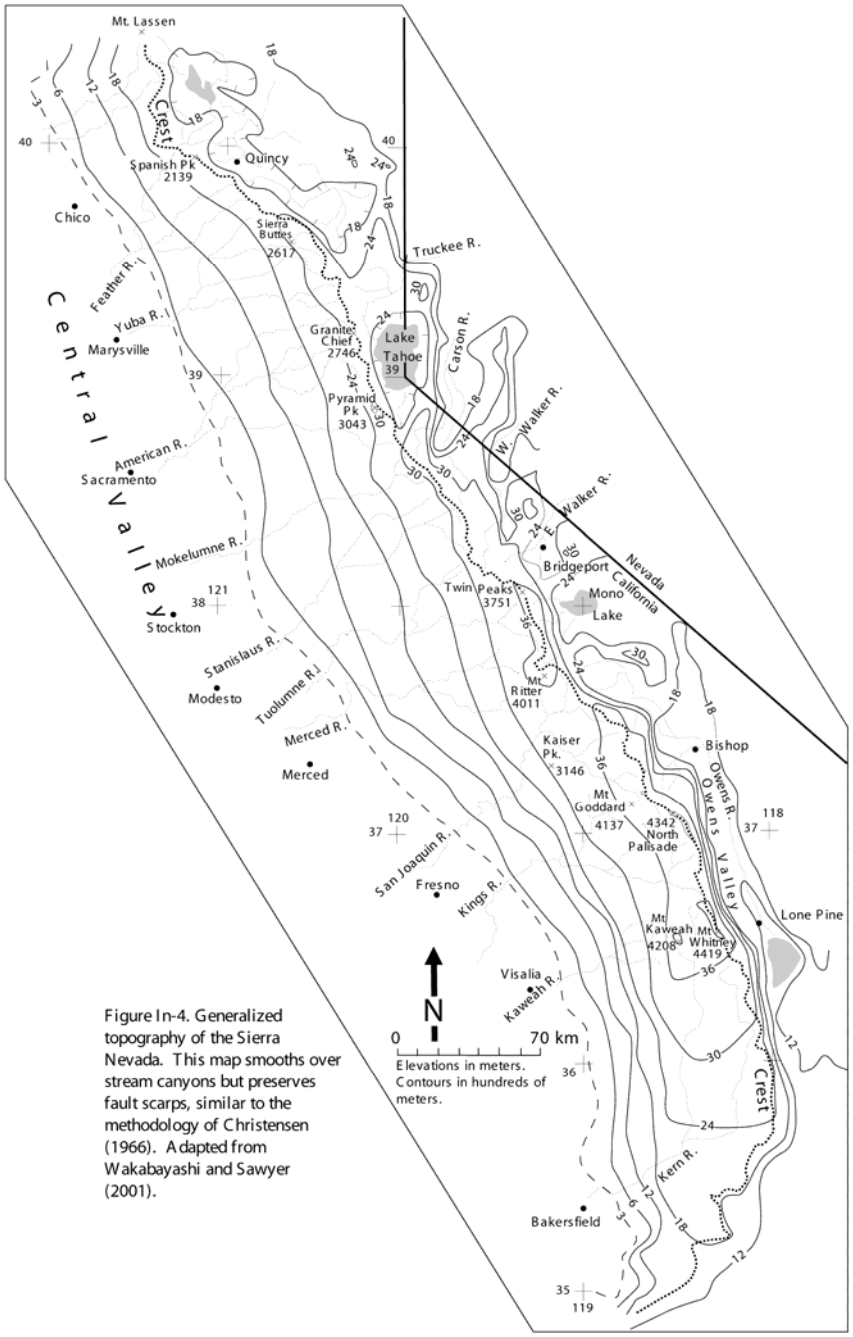

Figure In-4. Generalized topography of the Sierra Nevada. This map smooths over stream canyons but preserves fault scarps, similar to the methodology of Christensen (1966). Adapted from Wakabayashi and Sawyer (2001).

Sierra Nevada: A Geomorphology Field Laboratory

While most of the research on the neotectonics on the Walker Lane has taken place in the last two decades, the Sierra Nevada has served as a field laboratory for examining geomorphic processes and the relationship between tectonics and topographic development for over a century. The Sierra Nevada has long been regarded as a mountain range that attained most of its elevation as a consequence of westward tilting coupled with faulting along the Frontal fault system during the late Cenozoic (e.g., Whitney, 1880;

Ransome, 1898; Lindgren, 1911; Christensen, 1966; Huber, 1981; Unruh, 1991). In contrast to this view, thermochronologic data has been interpreted to suggest that late Cenozoic uplift did not occur and that the Sierra Nevada has been decreasing in elevation since the late Cretaceous (House et al., 1998). Small and Anderson (1995) suggested that the late Cenozoic uplift of the high ridges of the Sierra Nevada may have been climatically rather than tectonically triggered. Thus the Sierra has become the focus of debate on how some types of major mountain ranges form. The debate regarding the long-term topographic evolution of the Sierra Nevada has been discussed in Wakabayashi and Sawyer (2001), who proposed that late Cenozoic surface uplift did indeed occur, probably as a result of a tectonic transition, and that significant elevation was relict from pre-Eocene uplift. Some of the evidence bearing on models of long term development of the Sierra Nevada, particularly with regard to stream incision and development of relief, will be viewed and discussed at Stops 7 and 10.

Theories of landscape development, originally proposed in the Sierra Nevada, such as the stepped topography concept (Wahrhaftig, 1965) have been recently tested by quantification of erosion rates by cosmogenic nuclide dating (Granger et al., 2001) (Stop 1). Quantification of erosion rates in many different settings has allowed evaluation of many surface processes, including the relationship of weathering to parameters such as climate or erosion, and controls on erosion (in addition to the bedrock and boulder armoring effect discussed at Stop1) such as tectonic forcing (Riebe et al. 2000; 2001a, b) (discussed at Stop 4).

Following this introduction is a road log, followed by individual stop descriptions.

References

Argus, D.F., and Gordon, R.G., 1991, Current Sierra Nevada-North America motion from very long baseline interferometry: Implications for the kinematics of the western United States: Geology, v.19, p. 1085-1088.

Christensen, M.N., 1966, Late crustal movements in the Sierra Nevada of California: Geological Society of America Bulletin, v. 77, p. 163-182.

Dixon, T.H., Robaudo, S., Lee, J., and Reheis, M., 1995, Constraints on present-day Basin and Range deformation from space geodesy: Tectonics, v. 14, p. 755-772.

Dixon, T.H., Miller, M., Farina, F., Wang, H., and Johnson, D., 2000, Present-day motion of the Sierra Nevada block and some tectonic implications for the Basin and Range province, North American Cordillera: Tectonics, v. 19, p. 1-24.

Granger, D.E., C. S. Riebe, J. W. Kirchner, and R. C. Finkel, 2001, Modulation of erosion on steep granitic slopes by boulder armoring, as revealed by cosmogenic ^{26}Al and ^{10}Be, Earth and Planetary Science Letters v. 186, 269-281.

House, M.A., Wernicke, B.P., and Farley, K.A., 1998, Dating topography of the Sierra Nevada, California, using apatite (U-Th)/He ages: Nature, v. 396, p. 66-69.

Huber, N.K., 1981, Amount and timing of late Cenozoic uplift and tilt of the central Sierra Nevada, California-evidence from the upper San Joaquin river basin: U.S. Geological Survey Professional Paper 1197, 28p.Wakabayashi, J., and Sawyer, T.L., 2001, Stream incision, tectonics, uplift, and evolution of topography of the Sierra Nevada, California: Journal of Geology, v. 109, p. 539-562.

Lindgren, W., 1911, The Tertiary gravels of the Sierra Nevada of California: U.S. Geological Survey Professional Paper 73, 226 pp.

Ransome, F.L. 1898, Some lava flows on the western slope of the Sierra Nevada, California: U.S. Geological Survey Bulletin, v. 89. 71 pp.

Riebe, C. S., J. W. Kirchner, D. E. Granger, and R. C. Finkel, 2000, Erosional equilibrium and disequilibrium in the Sierra Nevada, inferred from cosmogenic ^{26}Al and ^{10}Be in alluvial sediment, Geology, v.28, p. 803-806.

Riebe, C. S., J. W. Kirchner, D. E. Granger, and R. C. Finkel, 2001a, Minimal climatic control of erosion rates in the Sierra Nevada, California, Geology, v. 29, p. 447-450.

Riebe, C. S., J. W. Kirchner, D. E. Granger, and R. C. Finkel, 2001b, Strong tectonic and weak climatic control of long-term chemical weathering rates, Geology 29, 511-514.

Small, E.E., and Anderson, R.S. 1995, Geomorphically driven late Cenozoic rock uplift in the Sierra Nevada, California: Science, v. 270, p. 277-280.

Unruh, J.R., 1991, The uplift of the Sierra Nevada and implications for late Cenozoic epeirogeny in the western Cordillera: Geological Society of America Bulletin, v. 103, p. 1395-1404.

Wagner, D.L. Saucedo, G.J., and Grose, T.L.T., 2000, Tertiary volcanic rocks of the Blairsden area, northern Sierra Nevada, California: in Brooks, E.R., and Dida, L.T., eds., Field guide to the geology and tectonics of the northern Sierra Nevada, California Division of Mines and Geology Special Publication 122, p. 155-172.

Wahrhaftig, C.W. 1965, Stepped topography of the southern Sierra Nevada, California: Geological Society of America Bulletin, v. 76, p. 1165-1189.

Wakabayashi, J., and Sawyer, T.L., 2000, Neotectonics of the Sierra Nevada and the Sierra Nevada-Basin and Range Transition, California, with field trip stop descriptions for the northeastern Sierra Nevada: in Brooks, E.R., and Dida, L.T., eds., Field guide to the geology and tectonics of the northern Sierra Nevada, California Division of Mines and Geology Special Publication 122, p. 173-212.

Wakabayashi, J., and Sawyer, T.L., 2001, Stream incision, tectonics, uplift, and evolution of topography of the Sierra Nevada, California: Journal of Geology, v. 109, p. 539-562.

Whitney, J.D. 1880, The auriferous gravels of the Sierra Nevada of California: Harvard College Museum of Comparative Zoology Memoir 6 (1) 569 pp.

Wills, C.J., and Borchardt, G., 1993, Holocene slip rate and earthquake recurrence on the Honey Lake fault zone, northeastern California: Geology, v. 21, p. 853-856.

2001 FRIENDS OF THE PLEISTOCENE PACIFIC CELL FALL FIELD TRIP ROAD LOG

Note: As with all road logs, there will be some difference, owing to differences in odometers for various vehicles. It is recommended that the individual segment mileages be considered more than the cumulative ones, as the cumulative mileage 'error' increases as the day goes on.

Thursday, October 11, 2001 Gathering of Friends

Assemble on grounds of Ramelli family homestead, west of the town of Vinton (see Fig. In-1 for generalized main roads in the area). The driveway to meeting place leaves Highway 70 3.0 miles west of Chilcoot (measured from the junction of Highway 70 and the Frenchman Lake road) and 10.7 miles east of the junction of county road A23 and Highway 70. Directly west of the driveway is a white, former one room schoolhouse "Summit School District" that is now an antique shop.

The first night's campsite lies in the northeast part of Sierra Valley, considered by many to be the largest valley within the Sierra Nevada. As discussed in the introduction, we would consider this tectonically-controlled basin to be within the Walker Lane belt, rather than part of the Sierran proper. The valley, which is bisected by several poorly understood northwest-striking faults, may have formed as a pull-apart basin, with right-lateral slip transferring across the valley. The Mohawk Valley fault, which bounds the valley on the southwest, is the subject of STOP 8.

During the Middle Pleistocene, Sierra Valley was occupied by pluvial Lake Beckwourth. Undissected lake sediments form the very flat floor of the valley, although the campsite actually sits on younger sandy alluvium of Little Last Chance Creek that spilled out onto the lake sediments. At the campsite, the lake was about 30 m (100 ft) deep during the most recent lake stand. During an earlier, higher stand (the subject of STOP 2), the lake was more than 90 m (300 ft) deep at this location.

Note that a short stretch of dirt road leading to stop 1 required 4 wheel drive for one of the vehicles in our dry run (but didn't for the other two). Those unsure about the capability of their vehicle may park at the Frenchman Lake road/Highway 70 junction in Chilcoot. Please make your arrangements before we get started on Friday morning.

Friday, October 12, 2001	Mileage from late noted point	Cumulative mileage for day
Start trip. Intersection of driveway from Ramelli homestead and Highway 70. <u>Make a right turn onto Highway 70 and drive eastward on Highway 70</u>.	0.0	0.0
Turn left off of Highway 70 onto the Frenchman Lake road in Chilcoot.	3.0	3.0
<u>Turn right onto an unmarked dirt road.</u> Here, the route traverses a	1.1	4.1

tombolo formed behind the granitic hill to the southwest. The crest of the tombolo, which is covered by a thick layer of eolian sand, is at an elevation of about 1,560 m (5,120 ft). The tombolo formed during the older, higher lake stand, and was likely lowered somewhat by subsequent erosion.		
Bear left at a fork in the road	0.5	4.6
Pass through gate	0.3	4.9
Keep straight at fork	0.5	5.4
STOP 1	1.6	7.0
Retrace route back to Highway 70 Drive southward on dirt road from stop, then turn left (south) onto the Frenchman Lake road	2.9	9.9
Turn left (east) onto Highway 70. The route climbs from the floor of Sierra Valley toward Beckwourth Pass. Beckwourth Pass, named for man who "discovered" it (James Beckwourth), is the lowest pass in the Sierra Nevada. This was a somewhat easier, albeit longer, variant of the mid-1800s emigrant trail.	1.1	11.0
Turn sharply left off of Highway 70 onto road that leads down the slope to some kind of facility (pump station?).	2.3	13.3
STOP 2	0.2	13.5
Drive back to Highway 70 and turn left (east)	0.2	13.7
Turn left (northward) onto Highway 395	3.3	17.0
The channel of Long Valley Creek is to our left (west) for the next 4 miles. The banks of the creek expose Holocene sediments.	7.0	24.0
Junction Doyle Grade (town of Doyle); stay straight on 395	12.5	36.5
Cross Long Valley Creek, stop 3 is just upstream to our right (east)	2.0	38.5
Turn right (east) onto Laver Crossing road, followed by an immediate right onto B&B Way-North Doyle Heights	0.4	38.9
Turn right at driveway, the entrance of which is flanked by two wooden posts	0.4	39.3
Turnaround at end of driveway **STOP 3**	0.2	39.5
Return to B&B road; turn left	0.3	39.8
Return to Laver Crossing road; turn right	0.4	40.2
Turn right onto Hackstaff Road	1.3	41.5
Turn left onto Fort Sage Road	1.2	42.7
Turn right onto an unmarked dirt road that leads up into the Fort Sage Mountains	3.3	46.0
Take left fork (smoothest most prominent track) after crossing dry creekbed	0.3	46.3
Road comes in from left, keep right	0.7	47.0
Road junction; park in this area. Some of the better parking spots come shortly after turning left at this junction, but parking is available both before and beyond this junction off the road to either side. This is the **CAMP FOR FRIDAY** and parking for **STOP 4**	1.0	48.0

Saturday, October 13, 2001	Mileage from late noted point	Cumulative mileage for day
Leave camp drive back to Fort Sage road	0.0	0.0
Bear left at fork	1.0	1.0
Turn left at Fort Sage road	1.0	2.0
Park on the margin of road. This is a very wide road. Park on it rather than off of it, because the shoulder is steep and vehicles may get stuck if they park off the road. **STOP 5**	1.0	3.0
Continue southward on Fort Sage road; turn right onto Hackstaff road	2.3	5.3
Turn left onto Laver Crossing road	1.2	6.5
Turn right (northward) onto Highway 395	1.3	7.8
Pass west-facing scarp of Honey Lake fault on right	0.8	8.6
Turn right onto Garnier Road (A26) toward Herlong	2.4	11.0
Turn left onto Herlong Access Road	3.7	14.7
Turn right onto Pole Line Road	0.4	15.1
Bear left, then follow main branch (both go to same place)	1.7	16.8
Turn left (due west) onto a section line road. follow it with minor detours around low areas	0.3	17.1
Turn left (due south) onto a section line road	5.0	22.1
Turn right onto section line road that bends northerly, then back to the southwest	1.0	23.1
Road junction; best parking is to the left by a corral. To the right is **STOP 6**	2.6	25.7
Turn left (north) on section line road	2.6	28.3
Turn right (east) on section line road	1.0	29.3
Main road turns right on section line; follow it	2.0	31.3
Univ. Nevada facility entrance, go straight, then round low area to right and continue	1.0	32.3
Bear right, several possible tracks cut the corner between section line roads	2.0	34.3
Bear right	0.3	34.6
Turn right (west) onto Herlong Access Road	1.7	36.3
Turn right onto Highway 395	4.2	40.5
Stay straight on Highway 36 toward Susanville (Hwy 395 turns right) you will stay on Highway 36 for the next 29 miles	25.9	66.4
Turn left onto Highway 147. Soon after turning onto Highway 147 you will turn right staying on Highway 147 and descend a short grade to the town of Clear Creek; the grade descends a west-facing fault scarp of the Walker Springs fault in 400 ka Basalt of Westwood.	28.5	95.4
After driving southward along the east shore of Lake Almanor, turn right (west) onto Highway 89	11.0	107.0
Take an immediate left (after about 0.05 miles) onto the Seneca Road	0.1	107.1
We pass a low west-facing scarp of the Eastside fault in 400 ka Basalt of Westwood.	0.1	107.2

Find parking along the Seneca Road. Fortunately it is wide for a fairly long distance. The drop off to the west is extremely abrupt. **STOP 7**	1.9	109.1
Return to Highway 89 and turn left (west)	2.0	111.1
Park along (north side of the road) on Lake Almanor Dam **STOP 8**	0.5	111.6
Continue westward on Highway 89 and turn left onto an unsigned dirt road.	0.6	112.2
Turn left onto another, narrower dirt road	0.1	112.3
Bear left at a fork	0.15	112.45
Turn right via one or two different possible routes into a large bowl with very small trees. Early arrivals should try to dry as far back in the bowl from the entrance point as they can. This is the **SATURDAY NIGHT CAMPING SITE (BUSINESS MEETING SITE)**. Note there is basalt bedrock exposed in the little gullies in this bowl. This is the 400 ka Basalt of Westwood. The steep slope bounding the southwest (upper) side of the bowl is the scarp of the Skinner Flat fault. This fault appears to be dying out to the northwest.	0.15	112.6
Sunday, October 14, 2001	Mileage from late noted point	Cumulative mileage for day
Starting point at exit from camping area onto perimeter dirt road	0.0	0.0
Bear right at fork	0.15	0.15
Turn right onto wide dirt road	0.15	0.3
Turn right (east) onto Highway 89: you will stay on 89 for a long time	0.1	0.4
Entering the Greenville area, we will pass through the town of Greenville. Greenville is situated in Indian Valley, a valley that appears drowned by alluvium as a result of tectonic damming near where Indian Creek flows out of it near its southwest corner. This is one of many tectonically controlled basins along the Mohawk Valley fault zone.	10	10.4
Highway 89 joins Highway 70; turn left and head toward Quincy	11.6	22.0
Entering American Valley, another tectonically controlled basin along the Mohawk Valley fault zone. To the west you can see a bare granite face. This is glaciated escarpment of the Spanish Peak fault, the main strand of the Frontal fault system in this area. The top of the ridge is the crest of the Sierra Nevada and you are viewing the eastern escarpment of the Sierra Nevada. North of American Valley, the Frontal fault system, and the Mohawk Valley fault zone broaden to a distributed zone of deformation some 30-40 km wide, whereas south of American Valley the faulting occupies a narrow zone of about 10 km in width.	8.8	30.8
On the right, at the start of a wide shoulder area, you will see a small	12.5	43.3

hill composed of very dark rock. This is the Lovejoy Basalt, a 16 m.y. old basalt that erupted east of the Honey Lake fault and flowed westward across the Sierra to the western margin of the Central Valley. The eruption of this unit predates movement on the Honey Lake and Mohawk Valley fault zones, and the unit is a good late Cenozoic marker horizon to record deformation, tilting, and rock uplift of the Sierra (see discussion for Stop 10). The Lovejoy Basalt caps ridges on both sides of the Mohawk Valley graben. More information and field trip stops related to the Lovejoy Basalt are found in Wagner et al. (2000; in reference list for introduction). Not long after passing the Lovejoy Basalt exposure the road crosses the curiously low divide between the North Fork and Middle Fork Feather River drainages. We now enter the Middle Fork drainage. We then drive through the little town of Cromberg. Southeast of Cromberg, the route traverses through the gorge that drains Mohawk Valley. Steep, unstable slopes can be seen on both sides of Highway 70. Landslides in this area are one possible mechanism for damming the outlet of Mohawk Valley and raising the level of Lake Beckwourth in Sierra Valley.		
Turn right onto Highway 89	11.3	54.6
We cross over the Middle Fork of the Feather River. The Feather River drainage is unique in that it is the only drainage to cross the entire width of the Sierra Nevada, draining a large area of easternmost California into the Central Valley. For much of the next 3 miles you will be driving across late Quaternary glacial outwash of Gray Eagle and Frazier creeks, two of the largest drainages heading along this part of the Sierran crest.	0.5	55.1
Turn left onto road at Clio (green Clio sign)	3.7	58.8
In 'downtown' Clio, Lower Main street curves 90° and becomes county road A40	0.2	59.0
Turn left onto C road, proceed northward toward railroad tracks	0.4	59.4
Intersection of C Road and railroad tracks. Park on either side of railroad tracks. We'll gather on the southside of the tracks about 100 m east of the crossing with C Road. **STOP 9**	0.3	59.7
return to Highway 89: drive southward on C Road, then turn right onto A40	0.3	60.0
Turn left onto Highway 89. We drive southward on Highway 89, crest over a pass, then eventually descend into Sierra Valley. This part of Sierra Valley is a good location for viewing the shorelines left by the most recent stand of pluvial Lake Beckwourth. Shorelines can be seen to the north along the west side of the valley, and to the east at the base of Hill 5348. Notice that shorelines are not evident from the higher, older lake stand.	0.6	60.6
Join Highway 49, turn left	13.4	74.0
In Sierraville, turn right (southward) onto Highway 89	4.8	78.8

Turn right onto road to Jackson Meadow Reservoir (Forest Road 07)	8.4	87.2
Turn right at an unsigned junction just before crossing dam. After turning you will pass a borrow quarry on your right	16.0	103.2
Keep straight at intersection	2.7	105.9
Keep straight at intersection	1.1	107.0
STOP 10. park at available turnouts on either side of the dirt road	3.4	110.4

STOP 1.

Clifford Riebe[1] and Darryl Granger[2]
[1]*Dept. Earth and Planetary Science, University of California, Berkeley*
[2]*Dept. Earth and Atmospheric Sciences, Purdue University*

Introduction for Stops 1 and 4

Chemical weathering and physical erosion jointly regulate soil development, sculpt landscapes, and deliver sediment and solutes to riverine habitats. Chemical weathering also generates nutrients and helps regulate global climate over million year timescales. Thus it is important to quantify long-term rates of weathering and erosion in different environments. Here we present results of a recent test that shows that cosmogenic nuclide techniques can be used to measure long-term, catchment-wide erosion rates (Stop 4; Granger et al., 1996). We used this technique to measure erosion rates at a series of sites in the Diamond and Fort Sage Mountains, and determined that the exposure of slowly eroding, bare rock plays an important role in granitic landscape evolution (Stops 1 and 4; Granger et al., 2001), much as was originally proposed by Wahrhaftig (1965). We also show how long-term chemical weathering rates can be measured by combining physical erosion rates, inferred from cosmogenic nuclides, with dissolution losses, inferred from the rock-to-soil enrichment of insoluble elements (Stop 4; Riebe et al., 2001b). Using this technique, we measured rates of weathering and erosion at a series of granitic Sierra Nevada study sites that span 20-145 cm/yr in average precipitation and 4-15 C in mean annual temperature (Stop 4). Our results show that both physical erosion and chemical weathering rates are insensitive to differences in climate and that long-term rates of chemical weathering and physical erosion are tightly coupled (Riebe et al., 2001 a&b). This result implies that chemical weathering rates may depend on tectonic uplift rates in many mountainous settings.

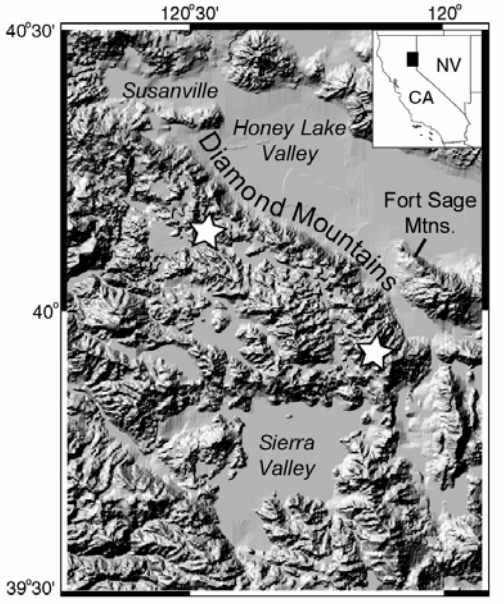

Fig. 1-1. Taken from Granger et al., 2001. Shaded relief map showing Diamond Mtn. study sites. Stars mark Adams Peak to the southeast and Antelope Lake to the northwest. Also shown is the Fort Sage Mtn. site of Granger et al., 1996. The Diamond Mtn. sites are developed in moderately uniform hornblende-biotite granodiorite/tonalite, which is similar to the bedrock of the Fort Sage Mtns (Oldenburg, 1995) Fort Sage sits in the rain shadow and is hotter and drier than the Diamond Mountain Sites.

Description of Stop 1

This is a gently sloped, soil-mantled ridge in the foothills of the Diamond Mountains. Gentler slopes in the area are generally mantled with less boulders and bare rock than their steeper counterparts. A good example of steep, boulder-mantled slopes can be seen on the ridge to the east.

Cosmogenic nuclide measurements from soils and ouctrops two miles North of Stop 1 show that exposed granitic bedrock weathers more slowly than the same rock buried beneath moist soil (Granger et al., 2001). Throughout the area, and at another Diamond Mountains site near Antelope Lake (Fig. 1-1), exposed bedrock and boulders are more abundant on steep slopes (Fig. 1-2) and apparently play an important role in regulating mountain erosion rates (Fig. 1-3). Rapid transport of fine sediment on steep slopes exhumes resistant corestones which accumulate on the surface. The resulting boulder lag apparently shields the underlying bedrock from erosion, even when the bedrock is deeply weathered and friable (Fig. 1-4). Where steep slopes have an abundant boulder lag, they erode as slowly as gentler slopes nearby (Fig. 1-2). On the basis of these observations and counterproof determined at the Fort Sage Mountains (to be discussed at Stop 4), we infer that boulder armoring can modulate hillslope erosion such that erosion rates of summits, steep mountain flanks, and gentle footslopes are indistinguishable, thus permitting local relief and steep mountain slopes to persist for long periods of time.

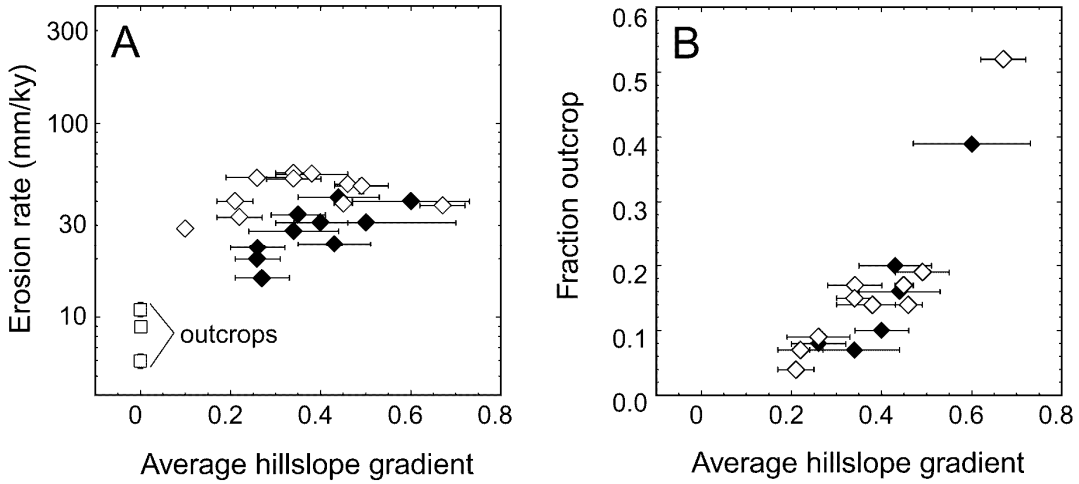

Fig. 1-2. Adapted from Granger et al., 2001. Catchment erosion rates (A) and fraction outcrop (B) plotted against average hillslope gradient for catchments at the Diamond Mountain sites (open diamonds are from Adams Peak, closed diamonds are from Antelope Lake). At both sites at gradients below ~0.4, there is weak correlation between erosion rates and hillslope gradients. More striking is the lack of correlation on steep slopes; for hillslopes with a gradient steeper than 0.45, erosion rates remain constant or even decrease. In contrast, bare rock abundance clearly increases with hillslope gradients. Below gradients of about 0.4, bare rock abundance remains uniformly low, whereas above it, the fraction of boulders and bedrock on the slopes increases rapidly. The steepest slopes are more than half covered with bare rock. The abundance of exposed rock suggests that bare rock weathering may play an important role in this landscape's evolution; it is therefore important to determine bare rock erosion rates. Three samples show that bare rock erosion is significantly slower than catchment averages, at 6-11 mm/ky (labeled "outcrops" in Fig. 2A). Because bare rock erodes more slowly than the catchment average, and because exposed bedrock and boulders comprise an increasing fraction of catchments as they become steeper, we suggest that bare rock exposure retards erosion of steep slopes and limits the range of erosion rate variability.

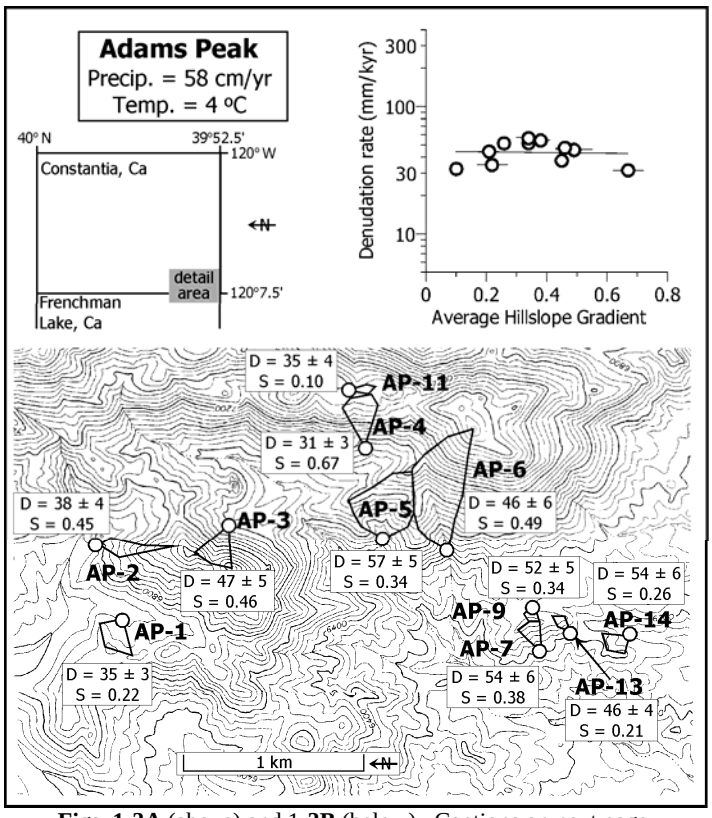

Figs. 1-3A (above) and 1-**3B** (below). Captions on next page.

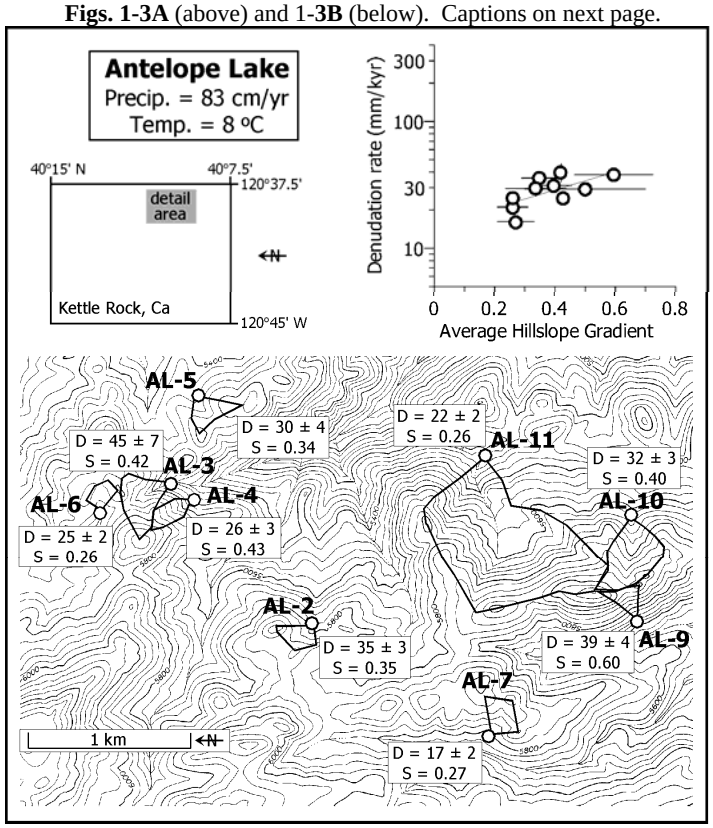

Caption for Fig. 1-3 (on the previous page, adapted from Riebe et al., 2000). Map of Adams Peak (Fig. 1-3A) and Antelope Lake (Fig. 1-3B) showing catchment boundaries, names, denudation rates ("D", equivalent to "Erosion rates" of Fig. 1-2), average hillslope gradients ("S" in m/m), and sampling localities (open circles). Maps are taken from USGS 7.5' topographic quadrangles (shown and named at the top of each panel as index maps). Contour interval = 40 ft. Not all study catchments are shown on the maps. Denudation rates are roughly uniform and are weakly correlated with hillslope gradient at these sites. We suggest that baselevel lowering rates are roughly uniform across each site, and that variations in hillslope gradients are largely controlled by differences in erodibility (as modulated by boulder abundance; see Fig. 1-2).

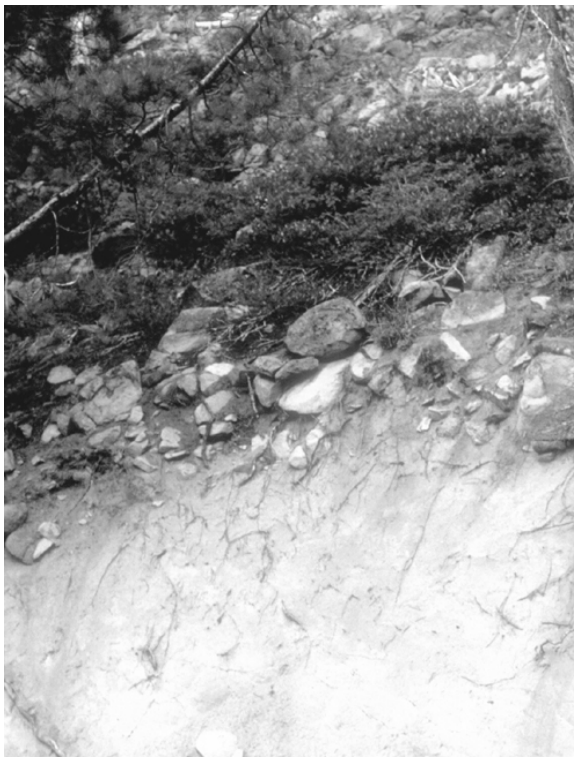

Fig. 1-4. Taken from Granger et al., 2001. Roadcut near Crystal Peak (~15 km northwest of Adams Peak) showing corestone boulders overlying hand-friable saprolite (horizontal field of view is ~5 m). We propose that on steep slopes, prone to rapid sediment transport by rainsplash, sheetwash, and biogenic processes, gruss will be rapidly stripped to expose corestones and bedrock. The exhumed rock will weather much more slowly than the saprolite. Provided that corestones do not roll downhill faster than they are exhumed and that intact bedrock is not exhumed first, a quickly eroding saprolite will accumulate a surface lag of boulders that will shield the underlying saprolite and interrupt rill development during rainstorms. Saprolite beneath such a boulder cover will continue to weather in place, but grussification and sediment transport will be strongly inhibited by the boulder cover. Exposure of slowly weathering boulders and bedrock provides a negative feedback that can modulate hillslope erosion rates. The faster saprolite is stripped, the more corestones and bedrock will be exhumed to slow the erosion.

References

Granger, D. E., J. W. Kirchner, and R. Finkel, Spatially averaged long-term erosion rates measured from in situ-produced cosmogenic nuclides in alluvial sediment, *Journal of Geology*, **104**, 249 (1996).

Granger, D.E., C. S. Riebe, J. W. Kirchner, and R. C. Finkel, Modulation of erosion on steep granitic slopes by boulder armoring, as revealed by cosmogenic ^{26}Al and ^{10}Be, *Earth and Planetary Science Letters* **186**, 269 (2001).

Oldenburg, E. A., Chemical and petrologic comparison of Cretaceous plutonic rocks from the Diamond Mountains, Fort Sage Mountains and Yuba Pass region of northeastern California, (M. S. Thesis, Humboldt State University, Humboldt, California, 1995) 99 p.

Riebe, C. S., J. W. Kirchner, D. E. Granger, and R. C. Finkel, Erosional equilibrium and disequilibrium in the Sierra Nevada, inferred from cosmogenic ^{26}Al and ^{10}Be in alluvial sediment, *Geology*, **28**, 803 (2000).

Riebe, C. S., J. W. Kirchner, D. E. Granger, and R. C. Finkel, Minimal climatic control of erosion rates in the Sierra Nevada, California, *Geology* **29**, 447 (2001a).

Riebe, C. S., J. W. Kirchner, D. E. Granger, and R. C. Finkel, Strong tectonic and weak climatic control of long-term chemical weathering rates, *Geology* **29**, 511 (2001b).

Wahrhaftig, C., Stepped topography of the southern Sierra Nevada, California, *Geological Society of America, Bulletin* **76**, 1165 (1965).

STOP 2.

Alan Ramelli[1] and Ken Adams[2]
[1]*Nevada Bureau of Mines and Geology, Reno, Nevada, ramelli@unr.edu*
[2]*Desert Research Institute, Reno, Nevada, kadams@dri.edu*

Spillover Point of Pluvial Lake Beckwourth into the Lahontan Basin, Railroad Tunnel Portal on East Side of Beckwourth Pass.

This stop looks at evidence that a mid-Quaternary pluvial lake in Sierra Valley (Lake Beckwourth) overtopped Beckwourth Pass at least once, spilling into Long Valley Creek and thence into the Lake Lahontan basin (fig. 2-1). This probably short-lived spillover has important biogeographic implications, because it likely transferred fish and other aquatic species from the Feather River, which flows to the Pacific Ocean, into the Lahontan system of the Great Basin.

Fig. 2-1. During the Middle Pleistocene, a pluvial lake/marsh system existed in Sierra and Mohawk Valleys. At least once, the lake in Sierra Valley (Lake Beckwourth) rose and overtopped Beckwourth Pass, spilling into the Lahontan basin and causing an exchange of aquatic species.

The existence of a Pleistocene lake in Sierra Valley is indicated by wave-cut platforms, spits, tombolos, rounded beach gravels, and sparsely exposed lake-bed sediments. This pluvial lake was briefly discussed by Van Couvering (1962), who named it Lake Beckwourth, and Durrell (1987), but no one has looked at it in detail. Our reconnaissance studies (Ramelli and Adams, 1999) add something to the picture, but much remains to be done, including surveying of shorelines, establishing better age constraints, and gaining a better understanding of outlet control.

Most recent stand of Lake Beckwourth

The most recent stand of Lake Beckwourth (fig. 2-2) is indicated by moderately preserved shoreline features at and below an elevation of about 1,540 m (5,050 ft). The best preserved of these include: 1) wave-cut benches on the west side of the valley about 10 km (6 mi) south of Beckwourth; 2) wave-cut benches and a tombolo around “Hill 5348" on the south side of Hwy 49 about 7 km (4 mi) west of Loyalton; and 3) broad spits on the east and west sides of “The Buttes” on the north side of Hwy 70 about 10 km (6 mi) west of Vinton. We haven’t surveyed the elevations of these features, but the crest of the tombolo on the back side of Hill 5348 is very close to the high shoreline, providing a close approximation of the high stand.

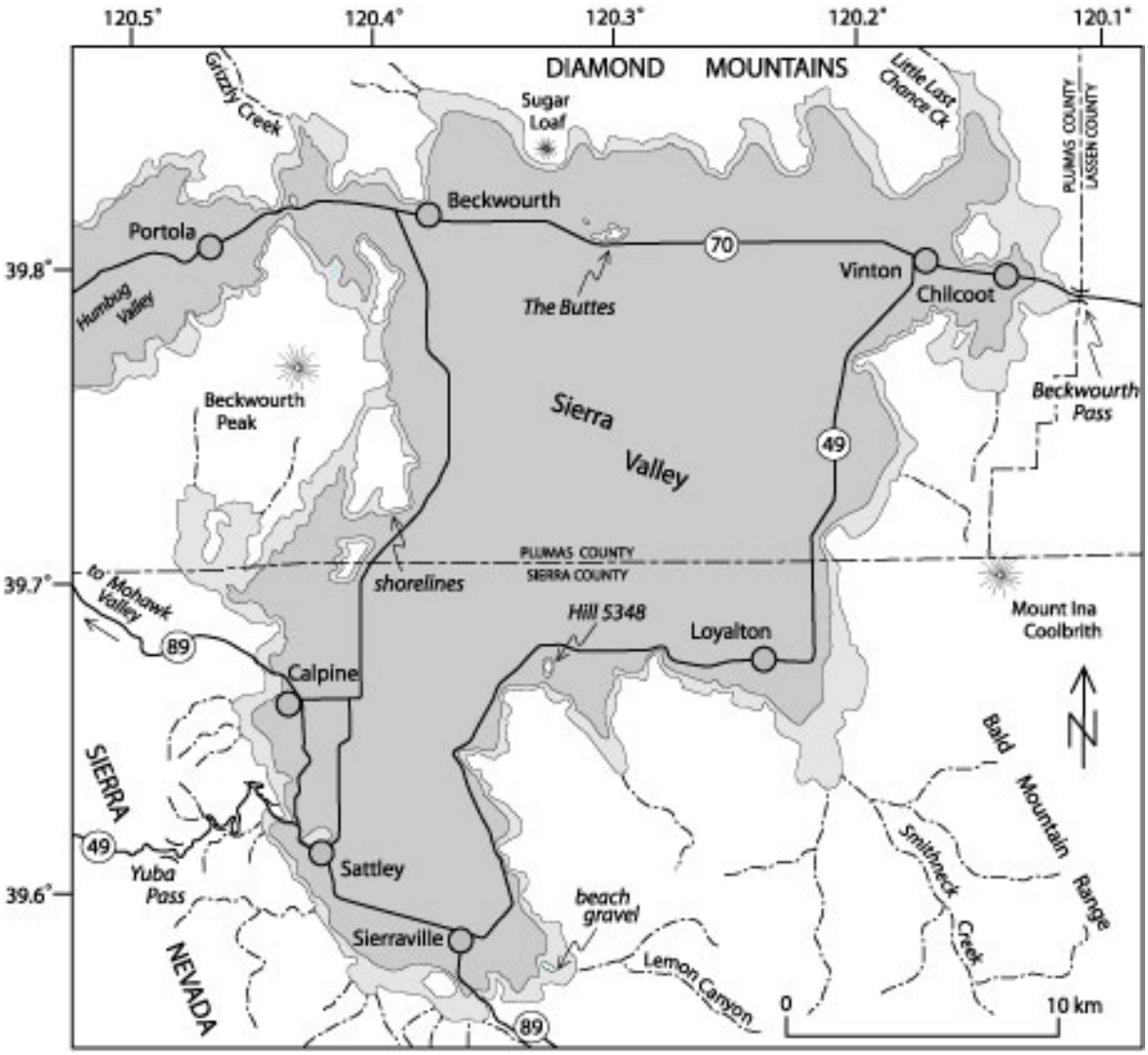

Fig. 2-2. Approximate outlines of two stands of pluvial Lake Beckwourth. The most recent stand (dark shading) reached an elevation of about 1,540 m (est. age about 150 ka). An earlier stand (light shading) reached an elevation of about 1,585 m (est. age greater than 300ka).

Durrell (1987) estimated the maximum elevation of the “Mohawk lake beds” in Mohawk Valley to be about 1,535 m (5,040 ft). This is very similar to the elevation of Lake Beckwourth and suggests the two basins were connected at that time. Durrell (1987) incorrectly interpreted the elevation of Lake Beckwourth to be 1,555 m (5,100 ft), and inferred that a fast-flowing stream connected the two basins. Work by Jim Yount (presented on the 1995 Pacific Cell FOP trip) showed that the Mohawk beds were

actually deposited within a marsh environment, rather than being lacustrine in origin as interpreted by Turner (1891), Mathieson (1981), and Durrell (1987). When this marsh existed, Mohawk Valley was drained at its western end by Poplar Creek, on the south side of Big Hill (see Durrell (1987) for a detailed discussion of the Poplar Creek outlet). The Feather River subsequently downcut through highly erodable materials on the north side of Big Hill, establishing a new outlet. Yount (1995) found several tephra layers within the Mohawk beds ranging in age from ~400 ka (Rockland ash) to about 150 ka, after which time the basin apparently became drained due to incision of the Feather River. We infer that this incision resulted in the death of Lake Beckwourth.

Older, higher stand of Lake Beckwourth

In several locations around Sierra Valley, poorly preserved features (e.g., wave-cut benches, tombolos, beach gravels, etc.) are located at elevations up to about 1,585 m (5,200 ft) indicating a higher stand of Lake Beckwourth. The most convincing evidence of this higher stand that we have found so far are rounded beach gravels present on the backside of a small hill to the south of Lemon Canyon Road about 3 km (2 mi) east of Sierraville. The geomorphic indicators of this higher lake stand are much more degraded than those of the most recent stand, indicating an age of substantially greater than 150 ka. Based on the poor preservation of shoreline features, we tentatively estimate the age of this stand to be at least 300 ka, and possibly much greater. Similar to the more recent stand, this high stand also appears to coincide with the maximum elevation of older deposits in Mohawk Valley (Yount, 1995).

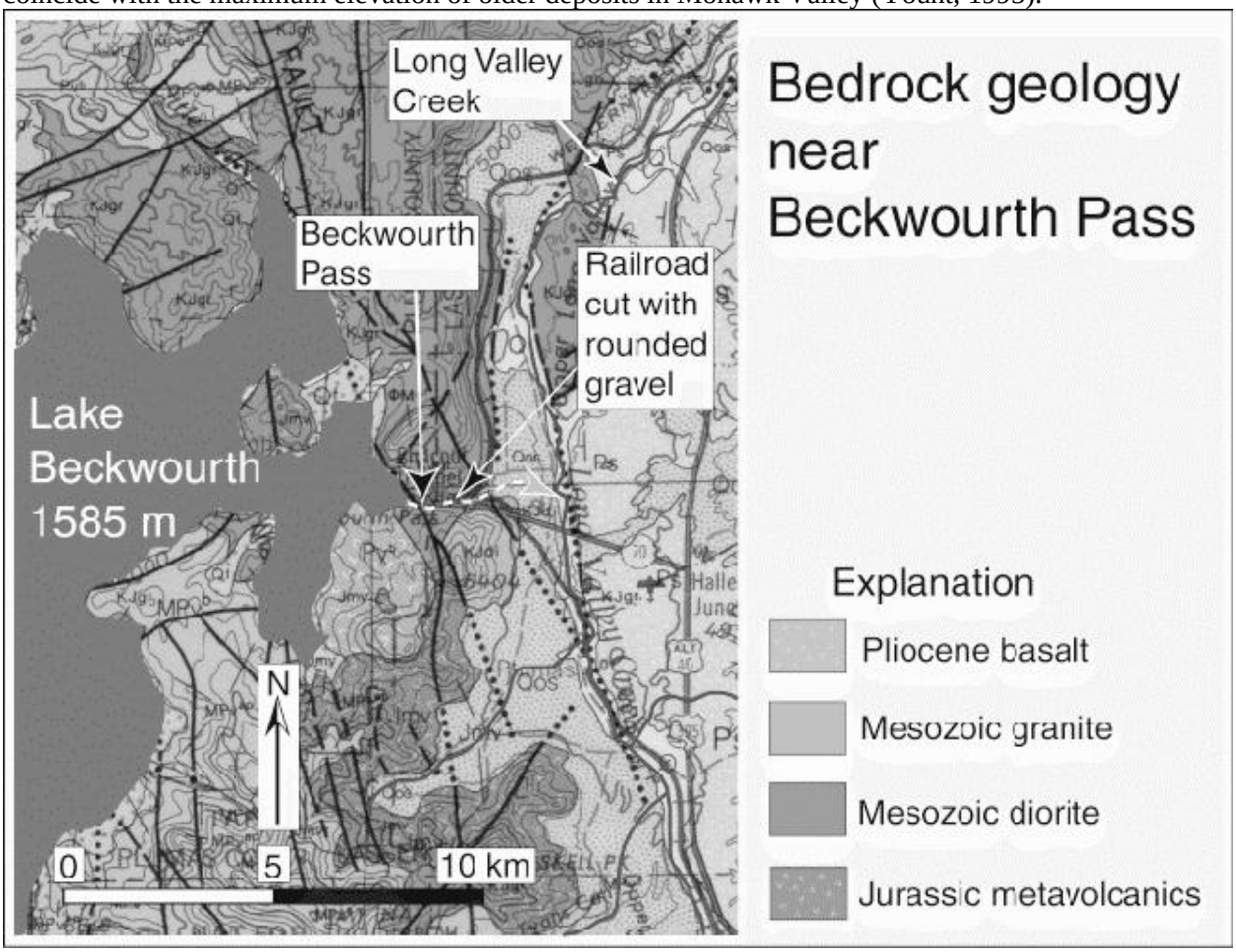

Fig. 2-3. Geologic map of the Beckwourth Pass area. The eastern portal of the railroad tunnel exposes evidence of a Middle Pleistocene spillover of pluvial Lake Beckwourth. Rounded volcanic clasts must have been derived from the west side of the pass.

At an elevation of 1,585 m (5,200 ft), Lake Beckwourth was very close to the 1,590 m (5,220 ft) elevation of Beckwourth Pass. This raised the question of whether the lake ever overtopped Beckwourth Pass, thus spilling into Long Valley and thence into the Lake Lahontan basin, rather than always spilling down the Feather River, which drains to the Pacific Ocean. The alluvial fan on the east side of the pass seems underfit in that it's quite large relative to the area it drains, lending credence to this possibility.

The eastern portal of the railroad tunnel through Beckwourth Pass (STOP 2) exposes fluvial deposits and a gravel lag on granitic bedrock. The gravel lag contains some rounded volcanic clasts that must have been derived from west of the pass, because only granitic and metamorphic rocks are present in the contemporary drainage area (fig. 2-3). The high degree of rounding provides further evidence that these were Lake Beckwourth beach gravels. Rounded volcanic clasts are also sparsely scattered on the surface in the area around the pass. We have found rounded clasts slightly above the pass, indicating the spillover caused at least some downcutting.

Discussion/Speculations

Lacking an outlet, pluvial lakes of the Great Basin (e.g., Lake Lahontan) fluctuate in response to changes in climate. Lake Beckwourth, on the other hand, was likely more controlled by its outlet history, and may not have coincided in time with pluvial lakes of the Great Basin. Similar to Lake Tahoe, Sierra Valley receives considerably more precipitation than does most of the Great Basin, especially along the Sierran front on the southwest side of the valley. Lake Beckwourth likely had a more sustained life, existing during all but the most extreme dry periods.

Shoreline features around Sierra Valley occur at fairly consistent elevations, seemingly precluding large-scale vertical tectonic changes over the time since Lake Beckwourth existed. To the contrary, much of Mohawk Valley may have been relatively downdropped by as much as 60 m (200 ft) over this period of time. This may indicate that late Quaternary tectonic activity has been concentrated along the Mohawk Valley fault system.

Inferred history of Lake Beckwourth

1) Late Tertiary (Plio-Pleistocene?) faulting created structural basins (Sierra, Humbug, and Mohawk Valleys) that received enough runoff that they filled to their respective spillover points, with Sierra Valley spilling into Humbug Valley, Humbug Valley spilling into Mohawk Valley, and Mohawk Valley in turn spilling down the west slope of the Sierra Nevada;

2) Through a combination of incision of the Sierra Valley outlet and sedimentation in Humbug and Mohawk Valleys, the basins became interconnected by a narrow gorge;

3) During the Middle Pleistocene, the lake in Mohawk and Sierra Valleys stabilized at an elevation of about 1,585 m (5,200 ft) for a period long enough to form features that persist until today;

4) The level of Lake Beckwourth then rose -- probably due to some sort of damming mechanism (possibly by a landslide, or possibly by glaciers from the Lakes Basin area extending across Mohawk Valley) -- until it overtopped Beckwourth Pass (>1590 m), thus spilling into the Lahontan Basin and causing an exchange of aquatic species;

5) Some incision of Beckwourth Pass occurred, but the outlet at the west end of Mohawk Valley soon reestablished...this time flowing down Poplar Creek;

6) The Poplar Creek outlet incised to about 1,540 m (5,050 ft) and then stabilized. For an unknown period of time, Lake Beckwourth occupied its most recent stand, with its outlet buffered by a marsh in Humbug and Mohawk Valleys;

7) Headward erosion of the Feather River then chewed through more easily eroded material on the north side of Big Hill, establishing a new outlet that drained Mohawk Valley and resulted in the death of Lake Beckwourth.

References

Durrell, Cordell, 1987, Geologic History of the Feather River Country, California; University of California Press, Berkeley, California

Mathieson, S.A., 1981, Pre- and post-Sangamon glacial history of a portion of Sierra and Plumas Counties, California; unpub. M.S. thesis, California State Univ., Hayward, 258 p.

Ramelli, A.R., and Adams, K.D., 1999, Probable short-lived middle Pleistocene spillover from pluvial Lake Beckwourth (Feather River/Pacific drainage system) into the Lake Lahontan basin: implications for biogeography: Geological Society of America Abstracts with Program, v. 31.

Turner, H.W., 1891, Mohawk Lake Beds, Plumas County, California; Philosophical Society of Washington Bulletin, v. 11, p. 385-409.

Van Couvering, J.A., 1962, Geology of the Chilcoot quadrangle, Plumas and Lassen Counties, California; unpub. M.A. thesis, Univ. of California, Los Angeles, 124 p.

Yount, James C., 1995, Mohawk beds in Plumas trough at Mohawk; in Quaternary Geology along the Boundary between the Modoc Plateau, Southern Cascade Mountains, and northern Sierra Nevada, W. Page ed., Friends of the Pleistocene 1995 Pacific Cell field trip.

STOP 3.

Chris Wills, California Division of Mines and Geology, San Francisco CA 94107, cwills@consrv.ca.gov

We have driven down from Beckwourth Pass into the Honey Lake basin, passing below the shoreline of Lake Lahontan. Because we are on the lake bed, we can be sure all of the landscape features around us (channels, terraces, fault scarps, etc.) post-date the lake. That is: we are looking at an almost exclusively Holocene landscape.

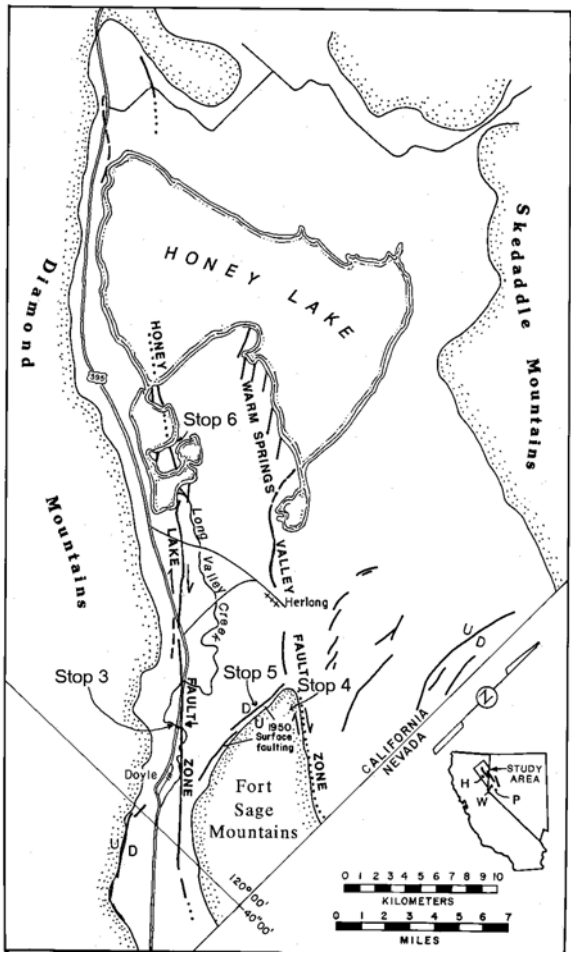

Fig. 3-1. Map of the Honey Lake basin showing major faults and stops for the 2001 FOP field trip. Modified from Wills and Borchardt (1993).

The features we are here to see are the Honey Lake fault zone and the channel and deposits of Long Valley Creek. At this site Wills and Borchardt (1993) used the right-lateral offset of the channel margin to calculate a slip rate of about 2 mm/yr. They logged the stream bank, cut in Holocene deposits in the inset terrace, and concluded that there had been at least 4 major ground rupturing earthquakes in the past 8000 years.

There have been extensive changes to this site since Wills and Borchardt did their work in 1989 and 1990. Most importantly, floods in 1998 filled much of the incised channel of Long Valley Creek and eroded the bank. According to Cindy Judd, who owns the property, the flood eroded up to 15 feet of the inset terrace. This means two things: 1) the stream bank logged by Wills and Borchardt is gone, and 2) the current exposure, which is steeper and possibly slightly higher has never been logged. Your intrepid field trip leaders spent almost an hour poking at the current exposure, enough to convince them that strands of the Honey Lake fault zone can still be observed cutting the Holocene sediments.

At this stop, then, one can observe a near-vertical 3+ meter high stream bank exposure of well-bedded Holocene sediments. The Mazama ash (Tsoyawata ash of J.O. Davis) is about a meter above the level of the creek bed. Many layers in the exposure are irregular and lens shaped, and show quite a bit of cross-bedding. We found one fault strand that appeared to cut layers up to near the surface, but did not have the time to clean or log much of the exposure.

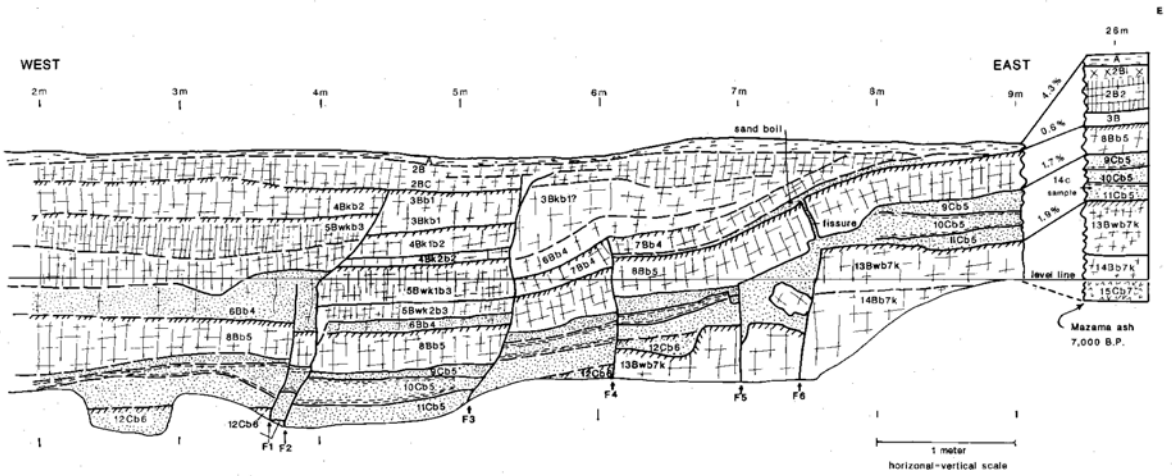

Fig. 3-2. Log of the bank of Long Valley Creek as it appeared in 1990. Note that Mazama ash was not observed in the fault zone itself, but several strands of the fault were logged cutting to different levels within the Holocene sediments. From Wills and Borchardt (1993)

The new exposures of the Holocene sediments in the channel of Long Valley Creek are similar to those described by Wills and Borchardt (1993), but it is not known if the current exposures would show evidence for more, or fewer, earthquakes or if additional datable material could constrain the ages of paleo-earthquakes. FOPers are encouraged to help scrape some of the slough off of the exposure and see how many strands of the fault can be observed, and how far up through the Holocene sediments they extend.

The second part of the Honey Lake fault story at this stop is the right-lateral offset of the top of the riser between the inset terrace and the surrounding lake bed. This has not changed since it was described by Wills and Borchardt, but is worth walking out. Briefly, this offset results in a slip rate because the top of the terrace riser can be traced on both sides of the fault and 16 m offset can be measured. The age of the terrace river must be younger than Lake Lahontan (it represents a channel cut into the floor of the lake). This riser was an active channel margin at least until the inset terrace material was deposited, protecting the riser from further erosion. Mazama ash in the inset terrace deposits was used to constrain the date of those deposits. If the inset terrace deposits, with Mazama Ash at the base, represent a relatively passive filling of the old channel, then the deposition of the inset terrace marks the abandonment of the old channel margin. The result is a feature with an age of between 8 and 14 ka is offset 16±2 m, giving a slip rate between 1.1 and 2.6 m, rounded to 2.0 mm/yr.

(**Fig. 3-3** on next page)

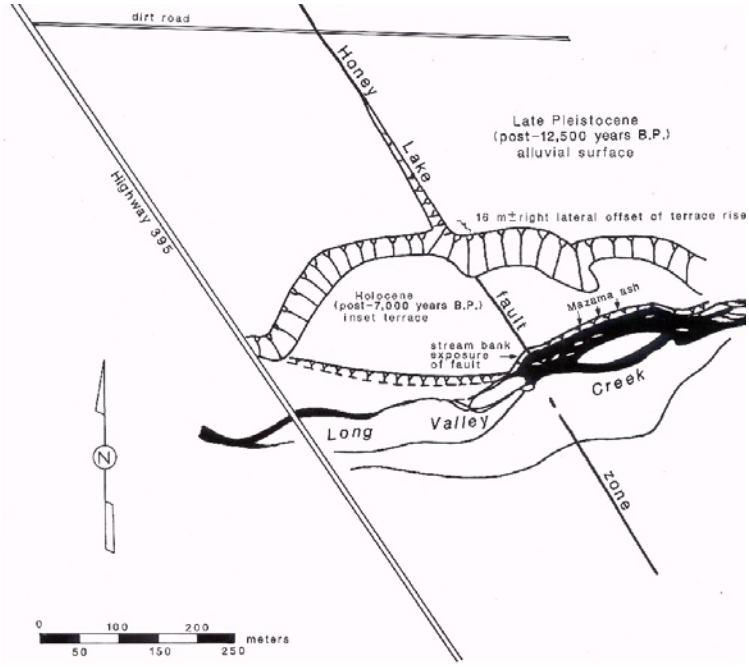

Fig. 3-3. Sketch map of Stop 3 showing inset terrace and offset of terrace riser from which Wills and Borchardt derived a slip rate estimate of 2 mm/yr. From Wills and Borchardt (1993)

Stop 4.

Clifford Riebe[1] and Darryl Granger[2]
[1]*Dept. Earth and Planetary Science, University of California, Berkeley*
[2]*Dept. Earth and Atmospheric Sciences, Purdue University*

Description of Stop 4 (Also see the introduction under Stop 1 for an overview.)

This is a flat-topped ridge on the fault scarp of the northeastern Fort Sage Mountains. The watersheds on either side of this ridge were the subject of the erosion rate study of Granger et al. (1996). Alluvial fans at the mouths of these catchments have been collecting their erosional debris since Lake Lahontan retreated from the scarp base, 16,000 years ago (Benson, 1993). The fan boundaries could once be distinguished by differences in vegetation (see Fig. 4-2), but the vegetation was consumed in a recent fire, and the fans are no longer obvious from this overlook. In the catchments, steeper slopes expose only slightly more boulders and bare rock than their gentler counterparts, in contrast to what was seen at Stop 1, where the steeper slopes are much more densely mantled by boulders and bare rock.

Cosmogenic nuclide measurements have come into wide use as chronometers for surface exposure and processes. It has been proposed that streams may mix eroding sediment such that the average cosmogenic nuclide concentrations in stream sediment samples should reflect the long-term erosion rates of the sediment contributing areas (Fig. 4-1; Brown et al., 1995; Bierman and Steig, 1996; Granger et al., 1996). The two Fort Sage Mountains catchments visible from Stop 4 provide an ideal setting for testing whether cosmogenic nuclides in sediment can be used to measure basin-wide erosion rates, because erosion rates inferred from cosmogenic nuclides can be compared with erosion rates recorded by accumulation in the alluvial fans (Fig. 4-2, after Granger et al., 1996). For both catchments, the two different techniques for measuring erosion rates are averaged over similar timescales and agree to within 30% (Table 4-1, after Granger et al., 1996).

Erosion rates at Fort Sage have a strong dependence on hillslope gradient, increasing exponentially with gradients up to 0.63, and with proximity to the fault scarp face, which is apparently a source of locally rapid baselevel forcing (Fig. 4-3). These results lie in stark contrast to the relatively uniform erosion rates of the Diamond Mountains over an even broader range of hillslope gradients. This disparity may be explained by the lack of boulder armoring at the Fort Sage study area. Boulder abundance at both of the Fort Sage catchments is uniformly low, never exceeding 20% even on steep slopes (Fig. 4-4; Granger et al., 2001). The Fort Sage Mountains, then, provide a counterproof to the boulder-armoring hypothesis by showing that steep slopes in the absence of boulder cover erode much more rapidly than gentle slopes in a granitic bedrock very similar to that of the Diamond Mountains.

We have also developed a new technique for measuring long-term chemical weathering rates, based on cosmogenic nuclide measurements and geochemical mass balance (Riebe et al., 2001b). The technique requires that, in addition to measuring cosmogenic erosion rates, we also have to measure representative concentrations of immobile elements in catchment rock and soil (Fig. 4-5). We did so across the subcatchments of Fort Sage watershed A (Fig. 4-6). Chemical depletions (which reflect the degree to which insoluble elements are enriched in catchment soils) are roughly uniform across the wide range of denudation rates at Fort Sage, while rates of chemical weathering and total denudation are tightly correlated, possibly because chemical weathering rates are regulated by rates of fresh mineral supply by physical erosion of rock (Fig. 4-7). This result implies that tectonic uplift rates may regulate chemical weathering rates.

We also used cosmogenic nuclides to measure long-term rates of erosion and weathering at five other Sierra Nevada granitic sites, including the two Diamond Mountain sites (Riebe et al., 2001b; Fig. 4-8; Table 4-2). Our sites span 22-145 cm/yr in average precipitation and 4-15 C in mean annual temperature. At our Fall River site (northern Sierra foothills), as is the case at Fort Sage, chemical

depletions are roughly uniform across a wide range of denudation rates, while rates of chemical weathering and total denudation are tightly correlated (Fig. 4-9). Note that Fall River is much wetter than Fort Sage, yet chemical depletions and the ranges of chemical weathering and denudation rates are very similar at the two sites (compare Figs. 4-7 and 4-9). The results shown in Fig. 4-9 lend further support to the notion that chemical weathering rates are regulated by rates of fresh mineral supply by physical erosion of rock. These results also strengthen the argument for strong tectonic control of chemical weathering rates. Across the suite of Sierra Nevada sites, differences in chemical weathering rates are strongly associated with differences in denudation rates across each individual site, and obscure any clear correlation of chemical weathering with average precipitation or temperature (Fig. 4-10). This implies that chemical weathering rates are more tightly coupled to erosion rates than they are to climate, at least across these sites.

References:

Benson, L., Factors affecting ^{14}C ages of lacustrine carbonates: Timing and duration of the last highstand Lake in the Lahontan Basin, *Quaternary Research*, **39**, 163 (1993).

Bierman, P., and E. J. Steig, Estimating rates of denudation using cosmogenic isotope abundances in sediment, *Earth Surface Processes and Landforms*, **21**, 125 (1996).

Brown, E. T., R. F. Stallard, M. C. Larsen, G. M. Raisbeck, and F. Yiou, Denudation rates determined from the accumulation of in situ-produced ^{10}Be in the Luquillo Experimental Forest, Puerto Rico, *Earth and Planetary Science Letters*, **129**, 193 (1995).

Granger, D. E., *Landscape erosion and river downcutting rates from cosmogenic nuclides in sediment* (Ph.D. Thesis, University of California, Berkeley, 1996) 118 p.

Granger, D. E., J. W. Kirchner, and R. Finkel, Spatially averaged long-term erosion rates measured from in situ-produced cosmogenic nuclides in alluvial sediment, *Journal of Geology*, **104**, 249 (1996).

Granger, D.E., C. S. Riebe, J. W. Kirchner, and R. C. Finkel, Modulation of erosion on steep granitic slopes by boulder armoring, as revealed by cosmogenic ^{26}Al and ^{10}Be, *Earth and Planetary Science Letters* **186**, 269 (2001).

Riebe, C. S., J. W. Kirchner, D. E. Granger, and R. C. Finkel, Erosional equilibrium and disequilibrium in the Sierra Nevada, inferred from cosmogenic ^{26}Al and ^{10}Be in alluvial sediment, *Geology*, **28**, 803 (2000).

Riebe, C. S., Tectonic and climatic control of physical erosion rates and chemical weathering rates in the Sierra Nevada, California, inferred from cosmogenic nuclides and geochemical mass balance (Ph.D. Thesis. University of California, Berkeley, 2000) 212 p.

Riebe, C. S., J. W. Kirchner, D. E. Granger, and R. C. Finkel, Strong tectonic and weak climatic control of long-term chemical weathering rates, *Geology* **29**, 511 (2001b).

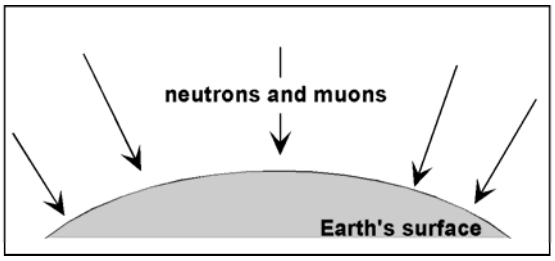

Cosmic rays bathe the earth's surface...

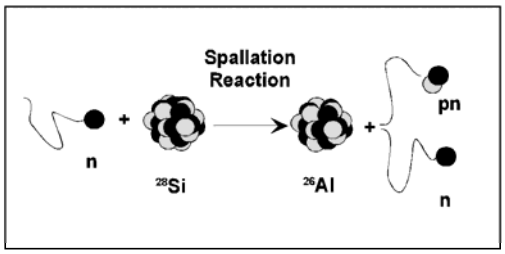

creating the cosmogenic nuclides ^{26}Al and ^{10}Be in quartz mineral grains

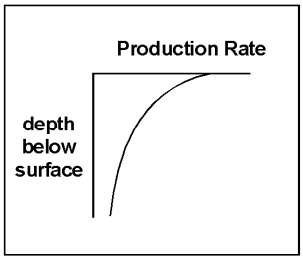

The cosmic ray flux declines rapidly as it passes through matter...

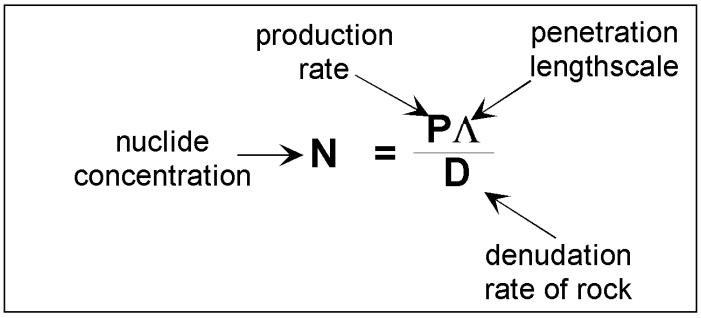

permitting us to model nuclide accumulation as a function of the steady exhumation rate of mineral grains.

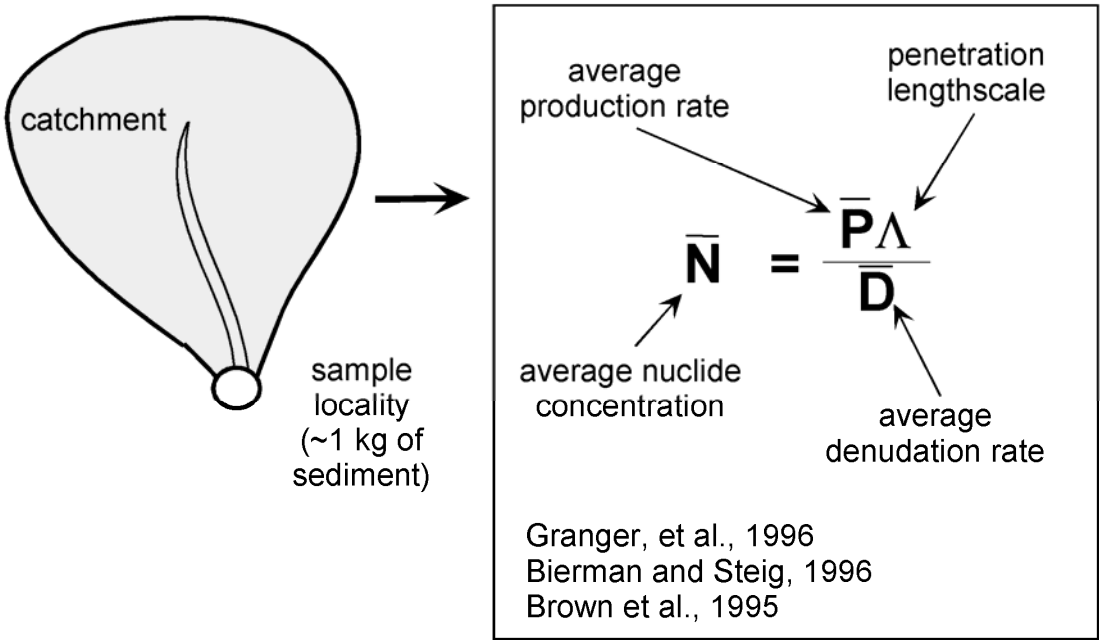

Fig. 4-1.

Fig. 4-2. Taken from Granger et al., 1996. Oblique aerial photo of the Fort Sage Mountains fault scarp, showing catchment boundaries (solid lines), subcatchment boundaries (dotted lines) and alluvial fan thickness contours (in m, from depths to beach sands below). The fans have accumulated each catchment's erosional debris since Lake Lahontan retreated from the scarp base ~16 ky ago. Thus the fans record long-term erosion rates of the contributing areas.

Table 4-1. Comparison of cosmogenic- and fan-based denudation rates. Adapted from Granger et al., 1996. The two techniques average denudation over similar timescales, so the agreement between the cosmogenic- and fan-based estimates within each catchment indicates that the cosmogenic nuclide method can be used to accurately measure long-term, catchment-wide denudation rates. Moreover, the denudation rates of the two catchments are notably different from one another, indicating that the cosmogenic nuclide technique can be used to quantify how denudation rates vary across landscapes.

	Catchment A	**Catchment B**
Fan volume (10^3 m^3)	188±34	310±52
Volume of eroded rock (10^3 m^3)[a]	111±29	178±45
Total volume of rock removed by denudation (10^3 m^3)[b]	133±43	212±67
Contributing area (10^3 m^2)[c]	132±20	408±12
Denudation rate from fan volume (mm/kyr)[d]	**63±19**	**33±9**
Denudation rate from cosmogenic nuclides (mm/kyr)	**70±8**	**44±5**

[a] To obtain volume of eroded rock, fan volumes were corrected for bulk density change from bedrock (2.7 g/cm^3) to soil (1.6±0.3 g/cm^3).
[b] To obtain total volume of eroded rock removed by denudation, I use equations reported in Riebe (2000) with the zirconium enrichment factor of catchment A (1.18±0.03) to adjust the volumes of both fans. Because post-depositional weathering and erosion of the fan itself cannot be ruled out, the weathering losses, and thus fan-based denudation rates, are minimum estimates.
[c] Contributing areas are as reported by Granger (1996).
[d] Fan age is 16.0±0.4 kyr (Granger, 1996, after radiocarbon dates for Lake Lahonton retreat reported by Benson, 1993).

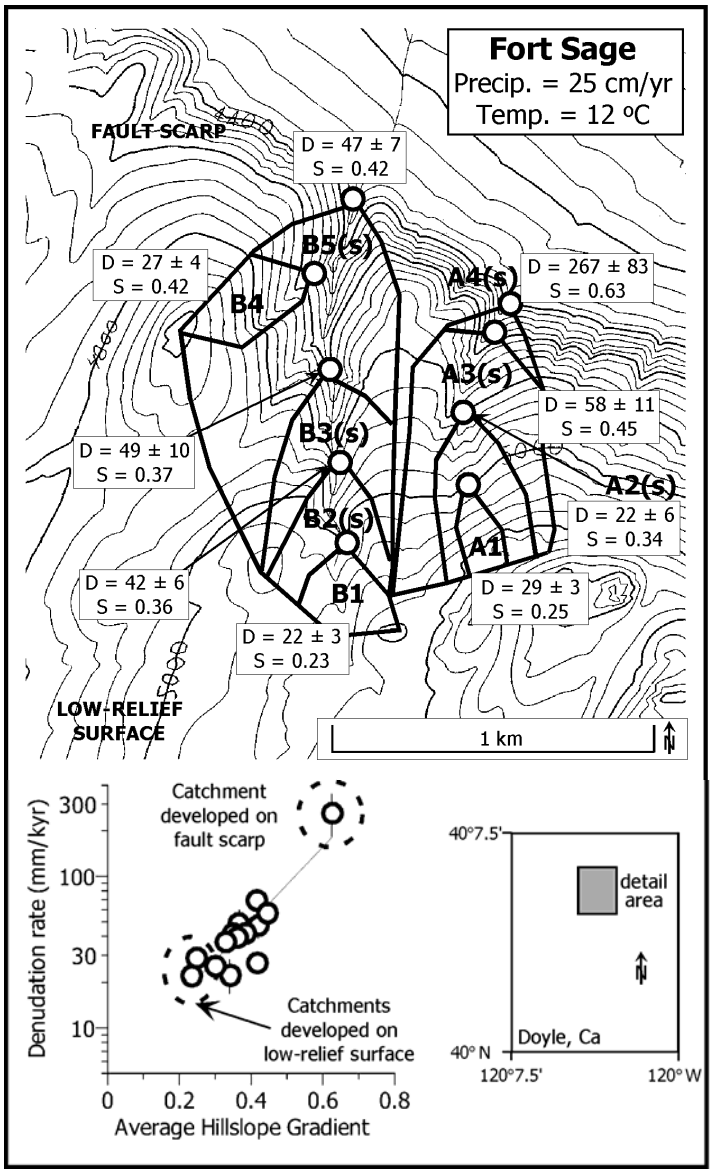

Fig. 4-3. Adapted from Riebe et al., 2000. Map of Fort Sage showing catchment boundaries, names, denudation rates ("D", equivalent to "Erosion rates" of Fig. 2), average hillslope gradients ("S" in m/m), and sampling localities (open circles). The map is excerpted from the USGS 7.5' topographic quadrangle Doyle, CA (shown as an index in the panel corner). Contour interval = 40 ft. Denudation rates increase with hillslope gradients and proximity to the fault scarp face, which is apparently a source of locally rapid baselevel forcing.

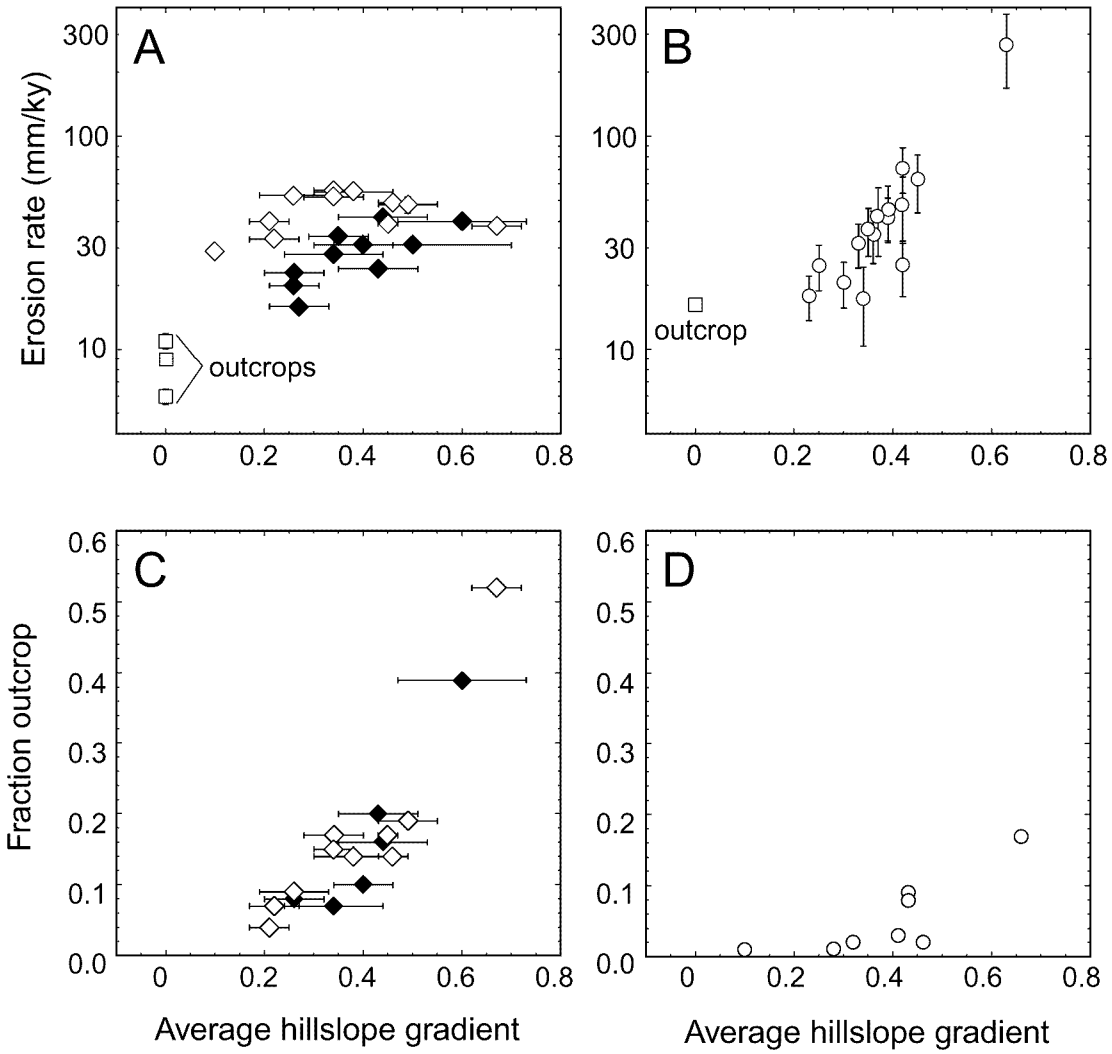

Fig. 4-4. Taken from Granger et al., 2001. Catchment erosion rates (A and C) and fraction outcrop (B and D) plotted against average hillslope gradient for catchments at the Diamond Mountain sites (A and C, with open diamonds from Adams Peak and closed diamonds from Antelope Lake) and at Fort Sage (B and D open circles). Erosion rates at Fort Sage have a strong dependence on hillslope gradient, increasing exponentially at gradients up to 0.63. These results lie in stark contrast to the relatively uniform erosion rates of the Diamond Mountains over an even broader range of hillslope gradients. This disparity may be explained by the lack of boulder armoring at the Fort Sage study area. Boulder abundance at both of the Fort Sage catchments remains uniformly low, never exceeding 20% even on steep slopes. The Fort Sage Mountains, then, provide a counterproof to the boulder-armoring hypothesis by showing that steep slopes in the absence of boulder cover erode much more rapidly than gentle slopes in a granitic bedrock very similar to that of the Diamond Mountains.

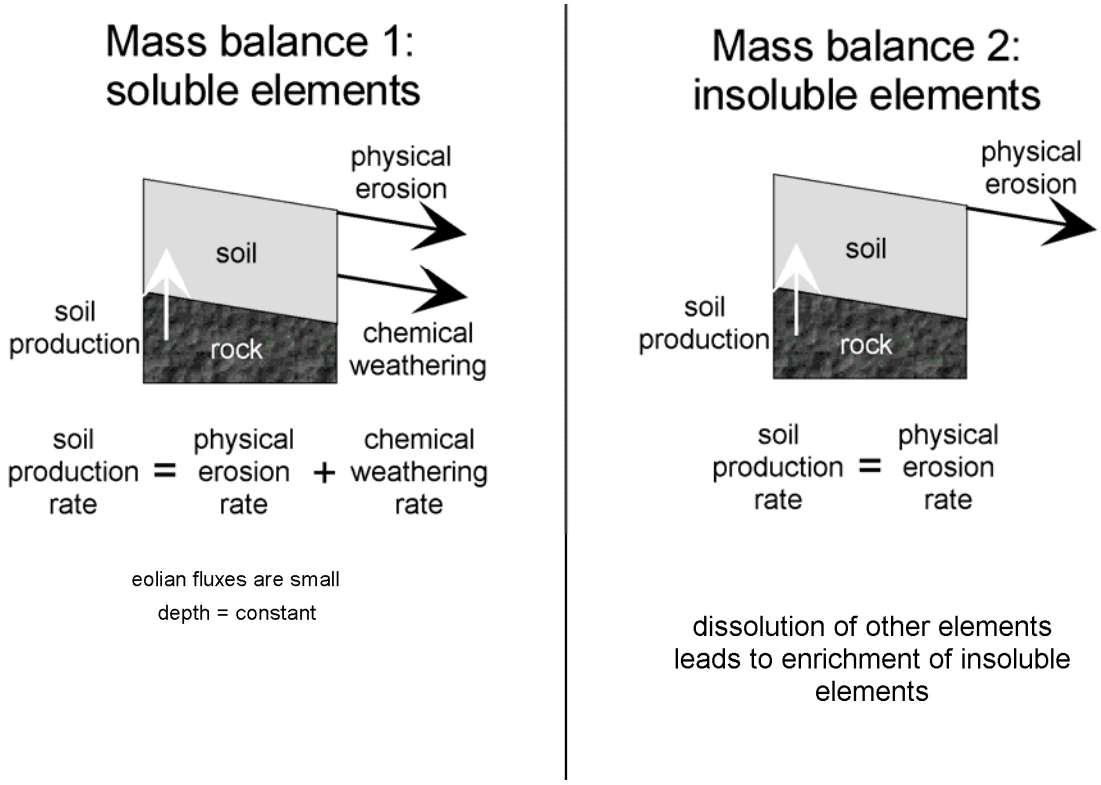

$$\text{chemical weathering rate} = \text{total denudation rate} \times \text{chemical depletion fraction}$$

$$W = \rho_{rock} \times D \times C$$

and

$$C = 1 - \frac{Zr_{rock}}{Zr_{soil}}$$

To estimate long-term chemical weathering rates for our catchments all we need are:

1) cosmogenic estimates of denudation rates
2) representative [Zr] from rock and soil

Fig. 4-5. Measuring long-term chemical weathering rates from cosmogenic nuclides and geochemical mass balance.

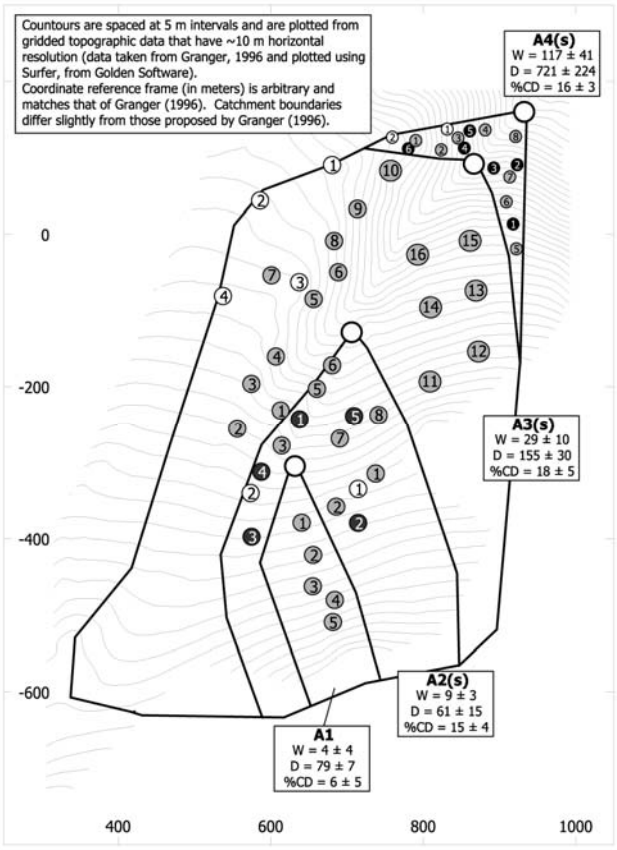

Fig. 4-6. Taken from Riebe 2000. Map of Fort Sage catchment A showing locations of soil pit (black circles), soil surface (gray circles), and bedrock (open circles) samples. These samples were analyzed for major and trace element concentrations by XRF. Large open circles are cosmogenic nuclide sampling localities. Labels include chemical weathering rates "W" in t km^{-2} yr^{-1}, denudation rates "D" in t km^{-2} yr^{-1}, and percent chemical depletion "%CD".

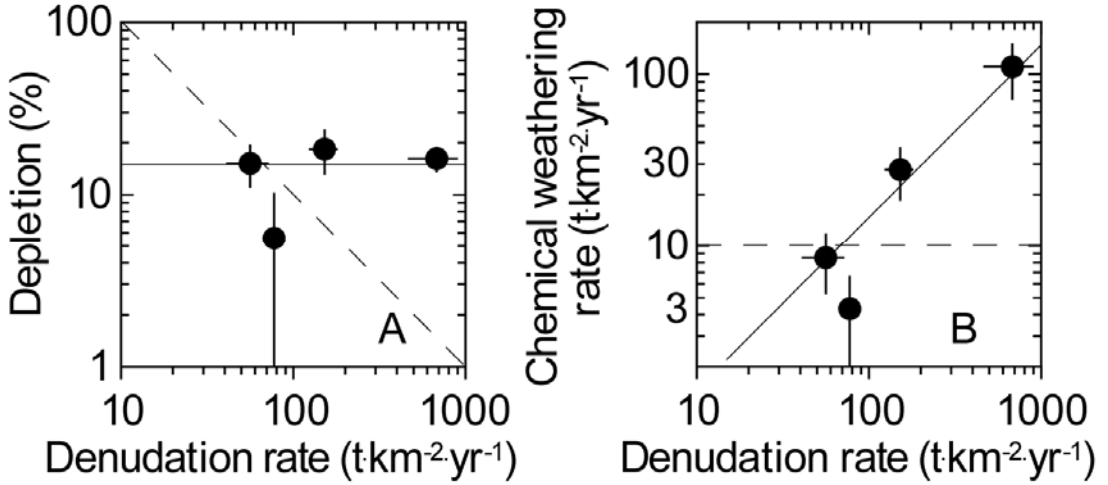

Fig. 4-7. Adapted from Riebe et al., 2001b. Plots of chemical depletions (A) and chemical weathering rates (B) versus total denudation rates for the Fort Sage site. Chemical depletions are roughly uniform across a wide range of denudation rates, while rates of chemical weathering and total denudation are tightly correlated, possibly because chemical weathering rates are regulated by rates of fresh mineral supply by physical erosion of rock. This result implies that tectonic uplift rates may regulate chemical weathering rates.

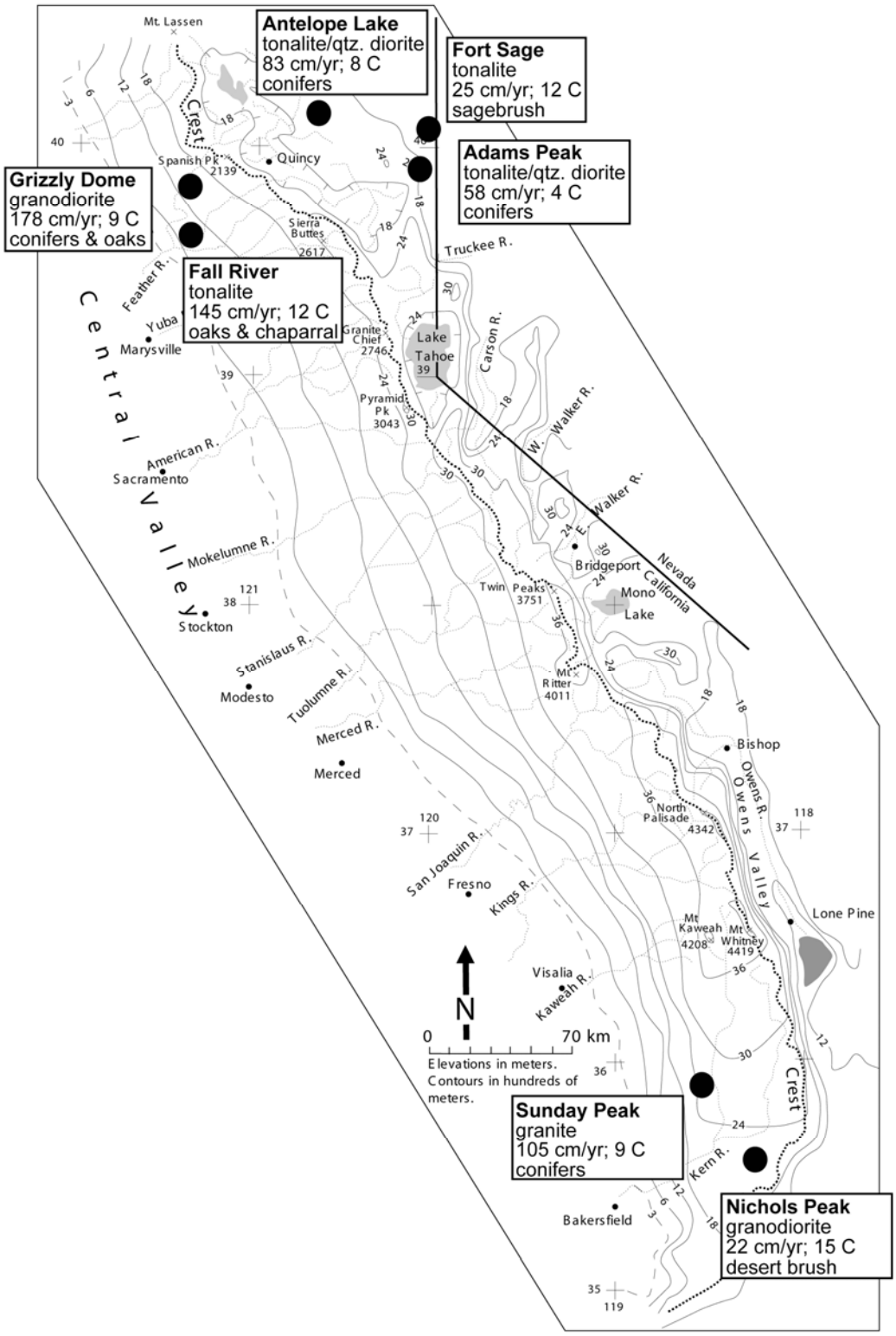

Fig. 4-8. Generalized topographic map of the Sierra Nevada (drafted by John Wakabayashi) showing locations, lithologies, annual averages of precipitation, mean annual temperatures and dominant vegetation types of sites where we have measured rates of erosion and weathering using cosmogenic nuclides.

Table 4-2. Denudation rates, [Zr], chemical depletion fractions, and weathering rates

Basin	Denudation rate	$[Zr]_{saprolite}$	$[Zr]_{outcrop}$	$[Zr]_{rock}$	$[Zr]_{soil}$	Chemical depletion fraction	Weathering rate	
							W_{Si}	W
	(t km^{-2} yr^{-1})	(ppm)	(ppm)	(ppm)	(ppm)	(%)	(t km^{-2} yr^{-1})	
Fort Sage (granodiorite; 25±3 cm/yr; 12.2±0.6 °C; average depletion = 15±3 %)								
A1	79±7	N.D.	112±3 (2)	112±3	118±5 (5)	6±5	0±1	4±4
A2(s)	61±15	120±4 (5)	112±3 (2)	118±3	139±5 (19)	15±4	3±1	9±3
A3(s)	155±30	N.D.	113±4 (4)	113±4	139±7 (16)	18±5	9±3	29±10
A4(s)	721±224	118±4 (4)	122±3 (2)	119±3	142±3 (22)	16±3	38±13	117±41
Fall River (tonalite; 145±5 cm/yr; 11.9±0.6 °C; average depletion = 19±2 %)								
FR-2	400±79	94±9 (12)	85±6 (3)	92±7	109±6 (13)	15±8	19±12	61±34
FR-5	325±48	121±5 (7)	114±3 (4)	119±3	150±5 (25)	21±3	23±5	68±15
FR-6	100±22	N.D.	83±5 (3)	83±5	102±3 (9)	19±5	7±2	19±7
FR-8	39±4	N.D.	87±1 (3)	87±1	106±3 (9)	18±3	2±1	7±1
Adams Peak (tonalite; 58±7 cm/yr; 4.2±0.5 °C; average depletion = 14±2 %)								
AP-3	127±13	111±4 (5)	112±1 (3)	111±2	135±3 (20)	17±2	6±1	22±4
AP-4	85±9	N.D.	108±1 (3)	108±1	115±4 (9)	6±4	1±1	5±3
AP-5	154±15	N.D.	112±3 (4)	112±3	129±7 (9)	12±6	5±3	19±9
AP-11	94±12	N.D.	109±6 (2)	109±6	129±5 (4)	15±6	4±2	14±6
AP-13	123±12	N.D.	112±5 (2)	112±5	131±3 (4)	14±4	5±2	18±6
Antelope Lake (tonalite; 83±6 cm/yr; 7.8±0.4 °C; average depletion = 18±5 %)								
AL-4	70±8	N.D.	166±15 (4)	166±15	227±8 (9)	27±7	6±2	19±5
AL-5	81±10	N.D.	165±48 (2)	165±48	211±10 (7)	22±23	5±6	18±19
AL-9	104±11	N.D.	211±25 (3)	211±25	271±18 (8)	22±11	6±3	23±11
AL-10	85±8	182±11 (8)	192±7 (2)	183±9	212±6 (26)	14±5	3±1	12±4
Sunday Peak (granite; 105±5 cm/yr; 9.4±0.4 °C; average depletion = 10±4 %)								
SP-1	111±12	228±16 (8)	214±7 (3)	225±12	252±7 (23)	11±6	4±2	12±6
SP-3	89±10	N.D.	238±12 (3)	238±12	245±16 (9)	3±8	1±2	3±7
SP-8	85±8	N.D.	244±13 (4)	244±13	278±7 (8)	12±5	3±2	11±5
Nichols Peak (granodiorite; 22±3 cm/yr; 15.4±0.5 °C; average depletion = 25±6 %)								
NP-1	119±12	119±8 (5)	140±4 (2)	125±7	160±10 (19)	22±6	8±3	26±8
NP-18	85±8	197±3 (4)	229 (1)	203±19	285±15 (14)	29±8	6±2	24±7

Site descriptions (underlined) include mapped lithology, average precipitation (in cm/yr), mean annual temperature (in °C), and average chemical depletion fraction (in %, weighted by inverse variance).

N.D. = not determined.

Denudation rates are inferred from cosmogenic nuclide concentrations in the quartz fraction of stream sediment draining from the catchments. For further details, see Riebe (2000).

Zr concentrations are measured by X-Ray Fluorescence (see Riebe, 2000, for further details) and reported as averages ± standard errors for *n* samples (in parentheses).

$[Zr]_{rock}$ is averaged from the combined pool of saprolite and outcrop samples (see Riebe, 2000, for further details).

Chemical depletion fraction = $W/D = (1-[Zr]_{rock}/[Zr]_{soil})$.

Weathering rates are inferred from equation 3, using chemical depletion fractions and denudation rates measured from cosmogenic nuclides.

See Riebe (2000) for explanation of W_{Si} is measured.

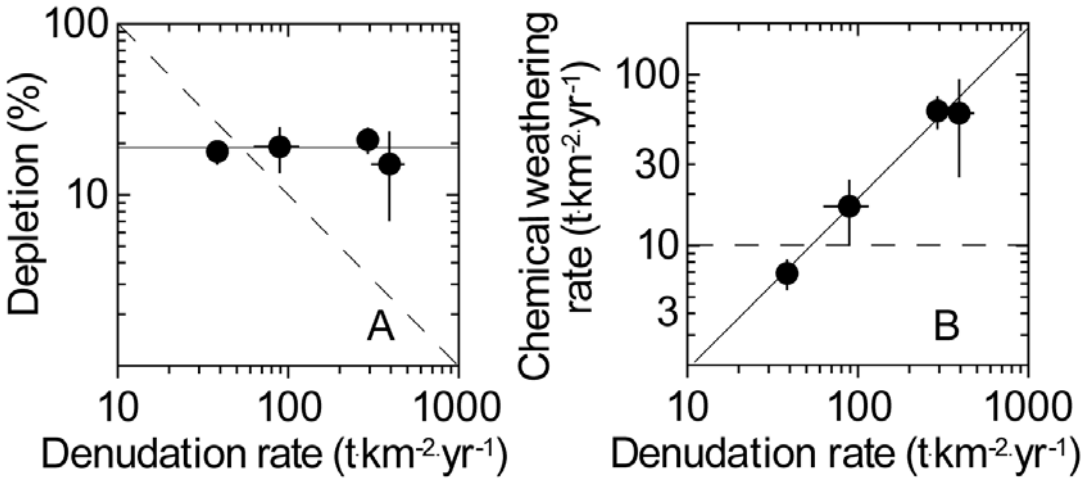

Fig. 4-9. Adapted from Riebe et al., 2001b. Plots of chemical depletions (A) and chemical weathering rates (B) versus total denudation rates for the Fall River site. As is the case at Fort Sage, chemical depletions are roughly uniform across a wide range of denudation rates, while rates of chemical weathering and total denudation are tightly correlated. Note that Fall River is much wetter than Fort Sage, yet chemical depletions and the ranges of both chemical weathering and denudation rates are very similar at the two sites (compare Figs. 4-7 and 4-9). The results shown here lend further support to the notion that chemical weathering rates are regulated by rates of fresh mineral supply by physical erosion of rock. These results also strengthen the argument for strong tectonic control of chemical weathering rates.

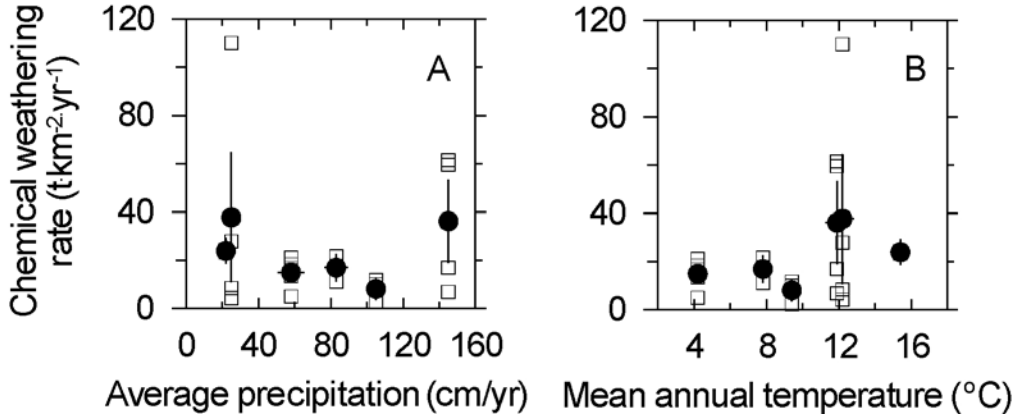

Fig. 4-10. Adapted from Riebe et al., 2001b. Chemical weathering rates plotted against average annual precipitation (A) and mean annual temperature (B) both for site wide averages (solid circles) and the individual catchments (open squares). Differences in chemical weathering rates are strongly associated with differences in denudation rates across each individual site, and obscure any clear relationship between chemical weathering and average precipitation or temperature. This implies that chemical weathering rates are more tightly coupled to erosion rates than they are to climate, at least across these sites.

FORT SAGE MOUNTAINS SUPPLEMENTAL STOP

William B. Bull, Dept. Geosciences, University of Arizona, Tucson, AZ

Reconnaissance for Lichenometry Sites in the Sierra Nevada of California

The 2001 Pacific Cell Friends of the Pleistocene field trip emphasizes paleoseismology and new tools for studying landscape evolution. To that great mix of topics I would like to add a few thoughts regarding the potential of lichenometry for dating and understanding geomorphic processes. Unfortunately, recent events did not allow me to fly back to the United States in time to participate in the dry run of this year's field trip. So, like the rest of you, I find myself in the position of making a reconnaissance for useful lichenometry sites. Selection of lichenometry sites has a crucial influence on precision of age estimates and resolution of closely spaced events.

The main purpose of this note is to outline features that we should look for while driving through, or walking across, the Sierra Nevada of northeastern California. With luck we might find an outcrop or a debris slope that is sensitive to seismic shaking. The FOP trip format virtually eliminates hands-on instruction, so I propose a 2002 lichenometry short course.

Searching for a Useful Site

One nice aspect of the new approach to lichenometry is that regional rockfall events caused by earthquakes should be represented by lichen-size peaks within your study area. Some times of abundant rockfalls are historical events, but the prehistorical events generally require independent confirmation of their times and locations. Once established, this basic catalog of lichen-size peaks caused by regional rockfall events is useful basis for assessing the quality and departures from the norm of your next lichenometry site. I refer you to 1998 article by myself and Mark Brandon for the details about a lichenometry method that provides precise, accurate age estimates for geomorphic events of the past 500 to 1,000 years. My 1996 article uses this method farther South in the Sierra Nevada, but the growth rate equations for four genera of lichens should be applicable in the northern Sierra Nevada.

Factors to consider in site selection include diversity and frequency of geomorphic processes, lichen species and abundance, quality of thalli, substrate smoothness, sizes of rockfall blocks, and ability to recognize old, stabilized block fields where lichen communities are not related to the times of substrate exposure because the first generation of lichens has died and has been replaced.

Much of the Sierra Nevada consists of soil -mantled hillslopes with scattered blocks of granitic rock. Are these useful sites to measure lichen sizes for dating purposes? Unfortunately, blocks on such stable slopes have lichen populations that do not reflect the times at which these rocks moved down the hill to their present locations. I mention this at the beginning because we do not want to waste time measuring the third or fourth generation of lichens growing on either an outcrop a joint face or a ridgecrest corestone if those lichen sizes do not provide information about a geomorphic event. I gather that Stop 1 has examples of such cruddy lichens.

Such undesirable sites are pretty obvious. Masses of lichens have grown together to the extent that circular or elliptical thalli are no longer present. Old stabilized block fields, on which several generations of lichens have grown and died, generally have minimal geochronologic information. Blocks may have weathered surfaces or may be largely buried by fine detritus. Such sites typically have slopes that are much less than the angle of repose for talus. Blocks whose oldest lichens colonized long after the time of initial substrate exposure typically have large thalli with highly irregular margins, or the lichens may have grown together to form a mosaic of thalli margins. Some block fields accumulate slowly and may have a mixture of datable and undatable blocks.

So, we seek nearly circular, isolated lichens that are suggestive of a first-generation lichen community. Our measurements consist of the largest lichen maximum diameters for each rock-fall block on a hillslope, or joint faces on the outcrops that are the source of blocks. The ideal Sierra Nevada rockfall lichenometry site is sensitive to both nearby and distant earthquakes. Such a site would have:

Unstable cliffs of fine-grained, strongly jointed rock.

Pervasive joints that parallel the cliff face.

Abundant blocks with smooth planar surfaces.
A limited size range for most blocks (such as 0.5 to 2 m).
A large repository of blocks close to the angle of repose.
Extensive, thick deposits of blocks devoid of plants, which might shade lichens or provide fuel for fires.
A local microclimate that favors the species of lichen being measured and that lacks persistent snow cover, or fierce winds, which can kill lichens.

Trip Stop 4 has some intriguing possibilities. The tonalite corestones on the soil-mantled slopes have black, irregularly shaped lichens according to Darryl Granger--probably another example of useless lichens. But, there is a volcanic neck that is only an easy 1/2 mile walk from the Stop 4 campsite. Darryl notes that it is 50% covered by yellow, circular lichens. Sounds like first generation Acarospora chlorophana to me. This is the best lichen for our purposes in the drier parts of the Sierra Nevada; tis easy to measure with digital calipers, is very slow growing, and has already been used to date earthquakes as old as 700 A. D.. There should also be rock-fall blocks at bases of the volcanic outcrops (the blocks produced at time of exposure of the outcrop joint faces). A data set here has potential of dating the very recent prehistorical earthquake that produced the fault scarp at nearby Trip Stop 3.

Lichenometry Short Course

I have run short courses for persons interested in lichenometry for the past three years, but these introductions to the subject have been in New Zealand.

A good short course site in the western United States is in the canyon of the South Fork of the Kings River in the Sierra Nevada a couple of miles up the valley from hamlet of Cedar Grove. The glaciated valley upstream from Cedar Grove ranges in altitude from 4600 feet to about 5000 feet. Rocky debris is being shed off the towering cliffs. The south-facing side of the valley has few usable lichens on it but the cooler north-facing side has several usable lichenometry sites.

The most convenient site is just downvalley from Roaring River bridge. Here jointing parallel to the hillslope, accentuated by some vertical fractures allows the formation of a debris cone. Off to one side is an area of sheet talus. Just upstream from the Roaring Fork waterfall is another cliffy area that has a sheet-like accumulation of talus. Both of these appear to be excellent sites for measuring sizes of lichens.

Advantages include:

1) Right by the road, so no long hikes are needed.
2) All four genera of the lichens for which we have growth rates are present,
3) A wide range of sizes should allow tying into the recent historical earthquake record, including the nearby 1872 earthquake in the Owens Valley.
4) Should be some old blocks (600 to 1000 years old)
5) Lack of fire on coarse blocky talus slopes makes for a more complete record of rockfall events.

I would expect the quality of lichen thalli to vary with microenvironment, plus the usual poorer quality for the big lichens. The chief disadvantage from a paleoseismology viewpoint is that one has to pick a measurement area fairly carefully or we are going to have a considerable signal from avalanches as well as seismically-generated rockfalls. This means that we will make a viorous reconnaissance, which could turn out to be an advantage from a short course instructional view.

Logistics appear good, there being both campgrounds and a store in Cedar Grove. Participants could fly into Fresno. Driving in takes several hours because of slow mountain roads. When working under NSF support, I had to get a permit from Sequoia-Kings National Park, mainly to collect samples of tree rings and of lichens. We may not need a permit for a short course if the activities of several people are restricted to walking, taking photos, and measuring sizes of lichens.

Timing. I live in New Zealand half of each year and expect to leave for my second home in late February or early March. Still snow on the ground in the Sierra Nevada then, so the only time for a California lichenometry Short course would be from late September to November. Not ideal because of shorter daylight hours, but cooler and much better chance of getting into a campground. Just send an e-mail to Bill@ActiveTectonics.com if you would like to join us for a day or two.

STOP 5.

James N. Brune, Seismological Laboratory, University of Nevada, Reno

This stop is along Fort Sage mountains road 1-2 miles SW of the north end of Turtle mountain (the northernmost extension of Fort Sage Mountains into Honey Lake Basin). From the road walk a few hundred yards East across the Lahontan shoreline and then across a young alluvial fault scarp about 1-2 meters high., representing recent slip on the western bounding normal fault of the Fort Sage Mountains horst. Although the scarp looks quite young, it is not observed extending into the sediments of the Honey Lake Basin. This suggests the slip occurred before the most recent high stand of Lake Lahontan. Alternatively the slip may be confined to the bounding horst faults and not extend into the basin. Other sections of the fault are confused by shorelines of high stands.

The 1950 M=7.2 Fort Sage Mountains earthquake produce small scarps (about 10 cm) along this fault, but no obvious remnants remain.

East of the alluvial scarp proceed East upslope about 1 km to spectacular balanced rocs which constrain the ground motion which could have occurred in the last few thousand years. In particular these rocks constrain the ground motion which could have occurred during the Fort Sage mountains earthquake, or any other recent earthquakes on the Fort Sage Mountains fault, and also constrain ground motion which could have occurred during earthquakes suggested for the Honey Lake fault during the last several thousand years by Wills and Borcherdt (1993).

We discuss the implications of the precarious rocks for earthquake hazard from the Honey Lake strike-slip fault, the Fort Sage Mountains normal fault, and for earthquake hazard in the broader Walker Lane and the Basin and Range in General.

The following are excerpts from a recently submitted paper

Precarious rock evidence for low near-source accelerations for trans-tensional strike-slip earthquakes

James N. Brune

Abstract

This paper describes precarious rock evidence for low ground motions associated with extensional sections of strike-slip faults. Recent evidence from physical and numerical models and data regressions has indicated that ground motion for extensional strike-slip regions may be lower than for strike-slip faults with a large fault-normal tectonic stress component, and for thrust faults in general. Data from compressional strike-slip and thrust earthquakes dominates the database used in most regression curves for ground acceleration, and in the calculation of current probabilistic seismic hazard maps. Therefore, estimates of ground accelerations on these seismic hazard maps may be too high for sites near extensional sections of strike-slip faults. This paper discusses precariously balanced rock data from three areas near extensional sections of strike-slip faulting: (1) the region of the Honey fault, California, with an active Holocene fault, (2) the Red Rock Canyon region of the Garlock fault, near a dilatational step-over, and (3) the region just south of Beaumont, California, near the Hemet dilatational step-over in the San Jacinto fault. These are all active strike-slip faults, with at least a few large earthquakes in the Holocene, and, in the case of the San Jacinto example, historic large earthquakes (M~7). Thus the precarious rocks at these sites are evidence of relatively low ground motions associated with extensional strike-slip faulting. The results of this study could be very important in developing more detailed seismic hazard maps in the future.

Precarious Rock Evidence from the Honey Lake Strike-slip Fault

A spectacular zone of precarious rocks exists in the Fort Sage Mountains near (2-7 km distance) the strike-slip Honey Lake Fault Zone, California (Figures 5-1 and 5-2). This fault has been interpreted to

be the locus of a total of 16 m of offset in Holocene time, a result of a few to several major earthquakes, with at least one major event in the last several hundred years (Wills and Borcherdt, 1993). The adjacent Honey Lake Basin is a major extensional feature. The rocks are thus strong evidence for low ground accelerations from this major strike-slip fault zone in an extending region. The appearance and geomorphic conditions of the rocks indicates they have been in precarious positions for thousands of years. The examples shown in Figure 5-2 are a selection from more than 50 such rocks in a relatively small region. Some of the rocks are only one or two kilometers from the trace of the fault. Preliminary estimates of toppling accelerations are about 0.3 g. Based on current attenuation curves it would appear that these rocks would be shaken down by ground motion from either an M=6.5 event on the Honey Lake fault (or an M =6 on the Fort Sage Mountains normal fault). The USGS-CDMG hazard maps for this region indicate a very high hazard, with 2500-year recurrence accelerations (2% in 50 yr probabilities) of over 0.8 g (Intensity X). The rocks suggest upper limit constraints on ground motion that is inconsistent with these maps.

The nearby Fort Sage Mountains normal fault was site of the 1950 M=5.6 Fort Sage Mountain normal faulting earthquake. Thus these rocks also provide support for low ground motions on the footwall of normal faults, further complementing the results of Brune (2000).

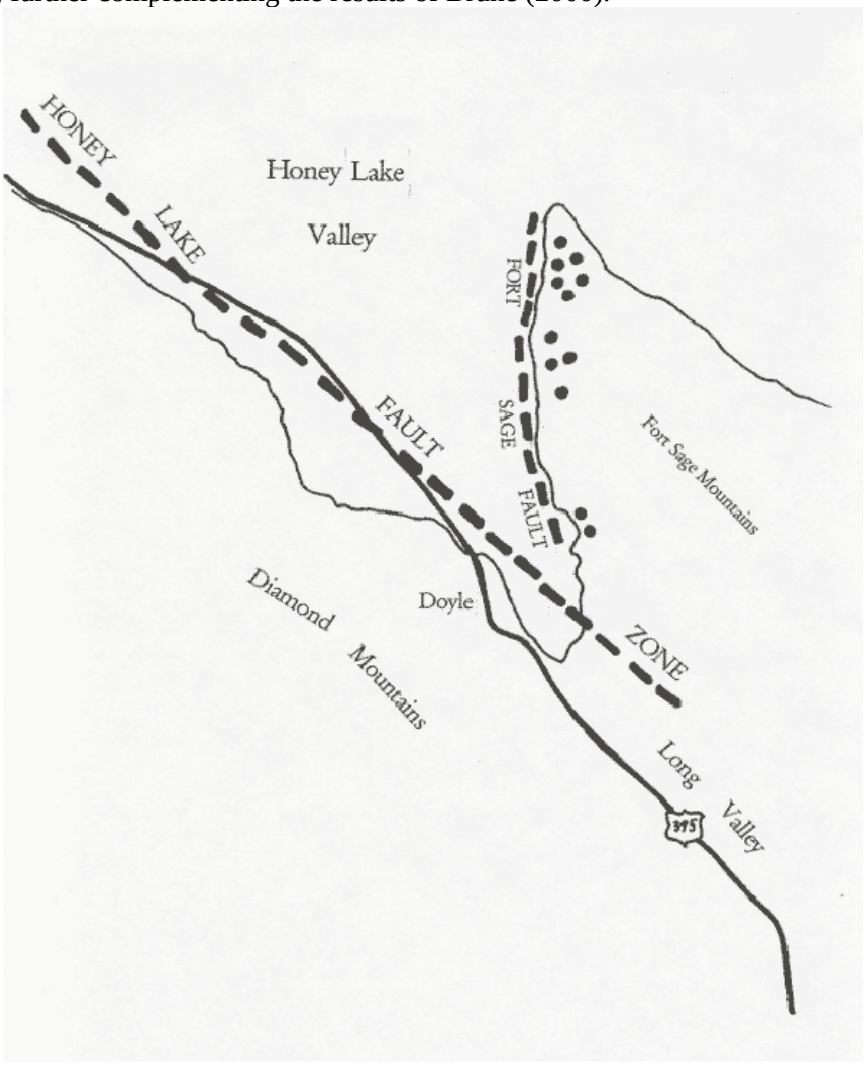

Fig. 5-1.

Fig. 5-2.

Conclusions

This paper has presented precarious rock evidence for low ground motions associated with three extensional sections of strike-slip faults. The results support recent evidence from physical and numerical models, and data regressions, indicating that ground motion for extensional strike-slip regions may be lower than for strike-slip faults with a large fault-normal tectonic stress component. Estimates of ground accelerations on some current seismic hazard maps may be too high for sites near extensional sections of strike-slip faults. The results of this study could be very important in developing more detailed seismic hazard maps in the future.

References

Brune, J.N., 2000. Precarious rock evidence for low ground shaking on the footwall of major normal faults. Bulletin Seismological Society of America 90, 1107-1112.

Wills, C.J., and Borchardt, G., 1993. Holocene slip rate and earthquake recurrence on the Honey Lake Fault Zone, Northeastern California. Geology 21, 853-856.

STOP 6.

Chris Wills, California Division of Mines and Geology, San Francisco CA 94107, cwills@consrv.ca.gov

At this stop we return to the Honey Lake fault zone. Several geologists working in the area, either mapping the geology or the fault itself, have visited this locality over the past 10 years or so, but no one has done any detailed work here as far as we know. There is a wealth of geologic features here and we expect the group will spread out along the shore of Honey Lake and several smaller groups will form focusing on some of the more spectacular features. While at this locality, don't spend too long looking at the exposures near the fault, though those are the first we come to. Be sure to walk out along the bluffs to the south and take time to look at the range of features exposed here.

The main features include the scarp of the Honey Lake fault zone that crosses this peninsula in Honey Lake. The 2-3 m high east-facing scarp is visible from the point that the dirt road reaches the shore of the lake, but you may want to walk back northeast away from the scarp to see more of it. Once again this scarp is developed in the bed of Lake Lahontan, so is essentially a Holocene feature.

The scarp projects into the bluffs and the fault can be easily found in the bluff exposures. The 'rocks' here are Pliocene or Pleistocene (?) lake (?) beds mostly of very light gray siltstone and claystone, the fault forms the boundary between the near-vertical beds found where we can first see these rocks and the much more gently dipping rocks that make up most of the bluffs. The fault also clearly offsets the Lake Lahontan deposits which overlie the older lake beds. Adjacent to the fault, the angular unconformity between the Plio-Pleistocene (?) lake beds and the Lake Lahontan deposits is marked by a gravel layer and overlain by grayish brown deposits including abundant tufa. That contact is offset vertically at least 3 m. Also visible at the fault zone, within the lake beds, is an area of dark brownish gray friable sand. We suspect this sand was injected into the lake beds by liquefaction.

Southward from the main fault exposures there are numerous minor faults, most of which do not cut the Lake Lahontan deposits that overlie the lake beds. There is also abundant evidence for soft-sediment deformation and/or slumping within the lake beds.

The most spectacular exposures of structural geology, including fairly tight folding and thrust faulting in the lake beds are just around the "nose" of the bluffs. Just south of that area, the lake beds contain numerous clean, white ash beds. A couple of these beds were sampled by Wills and Borchardt in 1989 and sent to Andrei Sarna for analysis. He reported that they were somewhat altered and not clearly correlated with any known ash deposits, but most closely resembled Pliocene ashes.

There are numerous questions to be asked here, beginning with the age and depositional environment of the "lake" beds, correlation of the ash layers, origin of the "plastic" appearing deformation of the lake beds by soft sediment deformation or slumping (or is some of it tectonic?), how much of the folding and low angle faulting is due to interactions with the current strike slip fault (or is some of it soft-sediment slumping?), development of the different strands of the fault over time, development of the broad warp in the former bed of Lake Lahontan and relation of that to faulting. You will no doubt come up with many more questions. Don't come to your field trip leaders for answers, we will be happy to speculate and wave our arms, but by the time we leave this stop you will have spent nearly as much time at these outcrops as anyone.

STOP 7

John Wakabayashi, 1329 Sheridan Lane, Hayward, CA 94544, wako@tdl.com,
http://www.tdl.com/~wako/

Soakies Grade Overlook Stop, Seneca Road, Lake Almanor Area

At this stop we can view features related to Quaternary volcanic history, stream incision, and faulting in this area. The Basalt of Rock Creek (~1 Ma) is exposed in the roadcut above where you will park along the Seneca road (a section of road known as Soakies Grade). The basal baked zone is easily seen in the roadcut. This steep baked zone overlies a thin zone of colluvium, that, in turn, overlies Paleozoic basement; this represents a buttress unconformity of the base of the flow against the old canyon wall. This is typical of the terrace-like remnants of basalt that occur in the North Fork Feather River canyon. More extensive remnants generally have a large wedge of colluvium on top of them and have stream gravels at their base. After looking at this basalt we can walk toward the northeast a bit along the road to get a view toward the Lake Almanor basin.

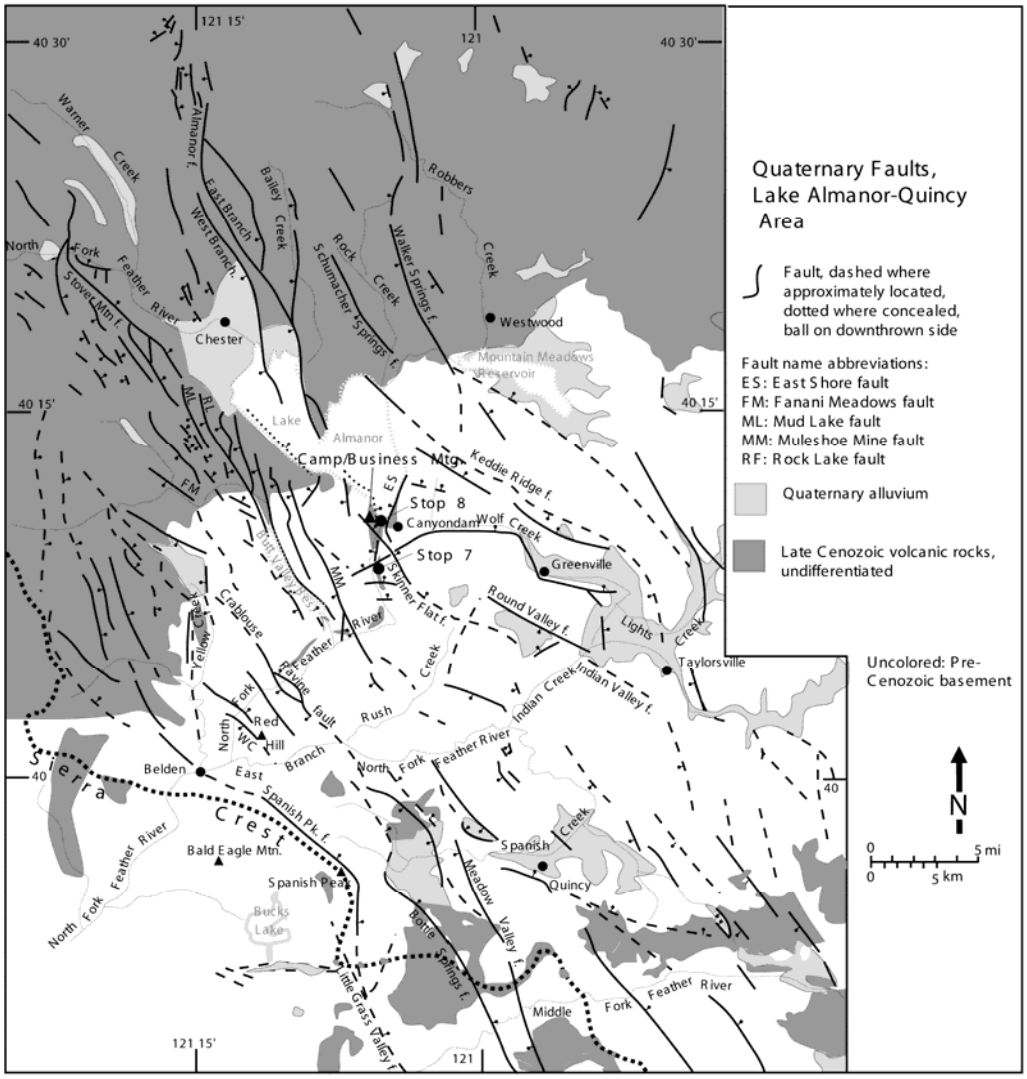

Figure 7-1: Quaternary faults of the Lake Almanor area. Adapted from Wakabayashi and Sawyer (2000).

Lake Almanor is a reservoir that floods a fault-bounded basin along some strands of the Mohawk Valley fault zone (Fig. 7-1). At this point we are at the northern limit of what is generally defined as the Sierra Nevada, as deposits of Plio-Pleistocene volcanic rocks cover essentially all older rocks to the north (the southern part of the Modoc plateau to the north and northeast or southern Cascades to the northwest).

In spite of the difference in rock types exposed at the surface, faulting along the Frontal fault system continues northward across the 'transition', part of a fault system that has been termed the Tahoe-Medicine Lake trough (Page et al., 1993). The Hat Creek fault, that forms the spectacular escarpment of the Hat Creek Rim north of this area, is part of the northern continuation of this fault system (e.g., Wills, 1990; Muffler et al., 1994). The Sierran-Modoc Plateau and Sierran-Cascades transitions are thus more a transition in rock types at the surface than a tectonic transition. Looking across the lake we observe a type of 'inverted topography' in which older volcanic rocks have been uplifted and younger volcanic rocks have flowed down channels cut into the older rocks. Across Lake Almanor, many of the highest areas are underlain by 2.2 Ma andesites. Younger basalt flows, the ~1 Ma Basalt of Rock Creek, ~0.6 Ma Basalt of Warner Valley, and ~0.4 Ma Basalt of Westwood, flowed down channels cut into older rocks (in the case of the 0.4 Ma basalts the rocks fill a channel cut into the 1 Ma rocks); these basalts flowed into the Almanor basin from the northwest, north, and northeast (Fig. 7-2). On the floor of the Almanor basin itself, beneath the lake and basin sediments, the volcanic flows likely overlie one another in stratigraphic sequence. Several of the basalts flowed through the Almanor basin and continued down the ancestral North Fork Feather River canyon, as will be discussed below.

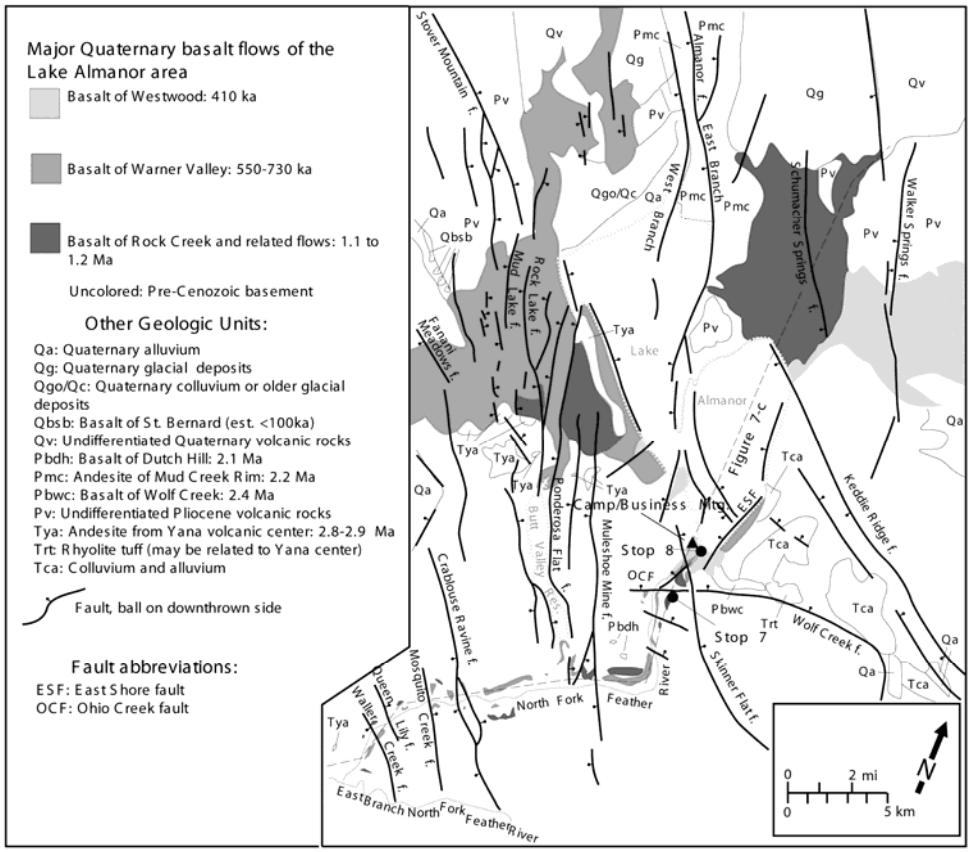

Figure 7-2: Plio-Pleistocene volcanic rocks, and Quaternary faults, Lake Almanor area. Adapted from Wakabayashi and Sawyer (2000).

At this viewpoint we are 'downstream' of the Almanor basin from the standpoint of the direction that the basaltic lavas flowed, yet we are significantly higher than the Almanor basin; because we are 'downstream' of the Almanor basin the elevation difference we see must be a consequence of faulting. The top of the basalt outcrop in the roadcut is 113 m higher than the high water level of Lake Almanor. The elevation difference between this remnant and the basin helps one visualize the vertical component of the faulting bounding this side of the Almanor basin (water depth is about 30 m). Note that the surface of this basalt in the Almanor basin is considerably lower than the bottom of the lake. In the basin, this basalt would be expected to be overlain successively by flows of the ~0.6 Ma Basalt of Warner Valley, the ~0.4 Ma Basalt of Westwood, and late Quaternary alluvial deposits that overlie these basalts in the basin.

Across the deep canyon of the North Fork Feather River to the north and northwest, we see a flat bench. The canyon walls reveal that the bench is underlain by Basalt of Westwood that overlies Basalt of Warner Valley; we will see this relationship at Stop 8. The Basalt of Westwood may not have made it much further downstream than the downstream limit of the bench, for it has not been found beyond that point. To the north of us, on our side (the east side) of the canyon, and partly blocking our view of the lake, is a wooded knob. This knob is capped with the Basalt of Warner Valley that overlies the Basalt of Rock Creek. The Skinner Flat fault, that passes northeast of this knob (backside of the knob relative to us), and a splay of the Ohio Creek fault, uplifts these exposures relative to Lake Almanor, and the bench on the west side of the river (Fig. 7-2). The relationships of the various basalts on each side of these faults suggest that the Skinner Flat fault may not have started significant movement until after the deposition of the Basalt of Westwood, whereas the main branch of the Ohio Creek fault may have moved after Basalt of Rock Creek time, but ceased movement before Basalt of Warner Valley time.

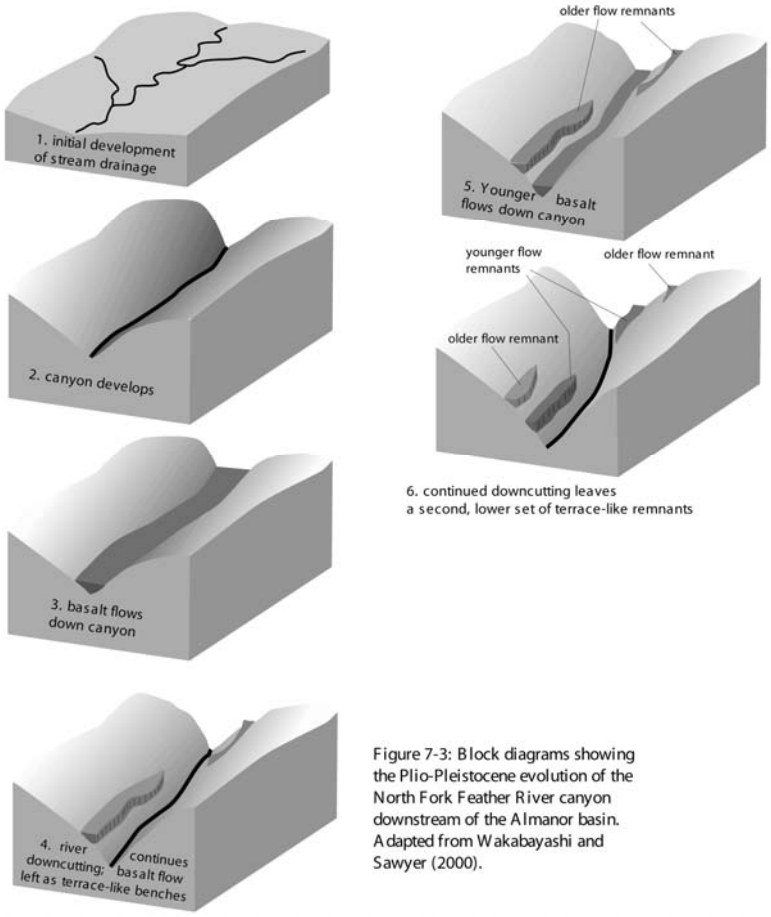

Figure 7-3: Block diagrams showing the Plio-Pleistocene evolution of the North Fork Feather River canyon downstream of the Almanor basin. Adapted from Wakabayashi and Sawyer (2000).

On the above-described wooded knob and the bench across the river basaltic units still overlie each other in normal stratigraphic fashion. Downstream of these outcrops, starting with the outcrops where we are stopped, an 'inverted' topographic series of basalt benches is seen, a consequence of successive river incision with periods of basalt flowing down the canyon (schematically shown in Fig. 7-3). The 'cross over' point is marked by the Ohio Creek fault that passes between the 'normal' stratigraphic sequences to our north and the outcrop that we are standing next to.

Now we will turn around and hike southeast up a dirt road onto the knoll on the east side of the main road, from which we can look downstream. From here we can see the river bend around a hill that has several prominent flat surfaces at different elevations. The lowest of the two flat surfaces are remnants of the 0.6 Ma Basalt of Warner Valley (lowest), and 1 Ma Basalt of Rock Creek (next bench up). Figure 7-4 was taken from a bit further down the canyon than our viewpoint, so that the lower bench

is more easily seen; it wraps around the bend in the canyon. Similar bench-like remnants exhibiting 'inverted' topographic relationships (oldest benches are highest) are present along the walls of the North Fork Feather River canyon as far downstream as the confluence of the North Fork with the East Branch North Fork. A canyon followed approximately the same course since at least 2.8 Ma, based on the oldest inset volcanic unit. The depth of the canyon at 2.8 Ma can be estimated by noting the position of the inset volcanic remnant of this age relative to erosion surfaces or basement topographic highs above it. The ages of the various terrace-like remnants of volcanic rocks in the North Fork Feather River canyon have been confirmed by Ar/Ar dating (Wakabayashi and Sawyer, 2000). Correlation of the terrace remnants in the canyon allow evaluation of vertical separation associated with faulting in the canyon (Fig. 7-5). Note that these are vertical separations on faults that appear to have a much larger strike-slip component (WLA, 1996). The Butt Valley fault zone, which has the largest vertical separation of any group of faults downstream of the Almanor dam area, appears to have the same separation of the Basalt of Warner Valley and the Basalt of Rock Creek, suggesting that faulting on these strands did not begin until after Basalt of Warner Valley deposition (~600 ka). Thus the two most significant fault zones in the North Fork Feather River canyon, the Skinner Flat fault and Butt Valley fault zones, both appear to have begun movement sometime after 600 ka. This start up of faulting may be a part of ongoing encroachment of the western margin of the Walker Lane or Frontal fault system into the Sierran block. Perhaps consistent with the immature state of the faults in this area is the fact that the Mohawk Valley fault zone/Frontal fault system in this area consists of many strands distributed over a zone 30 to 40 km wide. This zone is much narrower (about 10 km wide) south of Quincy.

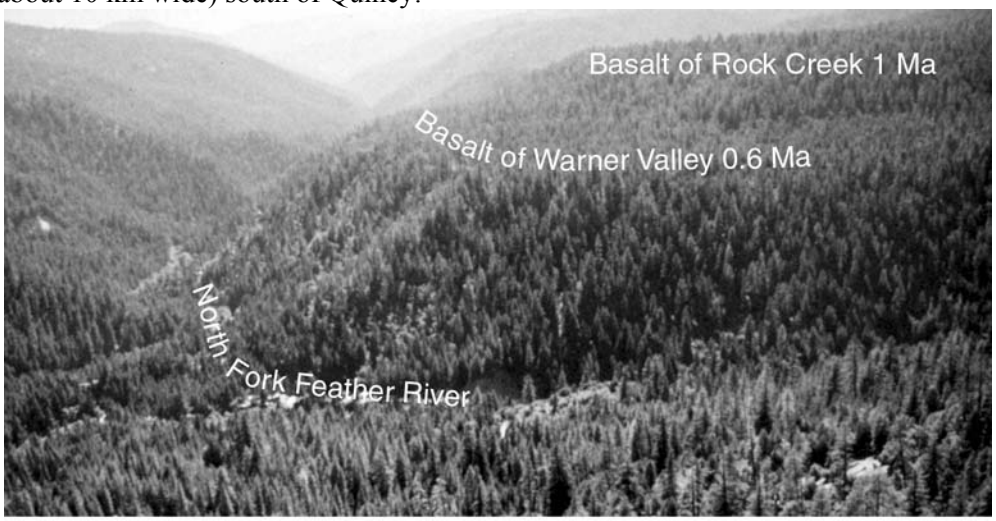

Figure 7-4. View down the North Fork Feather River Canyon from downstream of Stop 7, showing examples of terrace like remnants of Quaternary basalt flows in the canyon.

The terrace-like remnants of volcanic rocks in the North Fork Feather River canyon also allow estimation of incision rates. Incision relative to a volcanic unit can be measured in two ways: (1) from the top of the volcanic unit (includes the incision through the volcanic unit), referred to as 'total incision' (see also Fig. 10-1 for Stop 10), or (2) incision in rocks below the volcanic unit, referred to as 'basement incision' (Wakabayashi and Sawyer, 2001). For the various basalts in the North Fork Feather River canyon, incision can be measured between different times represented by the basalt flows. For example, basement incision between Basalt of Rock Creek and Basalt of Warner Valley time can be measured by the elevation difference between the base of a Basalt of Rock Creek flow remnant to the base of a Basalt of Warner Valley flow remnant along the same reach of the stream, whereas total incision between these two times can be measured by the elevation difference between the top of a Basalt of Rock Creek and the bottom of a Basalt of Warner Valley flow. The incision various between fault-bounded blocks is summarized in Table 7-1, and show diagramatically on Figure 7-5.

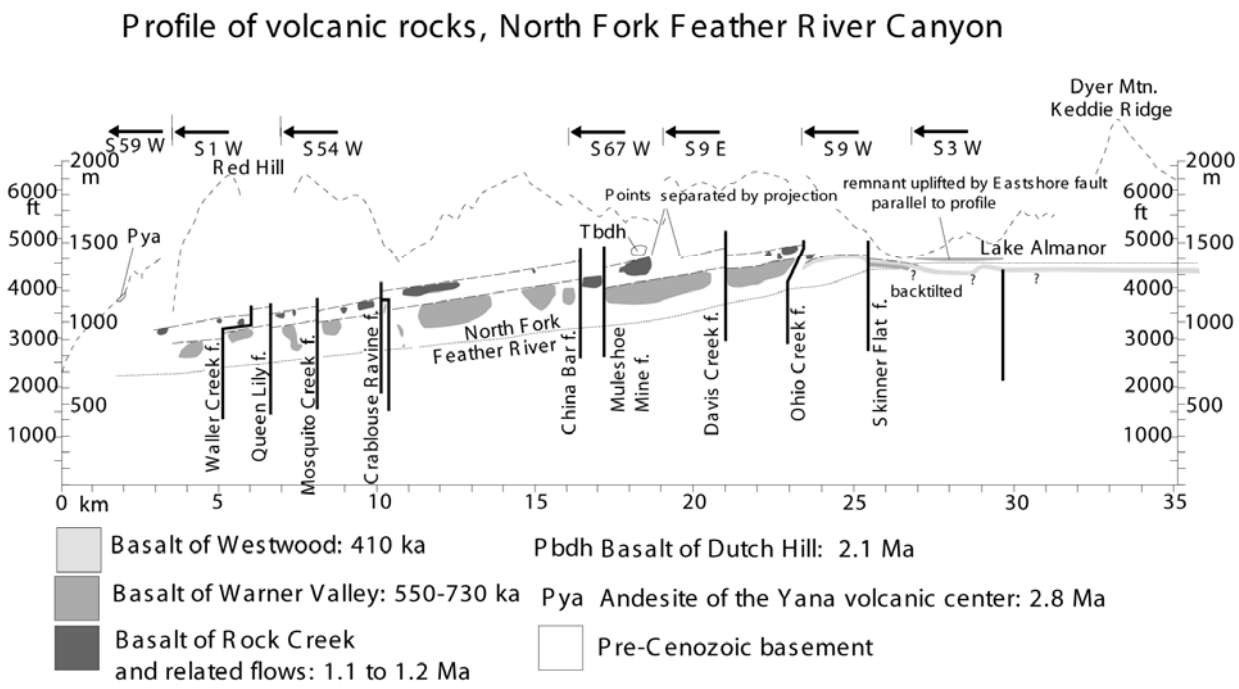

Figure 7-5: Profile of volcanic rocks, North Fork Feather River canyon projected to projection line shown in Fig. 7-2. Adapted from Wakabayashi and Sawyer (2000).

TABLE 7-1: INCISION RATE, NORTH FORK FEATHER RIVER, LAKE ALMANOR TO CONFLUENCE WITH EAST BRANCH NORTH FORK FEATHER RIVER

Fault Block or Reach of river	Total incision rate (mm/yr) with time interval; parentheses denote basement incision rate
Ohio Creek to Salmon Creek	0.57-0.73 Ma to present: 0.21-0.26 (0.096-0.12); 1.11-1.20 Ma to present: 0.22-0.24 (0.16-0.17); 1.11-1.20 Ma to 0.57-0.73 Ma: 0.31-0.52 (0.18-0.31)
Davis Creek to Meeker Bar	0.57-0.73 Ma to present: 0.30-0.38 (0.10-0.13); 1.11-1.20 Ma to present: 0.29-0.31 (0.24-0.25); 1.11-1.20 Ma to 0.57-0.73 Ma: 0.43-0.71 (0.33-0.54); 2.05 Ma to 1.11-1.20 Ma: 0.13-0.15 (0.052-0.058)
Butt Creek to Crablouse Ravine	0.57-0.73 Ma to present: 0.37-0.48 (0.15-0.19); 1.11-1.20 Ma to 0.57-0.73 Ma: 0.43-0.72 (0.31-0.51); 1.11-1.20 Ma to present: 0.32-0.34 (0.25-0.27)
Crablouse Ravine to Mosquito Creek	0.57-0.73 Ma to present: 0.28-0.36 (0.14-0.18); 1.11-1.20 Ma to 0.57-0.73 Ma: 0.32-0.54 (0.21-0.35)
Mosquito Creek to Queen Lily	0.57-0.73 Ma to present: 0.29-0.37 (0.067-0.086); 1.11-1.20 Ma to 0.57-0.73 Ma: 0.39-0.64 (0.31-0.51)
Waller Creek fault to East Branch confluence	0.57-0.73 Ma to present: 0.23-0.29 (0.12-0.15); 1.11-1.20 Ma to 0.57-0.73 Ma: 0.34-0.57 (0.24-0.40); 2.81 Ma to 1.11-1.20 Ma: 0.14 (0.082-0.086); 2.81 Ma to present: 0.17 (0.13)

STOP 8

John Wakabayashi, 1329 Sheridan Lane, Hayward, CA 94544, wako@tdl.com, http://www.tdl.com/~wako/

Canyon Directly Downstream of Lake Almanor Dam.

This is a brief stop to look at Quaternary basalts exposed in the walls of the narrow canyon directly downstream from Lake Almanor dam. The best viewing of this exposure is from the east side of the outlet of the dam. The cliffs on the west side of the canyon are made up of the 400 ka Basalt of Westwood overlying the 600 ka Basalt of Warner Valley. The base of the Basalt of Westwood is seen as

a degraded (less massive) zone possibly including an old soil, that overlies more massive basalt of the Basalt of Warner Valley. Argon-argon samples were collected from the cliff you are viewing; these samples verified the presence of the two flow units. From where we park our vehicles we can see a topographic step (facing us) on the west side of the river. This is the scarp of the Skinner Flat fault in Basalt of Westwood. The scarp is up to 10 m high and also bounds the southwest (uphill) side of the area that we will camp. In addition to the scarp, the surface of the Basalt of Westwood slopes northeastward toward the lake. Because this is the upstream direction, this slope is most likely of tectonic origin.

References (STOPS 7 & 8)

Muffler, L.J.P., Clynne, M.A., and Champion, D.E., 1994, Late Quaternary normal faulting of the Hat Creek basalt, northern California: Geological Society of America Bulletin, v. 106, p. 195-200.

Page, W. D., Sawyer, T. S., McLaren, M. , Savage, W. U., and Wakabayashi, J., 1993, The Quaternary Tahoe-Medicine Lake trough: the western margin of the Basin and Range transition, NE California: Geol. Soc. Amer. , Abstr. w. Programs, v. 25, no. 5, p. 131.

Wakabayashi, J., and Sawyer, T.L., 2001, Stream incision, tectonics, uplift, and evolution of topography of the Sierra Nevada, California: Journal of Geology, v. 109, p. 539-562.

Wakabayashi, J., and Sawyer, T.L., 2000, Neotectonics of the Sierra Nevada and the Sierra Nevada-Basin and Range Transition, California, with field trip stop descriptions for the northeastern Sierra Nevada: in Brooks, E.R., and Dida, L.T., eds., Field guide to the geology and tectonics of the northern Sierra Nevada, California Division of Mines and Geology Special Publication 122, p. 173-212.

Wills, C. J., 1990, Active faults north of Lassen Volcanic National Park, northern California: California Geology, v. 44, p. 51-58.

WLA (William Lettis and Associates), 1996, Lake Almanor and Butt Valley Dams Seismic Stability Assessment, Volume 1: Seismic Source Characterization and Estimated Ground Motions: report to Pacific Gas and Electric Company.

STOP 9

Thomas L. Sawyer[1] and Rich Briggs[2]
[1]*Piedmont Geosciences, Inc., 10235 Blackhawk Drive, Reno, NV 89506, Piedmont@USA.com*
[2]*University of Nevada Reno, Center for Neotectonic Studies, Reno, NV 89557, briggs@seismo.unr.edu*

with prior contributions by:
Mark A. Hemphill-Haley[3] and William D. Page[4]
[3]Geosciences Dept., PG&E, P.O. Box 770000, San Francisco, CA 94177
[4]Geology Dept., Humboldt State University, Arcata, CA 95521

Kinematics and late Quaternary activity of the Mohawk Valley Fault Zone

Objective

The main purpose of this stop is to discuss the late Quaternary activity of the Mohawk Valley fault zone (MVFZ) based on geomorphic and trenching studies, as well as discuss the possible significance the fault zone may have in accommodate northwest-directed right-lateral shear measured geodetically across the northern Walker Lane. In addition, our vantage point above the town of Clio in Mohawk Valley provides a general overview of the geomorphology of the eastern front of the Sierra Nevada, topography produced by late Pliocene to late Quaternary movement on the MVFZ.

Overview

The MVFZ is the frontal fault of the Sierra Nevada from south of Sierra Valley northwest to American Valley, a distance of 60 km or more. In addition to forming the present topography along this part of the northern Sierran front, the MVFZ is optimally oriented to accommodate northwest-directed right shear along the western edge of the Basin and Range/Sierra Nevada transition in the northern Walker Lane. In addition, the fault zone is expressed as the "Plumas Trough" of Durrell (1966), which is one in a series of en echelon late Neogene graben that extend from the Tahoe basin to the Medicine Lake volcanic field (Page et al., 1993) and probably another 100 km northward to the Klamath Lake region of Oregon, or beyond.

Recently, Henry and Perkins (2001) suggested that the uplift of the Sierra Nevada relative to the Basin and Range began at 3 Ma in the Reno area, based on structural analysis of the Verdi-Boca sedimentary basin and 40Ar/39Ar dating and tephrochronology of volcanic units underlying, within, and overlying sediment in the basin. Henry and Perkins (2001) reported that the results of their study are consistent with apatite-fission-track and U-Th/He results that show uplift of the Carson Range, also within the northern Basin and Range/Sierra Nevada transition, at 3 Ma (Surpless et al., 2000). However, northwest-directed right shear began after 3 Ma in the Reno area or was accommodated to the east (Henry and Perkins, 2001).

Considering that the fault zone is less than 30 km from the Carson Range and sedimentary remnants of the dismembered and formerly extensive Verdi-Boca basin presently lie less than 25 km south along the Sierran front (Henry and Perkins, 2001), movement on the MVFZ also may have began at 3 Ma and perhaps right-lateral shear began somewhat latter.

The MVFZ is one of the more seismically active frontal faults of the Sierra Nevada (Gotter et al., 1994). In addition to abundant microseismicity, nine earthquakes of M=4 or larger have occurred along or near the MVFZ since 1974 (USGS-NEIC Internet resource, 2001). The largest and most recent of these events, a M=5.5 earthquake on August 10, 2001, occurred near the north end of Mohawk Valley 17 km beneath the west flank of Grizzly Ridge. This event, which proceeded a M=4.2 event on the following day, has a focal mechanism that is consistent with right-lateral slip on a northwest-striking nodal plane parallel to the MVFZ. The largest historical earthquake reported in the region was a moderate earthquake (M~6) that occurred in April, 1888. This earthquake reportedly was associated with ground cracking in Mohawk Valley near Clio. However, Toppozzada and others (1981) re-evaluated the felt reports of this event and concluded that the earthquake likely occurred in the Honey Lake region.

Geodesy along the northern Basin and Range/Sierra Nevada transition

Kinematic models and geodetic studies have shown that 20-25% of the relative motion between the Pacific and North American plates occurs east of the Sierra Nevada at the latitude of the northern Walker Lane (Atwater, 1970; Minster and Jordan, 1987; DeMets et al. 1987; Ward, 1990; Argus and Gordon, 1991; Dixon et al., 1995). Recent GPS geodetic studies across the northern Basin and Range (the continuous BARGEN (Bennett et al., 1998) and campaign USGS (Thatcher et al., 1999) networks) and within the Sierra Nevada (Dixon et al., 2000) have significantly increased the resolution of strain data along the northern Basin and Range/Sierra Nevada transition. These studies demonstrate that the bulk of strain accumulation in the northern Basin and Range occurs between the Sierra Nevada and the Central Nevada Seismic Belt (CNSB) (Fig. 9-2), and that the Sierra Nevada effectively acts as a microplate with little internal deformation. From east to west, velocity vectors across the northern Basin and Range generally increase in magnitude and rotate from east-west orientations to northwest directions with respect to stable North America, reflecting a transition from primarily extension in the east to increasing northwest-directed, right-lateral shear near the Sierra Nevada (Fig. 1; BARGEN vectors only for clarity). While the big picture is in place, however, details of how strain is distributed with respect to active faults along the northern Basin and Range/Sierra Nevada transition are not yet clear.

Existence, persistence, and magnitude of the strain gradient associated with the northern Walker Lane

A significant velocity gradient, or suddenly increased strain rate, appears to be associated with the northern Walker Lane. USGS stations along the Highway 50 corridor show increase in station velocities corresponding to the Walker Lane (Fig. 9-2) (Thatcher et al., 1999). BARGEN stations aligned with the USGS transect (stations NEWP, UPSA, SLID) also show a subdued, but a detectable increase in station velocities near the southern edge of the northern Walker Lane. In contrast, BARGEN station velocities farther north (LEWI, TUNG, GARL, SHIN, QUIN) do not show a significant jump in velocities, but instead reflect more evenly distributed strain. Velocity differences between BARGEN stations UPSA or GARL and SLID in the south (5-6mm/yr) are large when compared to SHIN and QUIN in the north (2-3mm/yr) (Fig. 9-2), implying that strain becomes more broadly distributed to the north. Bennett and others (1999) interpret only 2-3 mm/yr of right-lateral shear remaining at 41^{o}, with the bulk of deformation transferred northeastward into Basin and Range extension. This is consistent with prior observations and kinematic models of the transition from strike-slip faulting in Mohawk Valley to extension in northeastern California and Oregon (Grose, 1986; Pezzopane and Weldon, 1993; Unruh, 1996).

Geodetic context of the Mohawk Valley fault zone

The MVFZ is optimally oriented to accommodate the northwest-directed deformation measured geodetically across the northern Walker Lane. Preliminary measurements of relative velocities across the northern Walker Lane appear to show a transition from 4-8 mm/yr at its southern extent to 2-3 mm/yr near Quincy. Fault slip rate estimates for the region do not presently account for this strain accumulation (Briggs and Wesnousky, 2001). With the exception of the Honey Lake fault zone (~2 mm/year; Wills and Borchardt, 1993), slip rates have not been determined geologically for active strike-slip faults in this portion of the Basin and Range/Sierra Nevada transition. It is likely, based on previous geomorphic and trenching work (Sawyer et al., 1993), that the MVFZ takes up a significant portion of the geodetically measured dextral shear at its latitude.

A first-order attempt to model the amount of slip taken up by the MVFZ based primarily on geodetic measurements has been pursued by Dixon and others (2000) (Fig. 9-3). A simple elastic half space is used to model only two faults, the Honey Lake fault slipping at 2 mm/yr (Wills and Borchardt, 1993) and the MVFZ. Boundary conditions are the stable Sierran microplate translating to the northwest at nearly 14 mm/yr to the west and near-zero velocity (fixed) to the east. This model yields slip of 6□3 mm/yr on the MVFZ. Preliminary geologic work (Sawyer et al., 1993) indicates that a slip rate near or below the lowest limit (3 mm/yr) is most likely.

While the simple model of Dixon and others (2000) appears to overstate the slip rate on the MVFZ, it does highlight the potential for this fault to accommodate significant slip in this region. Increased geologic and geodetic information across the northern Walker Lane will be required if more realistic slip models are to be formulated. A campaign network of 16 GPS stations extending across this region has been in place since June 2000, and results will hopefully clarify strain distribution across the northern Walker Lane (Briggs and Wesnousky, 2001) (Fig. 9-4). Geodesy alone will provide only a rough sketch of strain accumulation across the region, however, and geologic and paleoseismic study of active northern Walker Lane faults will be necessary to understand how regional strain is released by earthquakes. This effort is underway - in addition to this investigation of the MVFZ, similar studies are ongoing on the Warm Springs fault zone (Craig dePolo and others), the Peavine fault (Alan Ramelli and others), and the Olinghouse and Pyramid Lake faults (Rich Briggs and Steve Wesnousky).

Mohawk Valley Fault Zone

The MVFZ is the frontal fault of the Sierra Nevada from south of Sierra Valley northwest to American Valley. However the steep, prominent Sierran front only extends along the western edge of southern Sierra Valley and of southern Mohawk Valley, where it is particular linear and relatively undissected. Paralleling the frontal fault or western branch of the southern MVFZ is an eastern branch that crosses the floor of Sierra Valley, between Sierraville and Calpine, and traverses the volcanic and granitic hills between Sierra and Mohawk valleys (Figure 9-1). The eastern branch appears to extend northwest along the east side of Mohawk Valley and American Valley and may account for most or all late Quaternary slip on the northern MVFZ. The character of the Sierran front changes near the town of Clio, apparently reflecting decreased activity on the western branch and a transfer of right slip across southern Mohawk Valley to the eastern branch in a releasing right stepover. Northwest from Clio, the front of the range is less steep and more dissected, and the western branch is concealed by massive landslide deposits and, further northwest, by unfaulted late Pleistocene lateral moraines and glacial till (Hawkins et al., 1986; Saucedo, 1992).

The parallel branches of the MVFZ are 3 km apart (Figure 9-1) and have contrasting geomorphic expressions and different styles of faulting. The western branch, first mapped by Turner (1897), downfaults the Miocene to middle Pliocene Mehrten Formation 500 to 700 m from the crest of the Sierra Nevada to the Mehrten capped hills between Mohawk and Sierra valleys (Turner, 1897; Sawyer et al., 1993) and 20 km to the northwest downfaults both the stratigraphically higher Mehrten Formation and the 16 Ma Lovejoy Basalt an estimated 1,200 m (Page and Sawyer, 1992) into the semi-rhombic depression at the town of Sloat. Whereas, the eastern branch is marked by a series of linear northwest-striking scarplets, deflected and ponded drainages, and tonal and vegetation lineaments crossing the floor of southern Sierra Valley, that were first mapped by Sawyer et al. (1993). In addition, the eastern branch lacks range-front relief and the more continuous fault traces display a left en echelon arrangement. The pattern of faulting and the contrasting geomorphic expression of the two branches are generally similar to that of the Owens Valley and Independence faults, respectively. Thus, as in the Owens Valley area, strain partitioning apparently occurs along the southern MVFZ.

Applying this late Neogene displacement data and assuming that vertical movement on the fault zone began at 3 Ma, a maximum long-term average, vertical slip rate of 0.2 mm/yr would characterize the western branch along the southern MVFZ and a rate of 0.4 mm/yr would characterize it along the central MVFZ.

Historical seismicity, recent geodetic data, and the pattern and geomorphic expression of faults in the zone, however, suggest that in addition to vertical displacement, the MVFZ accommodates a possibly significant component of right-lateral slip in the northern Walker Lane. Right-lateral strike-slip faulting is consistent with results of our paleoseismic study as well, which was conducted at the toe of the Sierran Front between Mohawk Valley and Sierra Valley and west of the town of Calpine (Figure 9-1).

Although uncharacterized, the cumulative amount of right slip on the MVFZ may be substantial. For example, the Middle Fork Feather River abruptly jogs northwest at Clio and does not resume its westerly course until near the town of Cromberg, possibly reflecting a 18 to 20 km right-lateral deflection

and/or offset along the northern MVFZ. The unique aspect of the Feather River as being the only drainage system to flow across the entire width of the Sierra Nevada may reflect an antecedent drainage condition, which would tend to support the inference that the drainage has been laterally offset.

Assuming that the Middle Fork Feather River is offset 18 to 20 km along the MVFZ and, further that strike-slip faulting began at 3 Ma or latter in the Mohawk Valley area, then a maximum right-lateral slip rate of 6-7 mm/yr is permissive, albeit unlikely, on the MVFZ. It is interesting to note that this rate is comparable to results of kinematic models and geodetic studies. Further study and additional information will be required to constrain the rate of slip on the MVFZ.

Paleoseismic investigation of the MVFZ at the Calpine trench site

Alt (1990) identified a site for paleoseismic investigation along the west branch of the southern MVFZ, 4 km west of Calpine, based on interpretation of aerial photographs and aerial reconnaissance. The "Calpine trench site" is at the abrupt toe of the steep and high Sierran front at 5,800 ft in a dense conifer forest. The initial trenching target was a distinct range-front graben. An additional trench was sited across a steep well-defined scarp on colluvium identified along a sympathetic fault splaying from the frontal fault (Figure 9-1).

Two exploratory trenches were excavated in December, 1990 at the Calpine trench site. Trench 1 was excavated within the range-front graben and crossed an antithetic fault. Trench 2 crossed a 3.7-m-high, northeast-facing scarp marking the arcuate splay fault (Figure 9-1). The prominent scarp trends N67ºW at the trench, slightly oblique to the N50ºW-trend of the nearby range front. As a result of inclemental weather, however, shallow groundwater seeping from small pores in the trench walls immediately froze forming 2-3 inch long needles of ice that completely obscured the walls of the trenches and forced us to postpone the trench study. In August, 1991, we re-excavated and logged the eastern part of trench 1, which exposed the antithetic fault, and re-excavated and logged all of trench 2.

Trench 1 Findings: Trench 1 was approximately 60 m long and up to 3 m deep. The trench exposed coarse colluvium interfingering eastward with flat-lying, fine-grained alluvial deposits near the axis of the graben. The alluvial deposits interfingered eastward with another package of colluvial deposits. A fragment of charcoal from near the base of unit C1, the uppermost deposit in this package, yielded a radiocarbon date of 3,395 + 105 ^{14}C yr BP. A second charcoal fragment was collected from an irregular shaped and bioturbated deposit that infilled above a burned tree stump in growth position. This sample yielded a date of 4,735 + 155 ^{14}C yr. BP.

A common problem in attempting to date near-surface deposits in a dense forest setting is the introduction of secondary or intrusive organic matter as a result of extensive bioturbation. Radiocarbon dates on intrusive charcoal postdate the age of the host deposits and may best explain the stratigraphic inversion problem of the two dates from trench 1. Therefore, unit C1 most likely is not younger than middle Holocene in age (Figure 9-5).

Although the range front fault was not exposed, it presumably lies further to the west and higher on the range front, trench 1 did expose the antithetic fault bounding the east side of the range-front graben. Two steeply west-dipping faults in a 4-m-wide zone of near-vertical fractures were exposed cutting and juxtaposing colluvial deposits (Figure 9-5). The eastern of the two faults, F1, is marked by a 25-cm-wide zone of prominent shear fabric that strikes N40º-45^{O}W and dips from 34^{O}-81^{O}W. The fault truncates upwards at the base of colluvial unit C2, which is overlain by the middle(?) Holocene unit C1. The cumulative stratigraphic separation across fault F1 probably exceeds 2 m, down to the southwest. The western fault, F2, was identified as a 10-cm-wide zone of shears and fractures that strikes N25^{O}W and steepens downward from 52^{O}W near the top of the trench to 72^{O}W near the bottom. The expression of this fault diminishes towards the surface, but can be identified to where it also truncates against the base of unit C2 (Figure 9-5). Stratigraphic separation across fault F2 exceeds 2 m.

The zone of steeply-dipping fractures is confined to the footwall of the fault F1 (Figure 9-5). The fractures generally strike N65^{O}W and dip from 75^{O}W through vertical to approximately 87ºE. Roots and

root mats commonly occur along, and aid in identification of, these fractures. The fracture zone cuts units C6 and C7 and truncates at the base of unit C5 (Figure 9-5).

Trench 2 Findings: Trench 2 was nearly 50 m long, up to 5.5 m deep, and exposed colluvial deposits, including scarp-derived colluvium, overlying and juxtaposed against weathered granitic bedrock. From youngest to oldest, the colluvial deposits are designated C1 through C8 and Cw1 through Cw5 (Figure 9-6). Bedrock was encountered in the footwall of the splay fault.

Two samples of charcoal collected from the youngest colluvial deposit, unit C1, yielded radiocarbon dates of 3,055 + 130 ^{14}C yr BP and 12,081 + 94 ^{14}C yr BP (Figure 9-6). Two additional samples of charcoal collected from the subjacent colluvial unit, C2, yielded dates of 1,032 ± 50 to 3,360 ± 56 ^{14}C yr BP (Figure 9-6). The spread and stratigraphic inversion of these dates likely results from the introduction of secondary charcoal by bioturbation. Although these deposits may be Holocene in age, units C1 and C2 are likely latest Pleistocene in age given the apparent problem with intrusive organic matter.

Trench 2 exposed a rather wide zone of steeply- to near-vertical faults and fractures. The main fault, F1, juxtaposes granitic bedrock and colluvial deposits in the footwall against colluvial deposits in the hanging wall. The upper extent of the fault bounds a fissure-fill deposits, unit FF2 (Figure 9-6). The fault strikes N72^{o}W, slightly oblique to the local trend of the scarp, and dips 57^{o}E. The fault exhibits distinct shear fabric and near vertically aligned clasts within a shear zone up to 60 cm wide. The vertical separation across fault F1 exceeds 3.9 to 4.4 m. Slickenside striations plunge a modest 15^{o}SE, suggesting dominantly right-lateral slip with a subordinate normal component on the range-front splay fault. The stratigraphic separation across fault F1 and these shear-sense indicators suggest that fault F1 may have produced 15 to 17 m of right-lateral displacement in the late Quaternary.

Trench 2 exposed three additional and subordinate faults, F2, F3 and F4 (Figure 9-6). Fault F2 is oriented N53^{o}W55^{o}E and exhibits only minor stratigraphic offset. This fault extends upwards to the base of unit C3 as a single fracture. Fault F3 strikes N51^{o}W, dips 85^{o}E, and also truncates upwards at the base of C3. This fault juxtaposes bedrock against colluvium in an apparent reverse sense, indicating lateral slip also occurs on fault F3. The down-to-the-east offset of the top of bedrock across fault F3 is estimated to be about 3.8 meters. Fault F4 is oriented N31^{o}W85^{o}E and offsets of the top of bedrock about 50 cm. This fault is associated with numerous fractures, an infilled fissure, and a small "colluvial-wedge" deposit, unit Cw3.

In addition, several high-angle fractures were exposed in trench 1. Most of these fractures are planar and strike N51º to 77^{o}W and dip steeply to the east. However, a few fractures are slightly arcuate and some dip westward. Although none of the faults were found to cut deposits younger than unit C4, three distinct fractures cut through the lower two-third's of overlying unit C2.

Paleoseismic Interpretation: Our interpretation of 6 to 7 earthquakes during the late Quaternary along the western branch of the MVFZ is based on the upward termination of faults and fractures, fissure-fill deposits, scarp-derived colluvium, the relative degree of clast weathering and soil development, and radiocarbon dates in trench 2 (Figure 9-7). Some or all of the events interpreted from trench 1 exposures may be represented in the other trench.

The first of a minimum of four surface-faulting events, "earthquake X", interpreted from trench 1 exposures of the antithetic fault (Figure 9-7) is evidenced by a set of fractures that disrupt units C6 and C7, but are abruptly truncated at the base of unit C5 (Figure 9-5). The second event, earthquake V, is interpreted to have separated units C5 through C7 a minimum of about 180 cm, down to the west, along fault F1. Unit Cw2 is thought to be a colluvial wedge derived from, and deposited against a scarp produced during this event. The penultimate event (earthquake U) faulted unit Cw2 along fault F2, and is associated with a comparable amount of vertical separation and with scarp-derived colluvial . The colluvial wedge resulting from the penultimate earthquake, unit Cw1, is buried by units C2 through C1a which likely provide a minimum time since the occurrence of the penultimate event of at least 5 ka . The

fourth, and most-recent event (earthquake T?, Figure 9-7), is inferred from youthful scarps and small closed depressions, that were first noted by Craig M. dePolo as extending northward along strike of the antithetic fault from trench 1. Evidence for this event was not recognized in the trench, presumably because it was obliterated by bioturbation in the fault zone.

The earliest of 6 to 7 events interpreted from trench 2 exposures, earthquake Z (Figure 9-7), produced a bedrock scarp along fault F3. Unit Cw5 is a colluvial wedge (Figure 9-6) derived from weathered bedrock exposed in the footwall of the fault during the event. The second event, earthquake Y, re-ruptured fault F3 and may have triggered minor slip along fault F2. Unit Cw4 is a colluvial wedge deposited at the base of the second-event scarp. The estimated thickness of Cw4 against the fault suggests that the second event resulted in at least 2.6 m of vertical displacement on a fault having an inferred lateral slip component. Earthquake X is the third paleoseismic event interpreted from trench 2 exposures and it produced a scarp in weathered bedrock along fault F4, buried by colluvial-wedge Cw3. The fourth event, earthquake W, is inferred from stratigraphic relationships along fault F1. Unit Cw2 is a colluvial wedge deposit derived from a scarp produced during this event. The thickness of the scarp-derived colluvium suggests that this event produced 1.3 m, or more, of down-to-the-east normal slip on fault F1, which based on the orientation of slickensides has a significant component of lateral slip. The fifth event, earthquake V, is interpreted from fissure-fill deposit FF2, which is in fault contact with hanging wall units Cw2 and C5. The penultimate event, earthquake U, produced a scarp buried by unit Cw1. Fracturing in the lower two-third's of unit C2 is the only evidence in trench 2 for the most recent event.

This paleoseismic investigation suggests that rupture along the western branch of the southern MVFZ occurs during large earthquakes, that are possibly characterized by right-oblique-normal displacements in excess of 2-3 m.

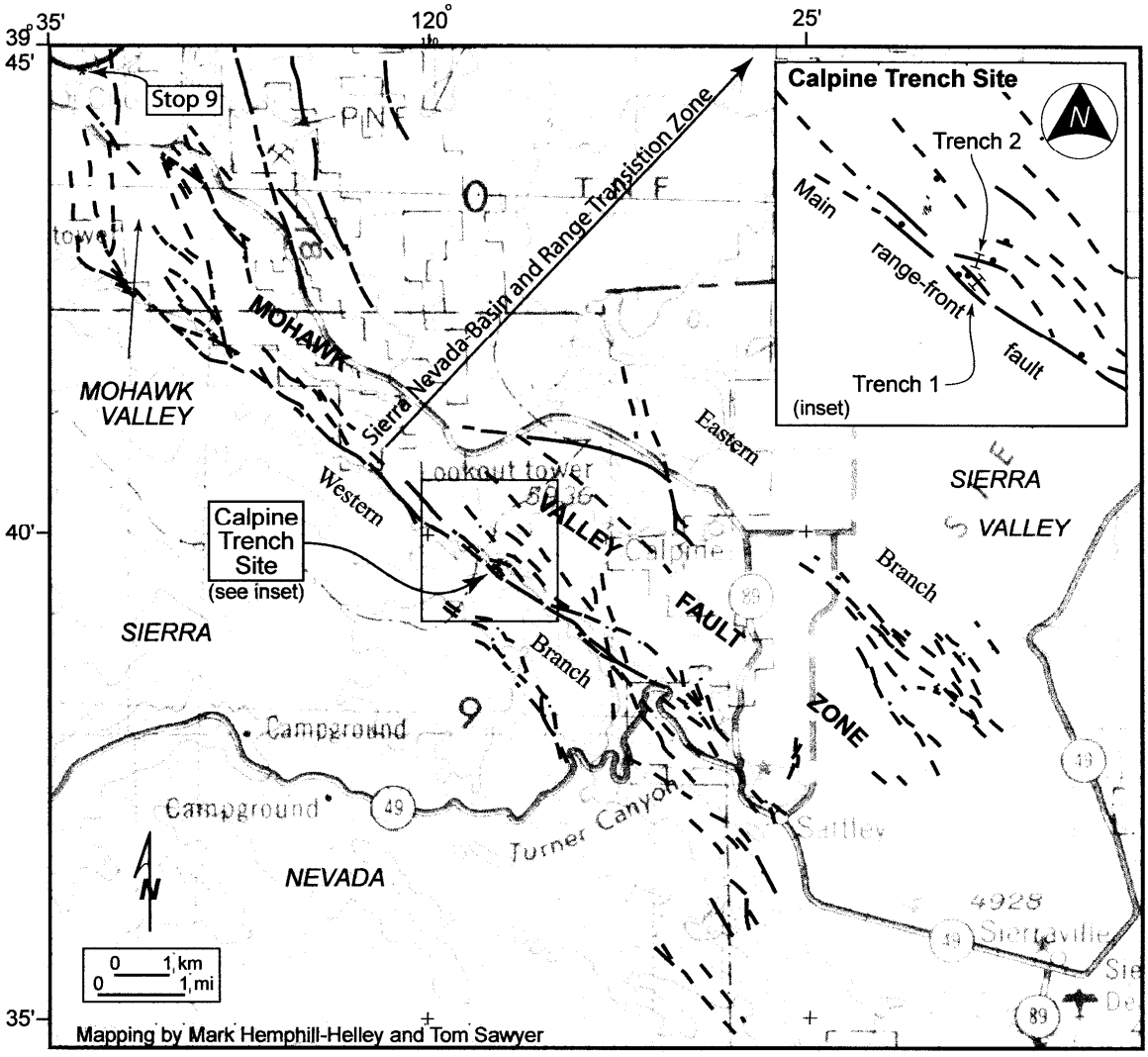

Figure 9-1. Map of the southern Mohawk Valley fault zone, based on interpretation of aerial photographs and limited field reconnainance.

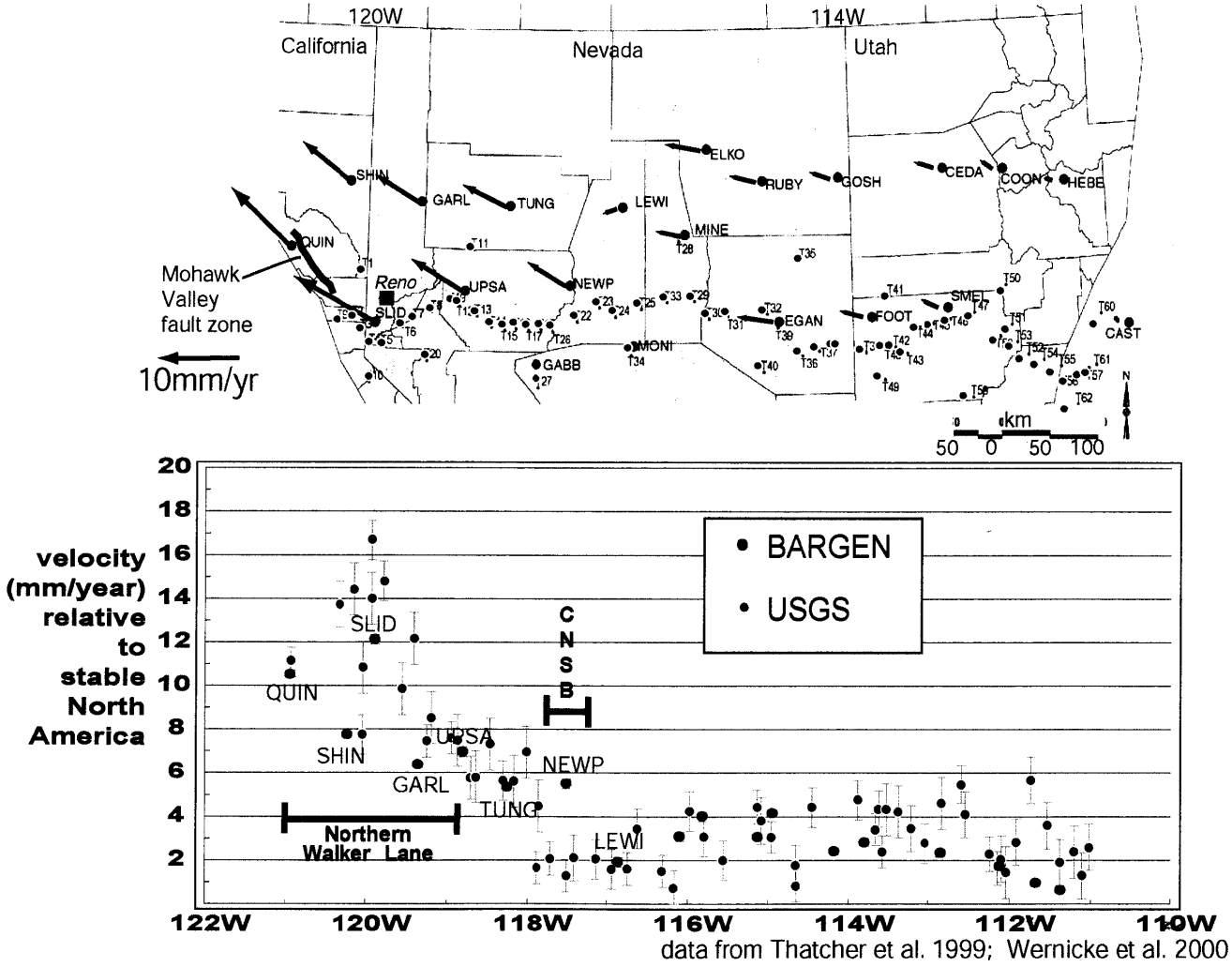

Figure 9-2. USGS and BARGEN geodetic networks. The top panel shows station locations for both networks and velocity vectors for the BARGEN network. The bottom panel shows absolute station velocities for both networks relative to stable North America. Note shared station QUIN.

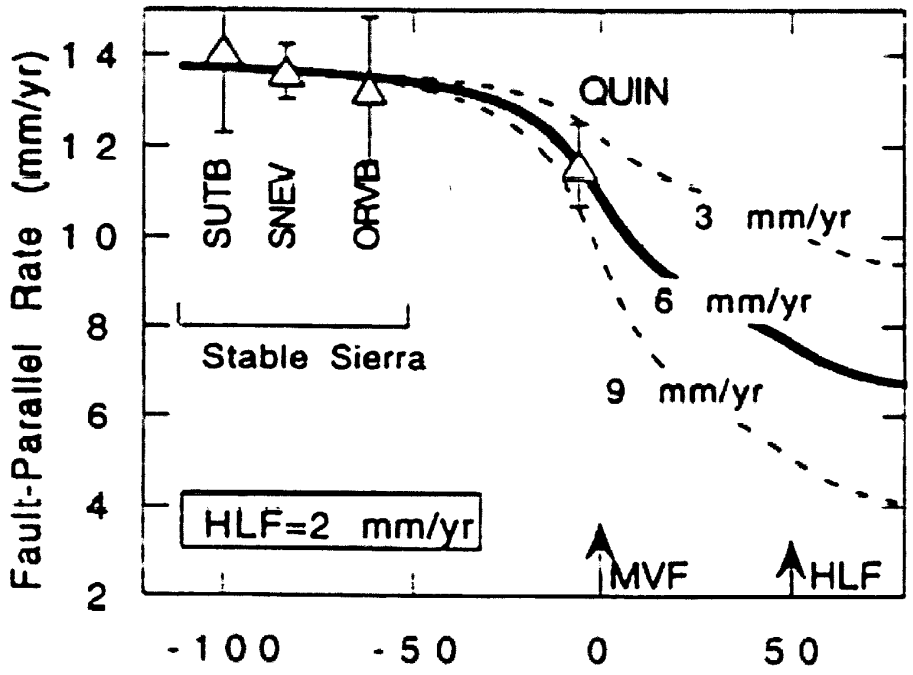

Figure 9-3. Simple strain accumulation model for two strike-slip faults in an elastic half-space (figure from Dixon et al., 2000). MVF = Mohawk Valley fault zone, HLF = Honey Lake fault zone. Honey Lake fault zone is fixed at 2mm/yr (Wills and Borchardt, 1993).

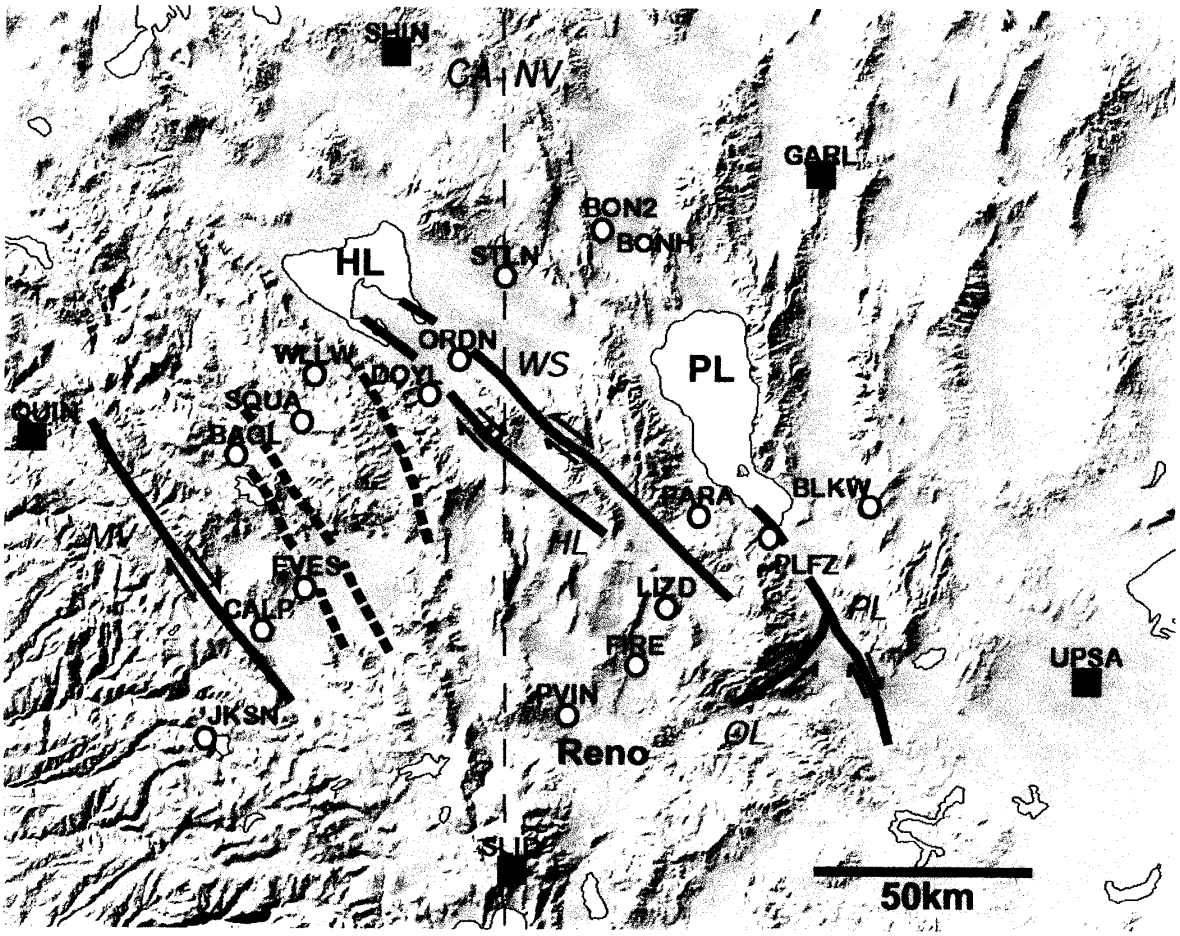

Figure 9-4. Circles denote stations of the Northern Walker Lane Geodetic Network. Existing continuous BARGEN (Bennett et al., 1998) stations are shown as squares. Major strike-slip faults are shown by solid lines (MV=Mohawk Valley; HL=Honey Lake; WS=Warm Springs; PL=Pyramid Lake; OL=Olinghouse).

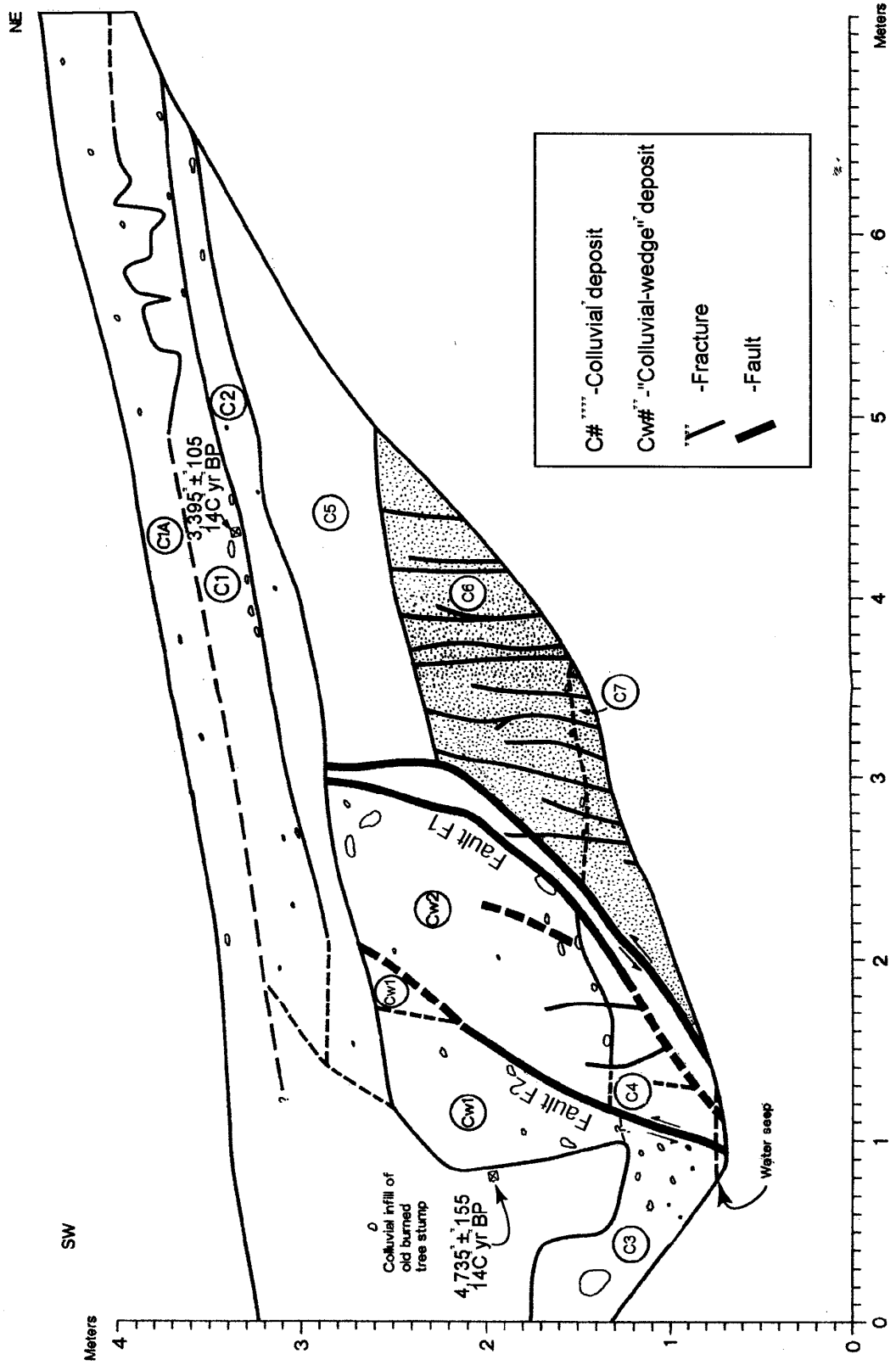

Figure 9-5. Graphical log of eastern part of Trench 1, Calpine trench site.

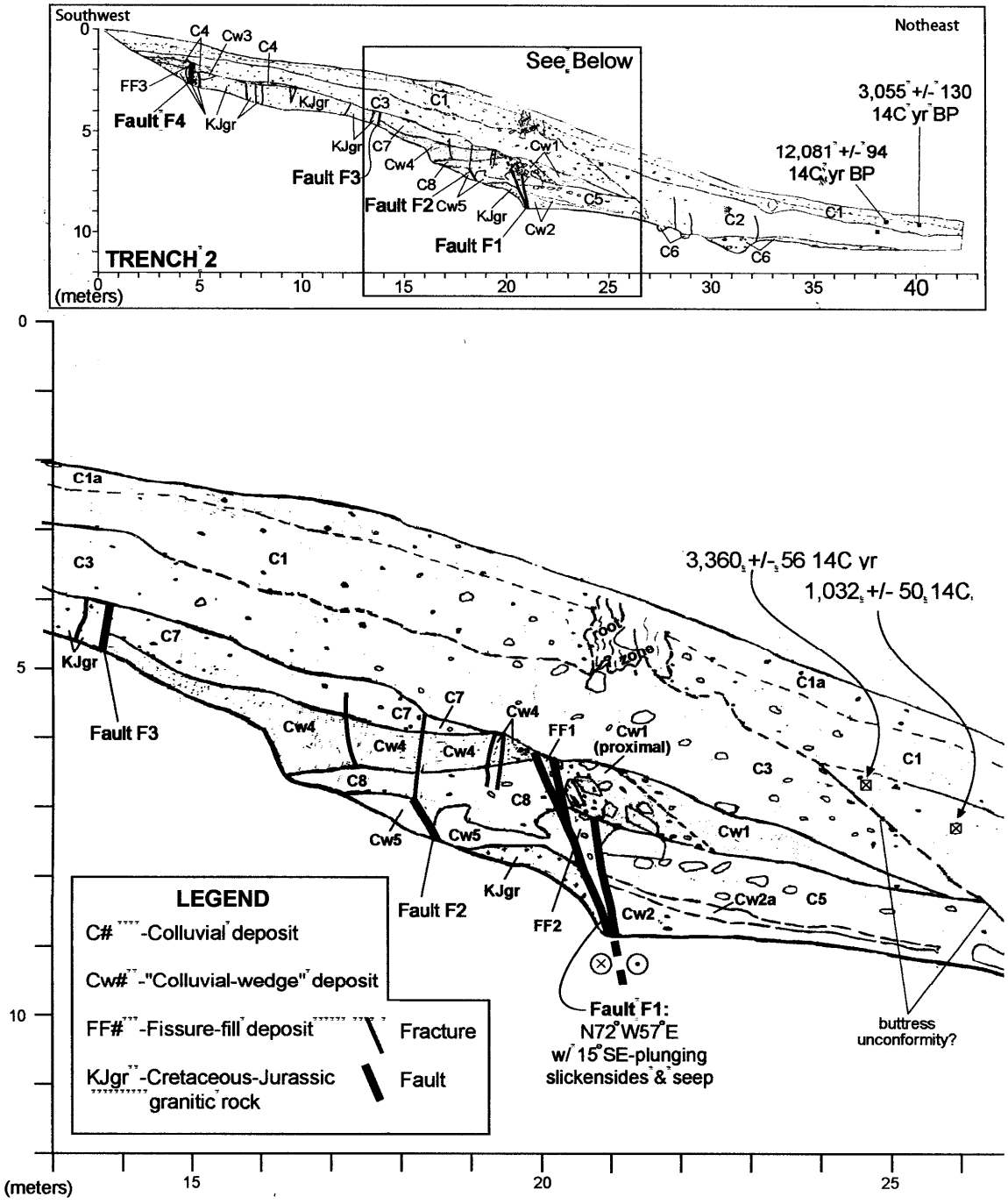

Figure 9-6. Graphical log of north wall of Trench 2, Calipine trench site.

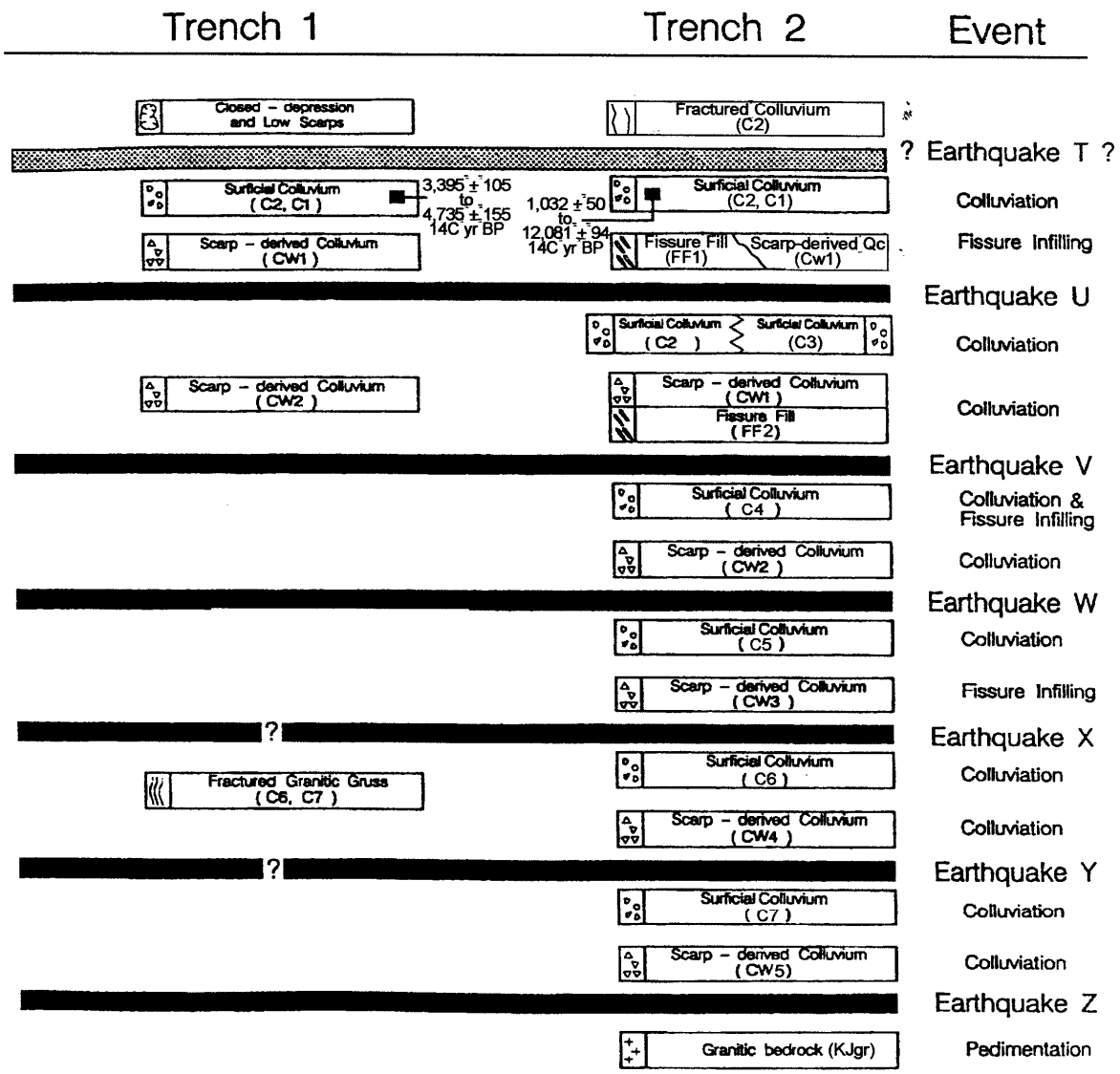

Figure 9-7. Relative chronology of paleoseismic surface-faulting events at the Calpine trench site.

References

Alt, J.N., 1990, Observations and Preliminary Conclusions from Mohawk Study, unpublished consultants report to PG&E, Geosciences Department, San Francisco, Ca, 2 p. with plates.

Argus, D.F., and R.G. Gordon, 1991. Current Sierra Nevada-North America motion from very long baseline interferometry; implications for the kinematics of the Western United States. Geology, vol.19, no.11, pp.1085-1088.

Atwater, T., 1970. Implications of Plate Tectonics for the Cenozoic Tectonic Evolution of Western North America. GSA Bulletin, v. 81, pp 3513-3536.

Bennett, R.A., B.P. Wernicke, and J.L. Davis, 1998. Continuous GPS measurements of contemporary deformation across the northern Basin and Range province. Geophys. Res. Letters 25:4, pp 563-566.
Bennett, R.A., Wernicke, B.P., Davis, J.L., Friedrich, A., and Niemi, N.A., 1999. Distribution of extension and shear across the northern Basin and Range from BARGEN continuous GPS data: The fate of the eastern California shear zone. Eos, Transactions, American Geophysical Union, vol.80, no.46, pp. F269.
Briggs, R.W. and S.G. Wesnousky, 2001. The Basin and Range Sierra Nevada Transition along the Northern Walker Lane: Geology vs. Geodesy. Seismological Research Letters, v.72, no.2, p.280.
DeMets, C., Gordon, R.G., Stein, S., and Argus, D.F., 1987. A revised estimate of Pacific-North America motion and implications for western North America plate boundary zone tectonics. Geophysical Research Letters, vol.14, no.9, pp.911-914.
Dixon, T. H., S. Robaudo, J. Lee, and M.C. Reheis, 1995. Constraints on present-day Basin and Range deformation from space geodesy. Tectonics 14:4, pp 755-772.
Dixon, T.H, M. Miller, F. Farina, H. Wang, and D Johnson, 2000. Present-day motion of the Sierra Nevada block and some tectonic implications for the Basin and Range province, North American Cordillera. Tectonics 19:1, pp. 1-24.
Durrell, C., 1966, Tertiary and Quaternary geology of the northern Sierra Nevada, in E.H. Bailey, editor, Geology of Northern California: California Division of Mines and Geology Bulletin 190, pp. 185-197.
Gotter, S.K. Oppenheimer, D.H., Mori, J.J., Savage, M.K., Masse, R.P., 1994, Earthquakes in California and Nevada: U.S. Geological Survey Open-File Report 94-647, scale 1:1,000,000.
Grose, T.L.T., 1986, Geologic map, Marlette Lake quadrangle: Nevada Bureau of Mines and Geology Map 2Cg, 1:24,000.
Grose, T.L.T., 1996. Tectonics of the Walker Lane in NE California and the Honey Lake anomaly. Eos, Transactions, American Geophysical Union, vol.67, no.44, pp.1211.
Hawkins, F.F., LaForge, R., and Hansen, R.A., 1986, Seismotectonic study of the Stampede, Prosser Creek, Boca, and Lake Tahoe dams, Truckee/Lake Tahoe area, northeastern Sierra Nevada, California: Seismotectonic Report No. 85-4, 210 p.
Henry, C.D. and Perkins, M.E., 2001, Sierra Nevada-Basin and Range transition near Reno, Nevada: Two-stage Development at at 12 and 3 Ma: Geology, v. 29, no. 8, p. 719-722.
Minster, J.B. and T.H. Jordan, 1987. Vector constraints on Western U.S. deformation from space geodesy, neotectonics, and plate motions. Journal of Geophysical Research, B, Solid Earth and Planets, vol.92, no.6, pp.4798-4804.
Page, W.D. and Sawyer, T.L., 1992, Tectonic deformation of the Lovejoy basalt, a late Cenozoic strain guage across the northern Sierra Nevada, California EOS v. 73, p 590.
Page, W.D., Sawyer, T.L., McLaren, M., Savage, W.U., and Wakabayashi, J., 1993, The Quaternary Tahoe-Medicine Lake trough: the western margin of the Basin and Range transition, NE California: Geological Society of America, Abstracts with programs, v. 25, p. 131.
Pezzopane, S.K. and R.J. Weldon, 1993. Tectonic role of active faulting in central Oregon. Tectonics, vol.12, no.5, pp.1140-1169.
Saucedo, G.J., 1992, Geologic map of the Chico quadrangle, California: California Division of Mines and Geology, scale 1:250,000
Sawyer, T.L., Page, W.D., and Hemphill-Haley, M.A., 1993, Recurrent late Quaternary surface faulting along the southern Mohawk Valley fault zone, NE California: Geological Society of America, Abstracts with Programs, v. 25, p. 142.
Surpless, B.E., Stockli, D.F., Dumitru, T.A., Miller, E.L., and Farley, K.A., 2000, Post-15 Ma westward structural and thermal encroachment of Basin and Range type extension into the northern Sierra Nevada: Geological Society of America Abstracts with Programs, v. 32, no. 7, p. A43.
Thatcher, W., G.R. Foulger, B.R. Julian, J. Svarc, E. Quilty, and G.W. Bawden, 1999. Present-Day Deformation Across the Basin and Range Province, Western United States. Science, Vol. 283.
Toppozada, T.R., Real, C.R., and Parke, D.L., 1981, Preparation of isoseismal maps and summaries of reported effects for pre-1900 California earthquakes: California Division of Mines and Geology Open-File Report 81-11 SAC, 182 p.
Turner, H.W., 1987, Description of the Downieville quadrangle, California: U.S. Geological Survey Geological Atlas of the United States, Folio 37, scale 1:125,000.
Unruh, J.R., 1991, The uplift of the Sierra Nevada and implications for late Cenozoic epeirogeny in the western Cordillera: Geological Society of America Bulletin, v. 103, p. 1395-1404.
Unruh, J.R., Humphrey, J.R., and W.D. Page, 1996. Northwest continuation of the greater Walker Lane Belt and counterclockwise rotation of the Sierra Nevada microplate, northeastern California. Abstracts with Programs - Geological Society of America, vol.28, no.5, pp.119.
U.S. Geological Survey National Earthquake Information Center, World Data Center for Seismology, Internet access.
Ward, S.N., 1990. Pacific-North America plate motions; new results from very long baseline interferometry. Journal of Geophysical Research, B, Solid Earth and Planets, vol.95, no.13, pp.21,965-21,981.
Wernicke, B., Friedrich, A.M., Niemi, N.A., Bennett, R.A., and J.L. Davis, 2000. Dynamics of plate boundary fault systems from Basin and Range Geodetic Network (BARGEN) and geological data GSA Today, vol.10, no.11, pp.1-7.
Wills, C.J. and Borchardt, G., 1993, Holocene slip rate and earthquake recurrence on the Honey Lake fault zone, northeastern California: Geology, v. 21, p. 853-856.

STOP 10

John Wakabayashi, 1329 Sheridan Lane, Hayward, CA 94544, wako@tdl.com,
http://www.tdl.com/~wako/

Overview Point Along Middle Fork-North Fork Yuba River Divide

This overview stop on the Middle Fork-North Fork Yuba River divide allows one to view the late Cenozoic incision of the North Fork Yuba River, in addition to relief that predated this incision (referred to as paleorelief). We park on a ridge that is capped by Tertiary volcanic rocks; our parking spot is near the base of these rocks where they overlie Paleozoic metamorphic rocks. From our parking area we can take a walk down a short logging spur on the north side of this ridge to the base of the volcanic rocks (only 5-7 m lower than where you park). From here one can look northward, down into the North Fork Yuba River canyon. The canyon bottom is about 650 m below this point. This represents the late Cenozoic incision of the North Fork Yuba River into the basement (pre Cenozoic) metamorphic rocks beneath the Tertiary volcanic cover (see Fig. 10-1). Because this area was blanketed with Cenozoic volcanic rocks, the river had to cut through the volcanic rocks and the basement. The maximum age for the start of this stage of incision can be estimated by the age of the youngest of these extensive volcanic deposits. This age is approximately 5 Ma (see discussions in Wakabayashi and Sawyer, 2001; and Unruh, 1991). Relationships between Tertiary units elsewhere in the Sierra, and the tilts of strata along the western margin of the range indicate incision through basement and tilting was minimal prior to 5 Ma. These same relationships indicate that tilting and major stream incision began not long after 5 Ma. Late Cenozoic incision in the Sierra Nevada is shown on Fig. 10-2.

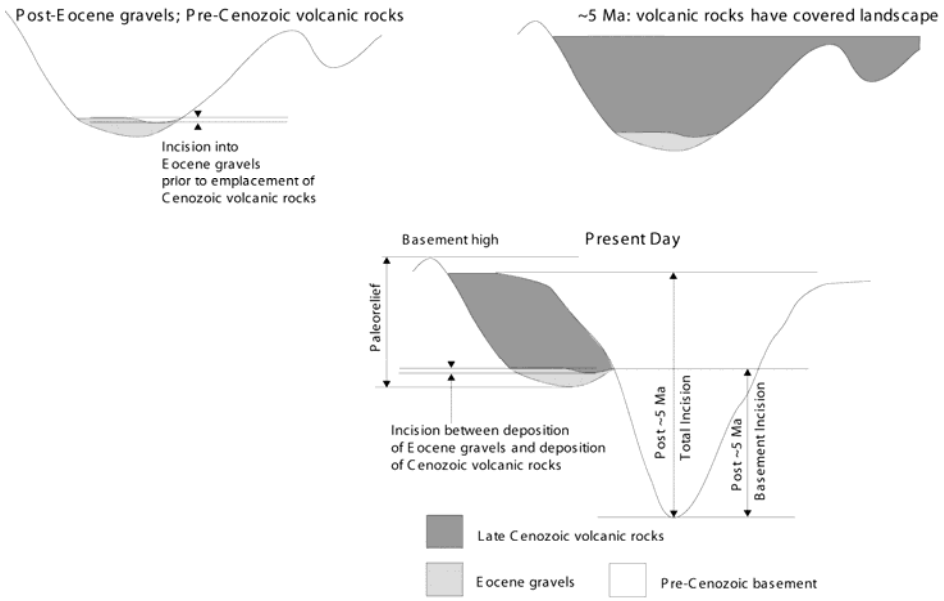

Figure 10-1: Diagram depicting the development of the cross section of a typical Sierra Nevada canyon. At many localities, late Cenozoic volcanic rocks directly overlie basement rather than Eocene gravels. Adapted from Wakabayashi and Sawyer (2001).

Looking northward across the canyon one sees the rugged summit of the Sierra Buttes, composed of Paleozoic metamorphic rocks, nearly 800 m higher than where you stand; this is the minimum amount of local relief represented by the Sierra Buttes at the time of the deposition of the volcanic rocks (paleorelief). The Sierra Buttes are the highest of several isolated basement highs in the northern Sierra. Other basement highs can be seen south of our viewpoint; some may be visible from south side of the ridge we are on, whereas others are visible on the drive to and from Highway 89. These paleorelief highs

include the Grouse Ridge area (about 500 m of paleorelief) and English Mountain, south of Jackson Meadow Reservoir (about 600 m of paleorelief). In general, there is little paleorelief in the northern Sierra except for these isolated highs (Fig. 10-3). In contrast, the Sierra Nevada from Yosemite southwards has a large amount of paleorelief. The bounding ridges of the San Joaquin River drainage, for example, have summits over 1000 m (locally over 1500 m) higher than the position of the 10 Ma ancestral San Joaquin River channel of Huber (1981).

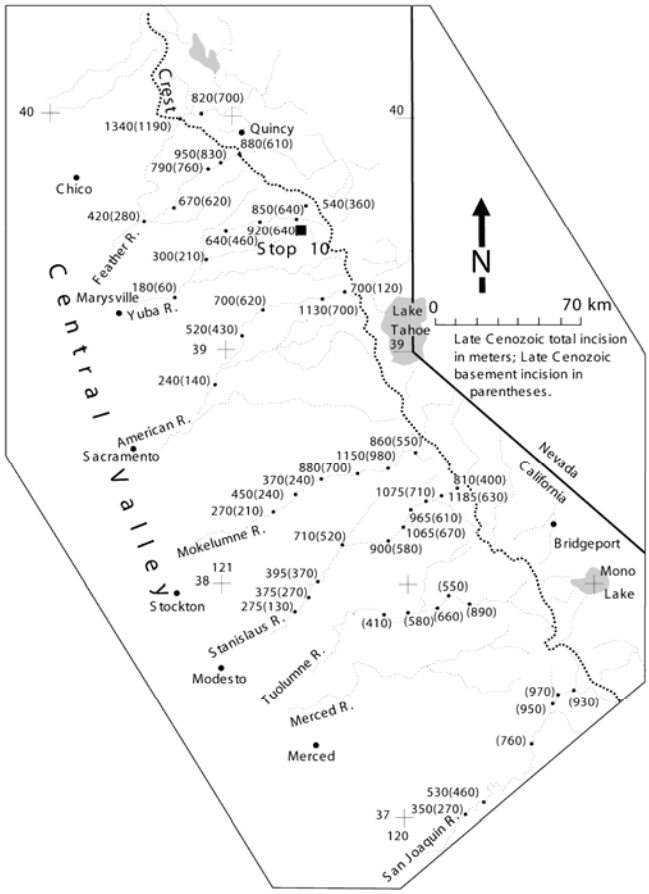

Figure 10-2. Late Cenozoic stream incision of the northern and central Sierra Nevada. Adapted from Wakabayashi and Sawyer (2001).

Stream incision and paleorelief offer clues to the long-term topographic evolution of the Sierra Nevada. Uplift of the range, however, cannot be evaluated unless there are features that can be tied to absolute elevation. In the Sierra Nevada the hingeline area (Fig. 10-4) has stayed at about the same elevation relative to sea level throughout the late Cenozoic (e.g., Huber, 1981; Unruh, 1991). Thus, well-preserved late Cenozoic units, such as the Lovejoy basalt and Table Mountain latite, can be used to record deformation, tilting, and rock uplift across the Sierra Nevada (Wakabayashi and Sawyer, 2000; 2001). The valleys down which the Lovejoy basalt and Table Mountain latite and other units flowed had lower gradients than the modern rivers. These paleovalleys were broad and alluviated in contrast to the narrow, deep canyons associated with today's rivers. Very low incision rates of streams from Eocene to Miocene time, recorded by the channeling of Miocene and/or Oligocene units through Eocene units are consistent with low stream gradients (Wakabayashi and Sawyer, 2001). Some estimates for ranges of paleogradients can be made for the drainages down which units such as the Lovejoy basalt and Table Mountain latite flowed; such estimates can be used with the present day configuration of well-preserved late Cenozoic units to estimate rock uplift in the Sierra (Fig. 10-4) (Wakabayashi and Sawyer, 2001). Late Cenozoic (post ~5 Ma) rock uplift of the Sierra Nevada is estimated at about 1700-1900 m. Erosion of bedrock summit flats in the Sierra has been very low (Small et al.,1997), so the uplift for the Sierra crest area, estimated from reconstructed late Cenozoic units approximates surface uplift for those summit

areas (Fig. 10-4). The fastest long-term late Cenozoic erosion rates are recorded by the most deeply incised parts of the modern canyons. Incision in such canyons can be compared to the rock uplift calculated for that area. Such an analysis shows that even the rocks at bottom of the deepest canyons have experienced surface uplift of 600-1100 m (schematically shown in Fig. 10-4) (Wakabayashi and Sawyer, 2001). Thus, there has been considerable mean surface uplift of the range in the late Cenozoic.

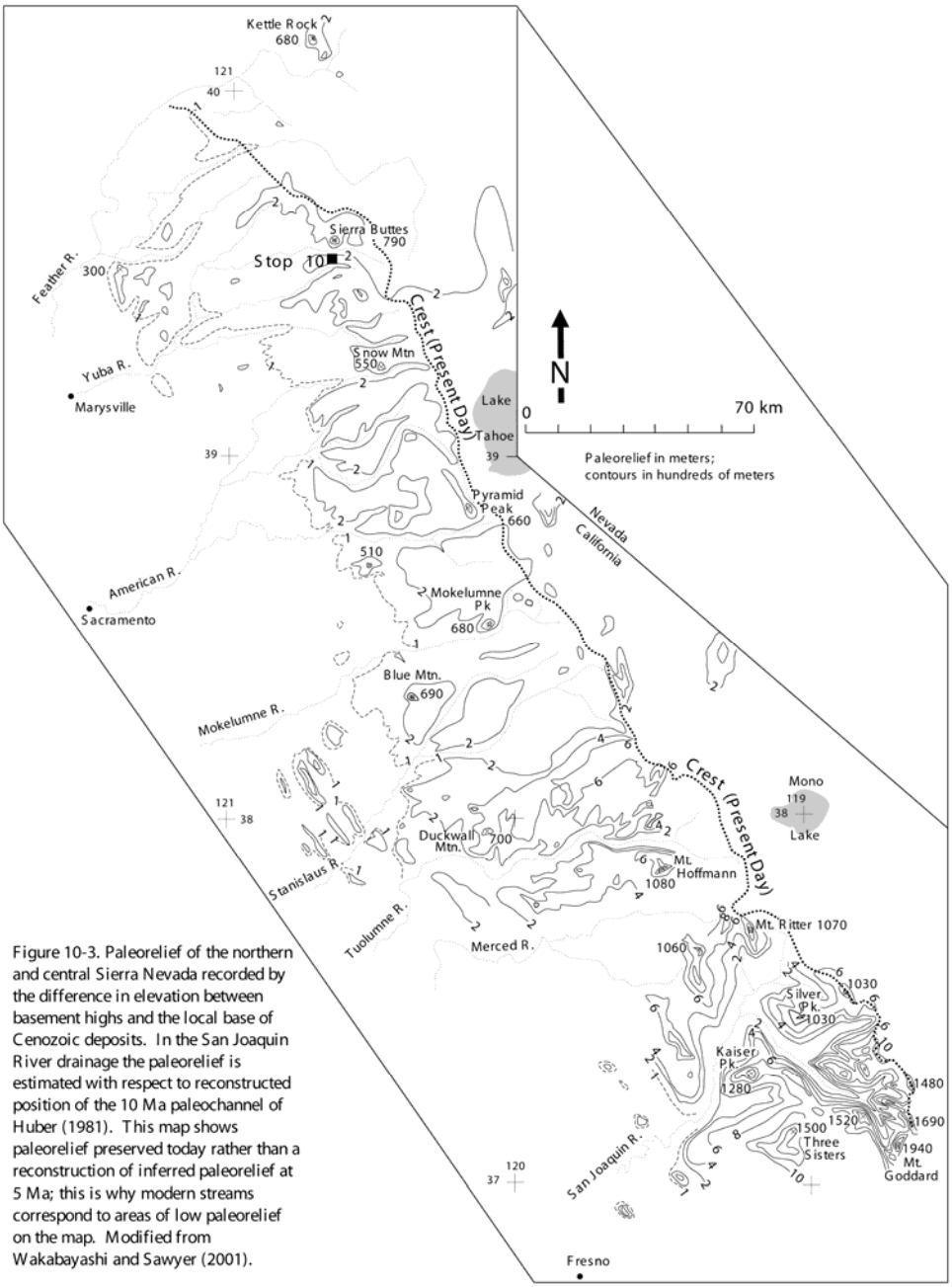

Figure 10-3. Paleorelief of the northern and central Sierra Nevada recorded by the difference in elevation between basement highs and the local base of Cenozoic deposits. In the San Joaquin River drainage the paleorelief is estimated with respect to reconstructed position of the 10 Ma paleochannel of Huber (1981). This map shows paleorelief preserved today rather than a reconstruction of inferred paleorelief at 5 Ma; this is why modern streams correspond to areas of low paleorelief on the map. Modified from Wakabayashi and Sawyer (2001).

The lack of Miocene-Eocene stream incision is associated with a lack of tilting and inferred Miocene-Eocene rock uplift. Eocene gravels underlie the late Cenozoic deposits throughout the northern and central Sierra, even in the Sierra crestal area. If significant Eocene-Miocene rock uplift and tilting had occurred, then Eocene deposits near the Sierran crest should be present as perched remnants high above the base of Miocene deposits. The Eocene deposits beneath Miocene and Oligocene volcanic rocks include exposures across (north) the North Fork Yuba River canyon from our viewpoint both upstream (east) and downstream (west) of Sierra Buttes. These exposures include deposits beneath Haskell Peak

that is on the crest of the range. The lack of significant rock uplift and stream incision between Eocene and Miocene time suggests that paleorelief we see today was created prior to the Eocene (Wakabayashi and Sawyer, 2001).

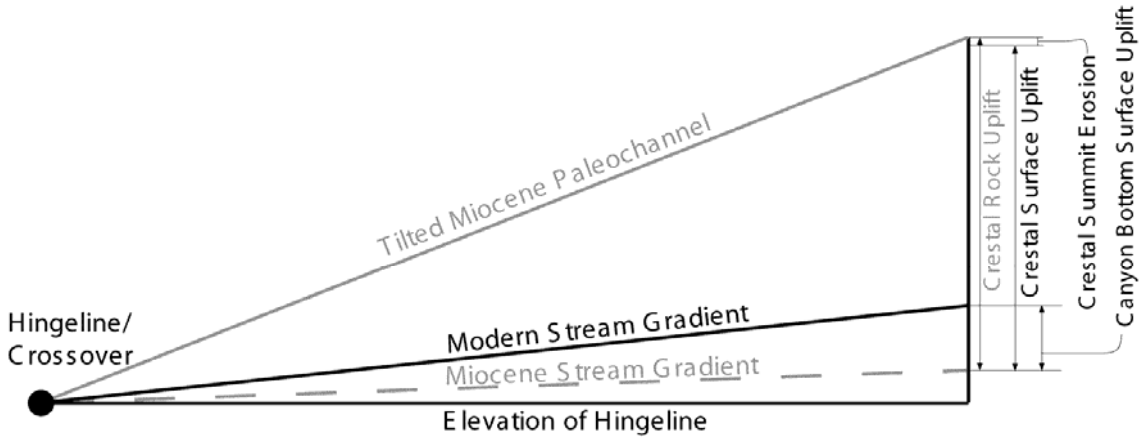

Fig.10-4: Diagram showing the relationship between tilted Tertiary paleochannels, Miocene stream gradients, and surface and rock uplift. Adapted from Wakabayashi and Sawyer (2001).

There has been considerable debate about whether or not late Cenozoic uplift occurred in the Sierra (e.g., Huber, 1981; Unruh, 1991; House et al., 1998; Wakabayashi and Sawyer, 2001), and what tectonic or other mechanisms influenced the topographic development of the Sierra Nevada (e.g., Small and Anderson, 1995; Wakabayashi and Sawyer, 2001); much of this debate is discussed in Wakabayashi and Sawyer (2001) and references therein. This final stop of the FOP trip affords a great backdrop to discuss various models for the evolution of California's most prominent mountain range.

References

House, M.A., Wernicke, B.P., and Farley, K.A., 1998, Dating topography of the Sierra Nevada, California, using apatite (U-Th)/He ages: Nature, v. 396, p. 66-69.

Huber, N.K., 1981, Amount and timing of late Cenozoic uplift and tilt of the central Sierra Nevada, California-evidence from the upper San Joaquin river basin: U.S. Geological Survey Professional Paper 1197, 28p.Wakabayashi, J., and Sawyer, T.L., 2001, Stream incision, tectonics, uplift, and evolution of topography of the Sierra Nevada, California: Journal of Geology, v. 109, p. 539-562.

Small, E.E., and Anderson, R.S. 1995, Geomorphically driven late Cenozoic rock uplift in the Sierra Nevada, California: Science, v. 270, p. 277-280.

Small, E.E.; Anderson, R.S.; Repka, J.L.; and Finkel, R. 1997. Erosion rates of alpine bedrock summit surfaces deduced from in situ 10Be and 26Al. Earth Planet. Sci. Lett. 150: 413-425.

Unruh, J.R., 1991, The uplift of the Sierra Nevada and implications for late Cenozoic epeirogeny in the western Cordillera: Geological Society of America Bulletin, v. 103, p. 1395-1404.

Wakabayashi, J., and Sawyer, T.L., 2000, Neotectonics of the Sierra Nevada and the Sierra Nevada-Basin and Range Transition, California, with field trip stop descriptions for the northeastern Sierra Nevada: in Brooks, E.R., and Dida, L.T., eds., Field guide to the geology and tectonics of the northern Sierra Nevada, California Division of Mines and Geology Special Publication 122, p. 173-212.

Wakabayashi, J., and Sawyer, T.L., 2001, Stream incision, tectonics, uplift, and evolution of topography of the Sierra Nevada, California: Journal of Geology, v. 109, p. 539-562.